Institut für Pharmakologie und Toxikologie
der Technischen Universität München

Control of vasculo-proliferative processes by the NO-cGMP-cGKI pathway

Robert Lukowski

Vollständiger Abdruck der von der Fakultät Wissenschaftszentrum Weihenstephan für Ernährung, Landnutzung und Umwelt der Technischen Universität München zur Erlangung des akademischen Grades eines

Doktors der Naturwissenschaften

genehmigten Dissertation.

Vorsitzender:	Univ.-Prof. Dr. D. Haller
Prüfer der Dissertation:	1. Univ.-Prof. Dr. M. Schemann
	2. Univ.-Prof. Dr. F. Hofmann
	3. apl. Prof. Dr. Chr. Prinz

Die Dissertation wurde am 04.09.2006 bei der Technischen Universität München eingereicht und durch die Fakultät Wissenschaftszentrum Weihenstephan für Ernährung, Landnutzung und Umwelt am 16.11.2006 angenommen.

CHAPTER

INDEX

FIGURE LEGENDS

1 INTRODUCTION

1.1 The NO-cGMP-cGMP-dependent protein kinase type I signaling pathway

The freely diffusible biological messenger nitric oxide (NO) is an important signaling molecule in the body of mammals, including humans and mice. Due to its chemical properties the half-live of the diatomic gas in biological fluids is very short, within few seconds (Wink et al., 2000). The potent vasorelaxant properties of NO were first discovered more than 25 years ago (Furchgott and Zawadzki, 1980; Ignarro et al., 1987; Palmer et al., 1987). Since then, numerous studies revealed that NO bioavailability and signaling are widespread and critical for the function of the nervous, cardiovascular, gastrointestinal, endocrine, and the immune system. It is widely excepted that NO plays a critical role in the pathogenesis of cardiovascular diseases such as hypertension, atherosclerosis, and restenosis (Lloyd-Jones and Bloch, 1996).

Endogenous NO is produced by NO synthases (NOS) expressed in many different cell types. In concert with multiple co-factors NOS catalyze the oxidation of the terminal guanidino nitrogen of L-arginine to form NO and L-citrulline. So far, three different NOS isoforms have been characterized. The enzymatic activity of the constitutively expressed neuronal isoform nNOS/NOS-1 and the endothelial isoform eNOS/NOS-3 is Ca^{2+}-calmodulin (Ca^{2+}-CaM) dependent, whereas the inducible iNOS/NOS-2 enzyme is generally independent of cellular Ca^{2+}-levels. iNOS expression is stimulated after exposure of macrophages, vascular smooth muscle cells (SMCs) or endothelial cells to lipopolysaccharides (LPS) or cytokines. The NO concentrations produced by iNOS are higher and are more persistent as compared to the other two isoforms. Since NO can not be stored in intracellular vesicles it diffuses immediately from the site of its production across cell membranes and exerts many of its physiological effects in target cells by activating the soluble guanylyl cyclase (sGC) (Fig. 1). The sensitivity of the cyclase to NO is conferred by a single prosthetic heme moiety. The sGC catalyzes the conversion of guanosine-5´-triphosphate (GTP) to the second messenger cyclic guanosine-3´,5´-monophosphate (cGMP) (Gross and Wolin, 1995; Hofmann et al., 2004; Lloyd-Jones and Bloch, 1996). Besides the NO-sGC-cGMP pathway, NO has also

other targets and signals via several cGMP-independent mechanisms (e.g. reaction with sulfhydryl groups forming nitrosothiols, hemeoxygenase, catalase) (Hanafy et al., 2001). Cellular cGMP levels can also be elevated by a NO-independent pathway via the membrane-bound particulate guanylyl cyclases (pGCs) that form cGMP in response to binding of natriuretic peptides (NPs), such as the atrial natriuretic peptide (ANP), brain natriuretic peptide (BNP), and the C-type natriuretic peptide (CNP) (Fig. 1) (Garbers and Lowe, 1994).

The duration, maximum level, and the intensity of an intracellular cGMP signal is affected by the phosphodiesterases (PDEs). The PDEs are a large gene family of cyclic nucleotide degrading enzymes identified in many cell types mediating the hydrolization of cyclic adenosine-3´,5´-monophosphate (cAMP) and/or cGMP to adenosine-5´-monophosphate (AMP) and/or guanosine-5´-monophosphate (GMP), respectively. The PDE-5 isoform is presumably the main cGMP-hydrolyzing PDE expressed in vascular and visceral SMCs. The importance of the enzyme for the regulation of vascular tone has been demonstrated by the effective application of its specific inhibitor, sildenafil. Therapeutically relevant, this drug is used for the clinical treatment of erectile dysfunction and pulmonal hypertension (Rybalkin et al., 2003).

The outcome of a cGMP signal is determined by the unique combination of its intracellular effectors. So far, three classes of cGMP-dependent receptor proteins have been identified (Fig. 1). (1a.) cGMP binds to and, thereby, regulates the activity of several PDEs specific for the degradation of cAMP. In this manner, an intracellular cross-talk of both cyclic nucleotide pools is established since cAMP and cGMP have the capability to modulate the degradation of its counterpart via the activity of PDEs. (1b.) However, high amounts of cGMP not only indirectly modulate the cellular cAMP level but they might as well modify the activity of cAMP-dependent protein kinase (cAK) by a direct cross-activation (Sonnenburg and Beavo, 1994). (2.) In olfactory sensory neurons and the visual system the activity of cyclic nucleotide-gated (CNG) cation channels is modulated directly by cGMP (Kaupp and Seifert, 2002). (3.) Finally, the cGMP-dependent protein kinases (cGKs) are presumably the major cGMP-dependent targets of NO in many cells (Fig. 1) (Hofmann et al., 2006).

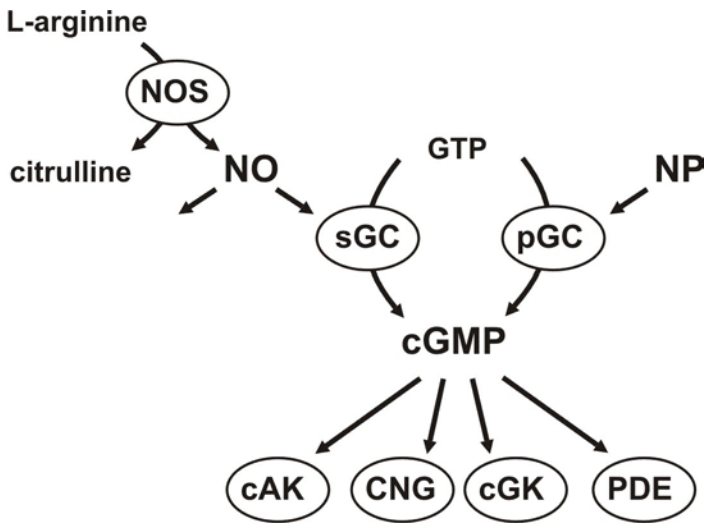

Fig. 1: Cellular synthesis and signaling pathways of cGMP. Nitric oxide (NO) is produced from L-arginine by the NO synthases (NOS). NO activates soluble guanylyl cyclase (sGC) to form cGMP using GTP. As indicated, NO has also cGMP-independent effects. An alternative pathway to produce cGMP involves the activation of particulate guanylyl cyclase (pGC) by natriuretic peptides (NPs). cGMP-dependent effectors are cAMP-dependent protein kinase (cAK), cyclic nucleotide-gated (CNG) cation channels, cGMP-dependent protein kinases (cGKs), and the phosphodiesterases (PDEs).

1.2 General properties of the cGKs

The cGKs are important intracellular cGMP receptors belonging to the serine-threonine family of protein kinases that phosphorylate substrate proteins at serine and/or threonine amino acid residues. Mammals express three different forms of cGKs encoded by two genes, *prkg1* and *prkg2*. The cGK type Iα (cGKIα) and cGK type Iβ (cGKIβ) isoforms are both products of the *prkg1* gene. cGKIα and cGKIβ differ in their individual NH_2-terminal ends that are encoded in transcripts produced from two alternative promoters. The cGKIs share many common structural features with the cGK type II (cGKII) enzyme, encoded by *prkg2* (Hofmann, 2005). cGKs are composed of three functional regions (Fig. 2):

(1.) The NH_2-terminal isoleucine-/leucinezipper region mediates the homodimerization of the identical cGK monomers. Partner proteins interact with these zipper regions and the kinases are targeted to different subcellular localizations by their specific amino termini. In the absence of cGMP, the activity of cGKs is suppressed by their NH_2-terminus, which acts as an autoinhibitory/pseudosubstrate site for the catalytic center. (2.) The catalytic domain contains the adenosine-5´-triphosphate (ATP) and substrate binding sites. This domain

catalyzes the γ-phosphate transfer of ATP to serine and/or threonine residues of substrate proteins. (3.) The regulatory domain of each cGK subunit is composed of two tandem cGMP-binding pockets with low and high affinity to cGMP (Corbin et al., 1986). cGMP binding to both pockets releases the autoinhibitory effect of the NH_2-terminus, induces a conformational change of the enzyme, and, thus, permits phosphorylation of target proteins by the cGKs.

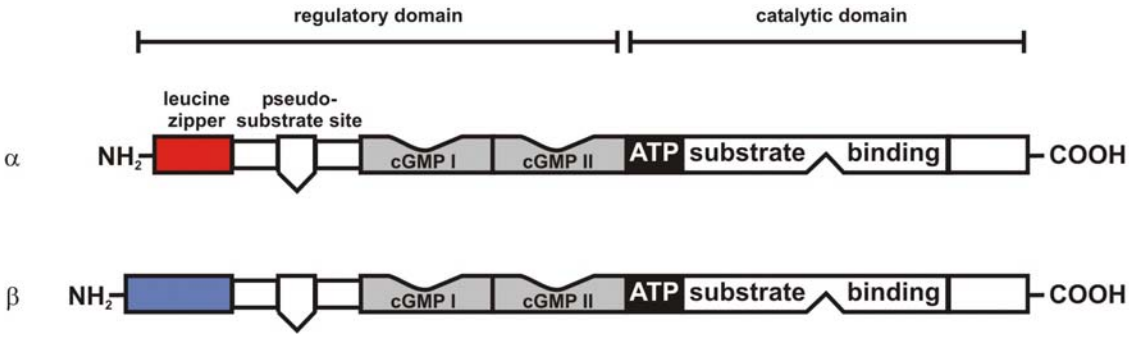

Fig. 2: Schematic domain structure of the cGMP-dependent protein kinase type I monomer. Structurally, the Iα and Iβ isoforms only differ in their approximately 100 NH_2-terminal amino acids (red and blue rectangle). Both isoforms are products of the same gene, *prkg1,* generated by the use of two alternative promoters. Further explanations in the text (modified from (Kleppisch, 1999)).

Besides these structural similarities of cGKI and cGKII, the kinases differ in their tissue distribution, subcellular localization, and their specific functions (Hofmann et al., 2000).

The type II cGK is anchored at the plasma membrane by an amino terminal myristoylation moiety. High concentrations of cGKII were found in chondrocytes, juxtaglomerular kidney cells, epithelial mucosa of the intestine, lung and the brain (El-Husseini et al., 1999; Gambaryan et al., 1996; Markert et al., 1995). The cGKII-deficient mice develop intestinal secretory defects, and, as a consequence of abnormal bone growth, a characteristic dwarfism (Pfeifer et al., 1996). The intestinal chloride and water secretion was stimulated by cGKII phosphorylation of the cystic fibrosis transmembrane conductance regulator (CFTR) ion channel (Vaandrager et al., 1998). In addition, the cGKII-deficient mice showed increased renin secretion (Wagner et al., 1998).

cGKI activity was first described in the rat cerebellum (Hofmann and Sold, 1972). Subsequently, expression of the cGKI protein was demonstrated in diverse mammalian tissues indicating its relevance as a major cGMP effector in different tissues. In the

cardiovascular system expression of the cytoplasmatic cGKI enzyme was found in platelets (Waldmann et al., 1986), in visceral and vascular SMCs (Keilbach et al., 1992), in the vascular endothelium (Draijer et al., 1995), in monocytes and monocyte-derived macrophages (Pryzwansky et al., 1995), in neutrophils (Werner et al., 2005), in the heart (Kumar et al., 1999), and kidney (Joyce et al., 1986). In the nervous system cGKI was localized in dorsal root ganglia (Qian et al., 1996), in neuromuscular endplates (Chao et al., 1997), in Purkinje neurons of the cerebellum (Lohmann et al., 1981), and in the hippocampus (Kleppisch et al., 1999; Kleppisch et al., 2003). Recently, it was shown that cGKI is broadly expressed in a number of additional brain regions (e.g. medulla, amygdala) and the retina (Feil et al., 2005c).

1.2.1 Function of the cGKIα/β isoenzymes

In the cardiovascular and nervous system increased cGMP concentration leads, at least in part, to the activation of the cGKIα/β isoenzymes, which mediate several effects of both NO and NPs. The Iα enzyme is expressed predominantly in the heart, lung, and cerebellum, whereas the cGKIβ is the major isoform in hippocampal neurons, the olfactory bulb, and platelets. Both isoforms are expressed in SMCs (Geiselhoringer et al., 2004; Keilbach et al., 1992). Here, only some of the cellular functions of the cGKIα/β isoenzymes as mediators of the NO-cGMP-cGKI pathway will be discussed briefly.

Using knockout mice it has been shown that cGKI mediates inhibitory effects on platelet aggregation *in vivo* (Massberg et al., 1999). Conversely, others demonstrated that cGKI stimulated the activation of platelets (Li et al., 2003b). In the isolated murine heart the negative inotropic effect of NO-cGMP was dependent on cGKI (Feil et al., 2003b; Wegener et al., 2002). In the nervous system cGKI was found to be involved in the sensitization of nociceptive neurons and distinct forms of synaptic plasticity and learning (Feil et al., 2003a; Feil et al., 2005b; Kleppisch et al., 1999; Kleppisch et al., 2003). Lessons from cGKI-deficient mice demonstrated that cGKI contributed to the cGMP-dependent relaxation of blood vessels, and, therefore, might play an important role in the regulation of blood pressure (Koeppen et al., 2004; Pfeifer et al., 1998; Sausbier et al., 2000). In particular, the cGKI activation was shown to interfere with the vasoconstrictory signaling that leads to an increase of intracellular Ca^{2+} concentrations ($[Ca^{2+}]_i$) in SMCs (Munzel et al., 2003).

Contraction and relaxation of SMCs are regulated by the phosphorylation and dephosphorylation of myosin regulatory light chain (RLC) by the Ca^{2+}-CaM dependent myosin light chain kinase (MLCK) and myosin light chain phosphatase (MLCP) (Fig. 3). MLCK induces phosphorylation of the RLC, which activates myosin ATPase to generate tension, whereas MLCP reverses the phosphorylation resulting in relaxation (Somlyo and Somlyo, 2003).

Ca^{2+}-dependent contraction is stimulated by binding of vasoactive agonists to G-protein-coupled receptors (GPCRs) that activate G_q and subsequently phospholipase C-β (PLC-β) to generate inositol 1,4,5-triphosphate (IP_3) (Demoliou-Mason, 1998). IP_3 mobilizes Ca^{2+} from intracellular stores by binding to the IP_3-receptor-I (IP_3RI). In addition, membrane depolarization opens voltage-dependent Ca^{2+}-channels resulting in Ca^{2+} influx (Karaki et al., 1997). As mentioned above, high Ca^{2+} concentrations activate the SMC Ca^{2+}-CaM dependent MLCK, which phosphorylates RLC leading to an increase in contractile force. Contraction of SMCs is also induced at constant Ca^{2+} concentrations by the Rho/Rho-kinase pathway. Phosphorylation of MLCP carried out by Rho-kinase inactivates the phosphatase, and, thus, increases the phosphorylation state of RLC.

Several potential mechanisms and targets for the cGMP-cGKI-dependent relaxation of smooth muscle (SM) have been identified that interfere with these pathways (Fig. 3):

(1.) cGKI can phosphorylate and activate the large conductance, voltage-dependent and Ca^{2+}-sensitive $BK_{Ca}{}^{2+}$-channel that contributes to the resting membrane potential of SMCs. Phosphorylation of the $BK_{Ca}{}^{2+}$-channel leads to a hyperpolarizing outward flux of K^+ from the cell, and, thus, inhibition of the Ca^{2+} entry via voltage-dependent Ca^{2+}-channels (Alioua et al., 1998; Fukao et al., 1999). (2.) At the endoplasmic reticulum (ER) of SMCs the cGKIβ isoform forms a trimeric complex together with the IP_3-receptor associated cGMP-kinase substrate (IRAG), and, presumably, the IP_3-receptor as well. cGKIβ-dependent phosphorylation of IRAG (Schlossmann et al., 2000), and/or the IP_3-receptor (Komalavilas and Lincoln, 1996) inhibits the agonist-induced Ca^{2+}-release from ER Ca^{2+}-stores. (3.) Ca^{2+}-independent inhibition of SMC contraction by cGKIα is mediated by the regulatory targeting subunit 1 (MYPT1) of MLCP. MYPT1 phosphorylation activates MLCP to dephosphorylate RLC (Surks et al., 1999; Wooldridge et al., 2004) resulting in Ca^{2+}-desensitation of SMC contraction, hence relaxation (Somlyo and Somlyo, 2003). (4.) cGKI-dependent phosphorylation of

PLC-β3 expressed in COS-7 cells blocked the activation of PLC by G-protein subunits. Whether this phosphorylation indeed inhibits G-protein mediated Ca^{2+}-release and contraction in SMCs *in vivo* is not clear (Xia et al., 2001). (5.) Recent evidence suggests that cGKIα directly phosphorylates the regulator of G-protein signaling-2 (RGS-2) (Tang et al., 2003). Phosphorylated RGS-2 increases the GTPase activity of G_q proteins by 100-1000 fold. Thereby, the half-live of GTP bound to G-proteins is significantly reduced, which attenuates the receptor-mediated vascular contraction induced by agonists (Hepler, 1999). (6.) cGKI-dependent phosphorylation of Rho was shown to interfere with the Rho/Rho-kinase pathway leading to relaxation (Murthy et al., 2003) (Fig. 3).

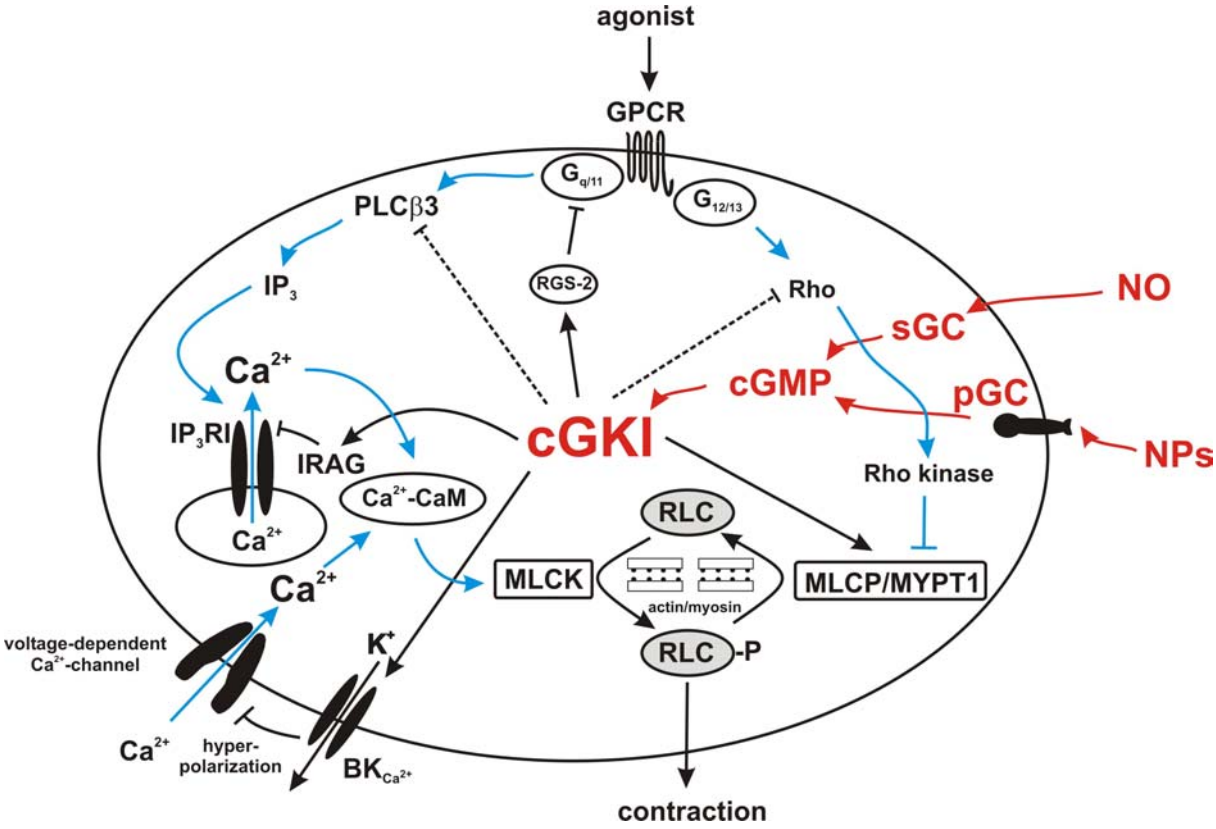

Fig. 3: SMC contraction pathways and cGMP-cGKI signaling leading to relaxation. Red lines point out pathways that lead to the activation of cGKI resulting in relaxation. Blue lines highlight pathways, which induce contraction of the SMC. Black lines are cellular targets that have been confirmed by *in vivo* studies. Dashed lines are pathways that have not been verified in intact SMCs. Abbreviations used are the same as in the text (modified from (Hofmann et al., 2006)).

1.2.2 The conventional cGKI knockout mice

To analyze the (patho-)physiological functions of cGKI *in vivo* a conventional knockout mouse line was generated. To ensure the disruption of both isoforms, the ATP-binding site, an identical region of Iα and Iβ, was deleted by gene targeting in embryonic stem cells. The cGKI mutants have multiple phenotypes and a reduced life expectancy. 50% of the mice die before 5-6 weeks of age. cGKI-deficient animals show a marked hypertrophy of the gastric fundus and pylorus, and severe disturbances of the gastrointestinal motility and relaxation of visceral SMCs. In the cardiovascular system cGKI knockouts do not show gross histological abnormalities, however, the cGKI ablation disrupts the NO-cGMP dependent relaxation of isolated aortic rings. Furthermore, platelet and immune function were disturbed in cGKI knockouts (Li et al., 2003b; Massberg et al., 1999; Ny et al., 2000; Persson et al., 2000; Pfeifer et al., 1998; Werner et al., 2005).

Taken together, the mutants with a chronic cGKI inactivation in every single cell throughout the development of the animal show multiple and severe defects. The analysis of the mice lacking cGKI is further complicated since it is difficult to discriminate whether an observed phenotype results from the primary deletion of cGKI in a given cell or arises secondary to defects in other cell types. Finally, conventional cGKI knockouts are inappropriate for long-term *in vivo* studies since most of them die before adulthood. To circumvent these limitations a mouse line was generated that allows the tissue-specific inactivation of the cGKI gene by using the Cre-loxP recombination technology (Wegener et al., 2002).

1.3 Conditional mutagenesis of genes using the Cre-loxP system in mice

The Cre-recombinase (cyclization recombination) is a 38 kDa protein derived from the P1 bacteriophage. Independent of any co-factors, Cre catalyzes the site-specific recombination between two of its loxP (locus of X-over of P1) consensus sequences. The actual outcome of a recombination event depends on the location and orientation of the loxP recognition sites. A chromosomal DNA segment flanked by two loxP sites in the same orientation (a *floxed* sequence) will be excised by Cre as a circular product with one loxP site remaining on the chromosome (Fig. 4). Other possible DNA rearrangements to modify the genome that can be

generated with the Cre-loxP system are inversions, integrations, and chromosomal translocations (not shown) (Nagy, 2000).

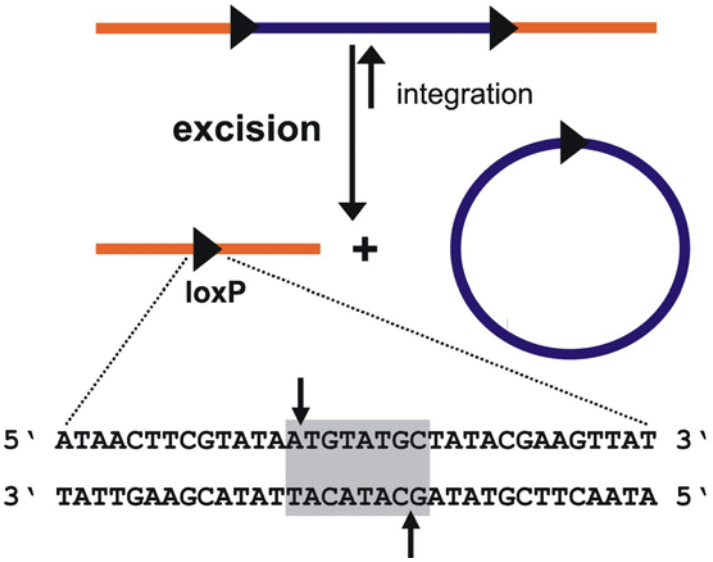

Fig. 4: Cre-loxP mediated excision and integration of DNA. The loxP recognition site consists of a core spacer sequence of 8 bp (gray) and two palindromic flanking sequences of 13 bp. Arrows indicate the phosphodiester bounds cleaved by Cre. Recombination between loxP sites in the same orientation results in excision of the flanked DNA segment. For kinetic reasons the intermolecular integration of the circular product is unfavorable as compared to the intramolecular excision process (modified from (Lukowski et al., 2005)).

About twenty years ago it became clear that the Cre-loxP system works in mammalian cells (Sauer and Henderson, 1988) and was effective in transgenic mice as well (Lakso et al., 1992; Orban et al., 1992). In particular in mouse genetics, the Cre-mediated excision of DNA segments was used as an important tool to generate conditional, i.e. cell- or tissue-specific, inactivations of selected genes. Using homologous recombination technology in embryonic stem cells the basic approach is to insert loxP sites into intronic gene sequences flanking an essential exon. This so called *floxed* version of the gene should be intact as the loxP sites do not interfere or disturb gene expression or alter the animal's phenotype (Metzger and Feil, 1999). To generate mice with a conditional inactivation of the *floxed* gene the *floxed* target mouse is crossed with a Cre transgenic mouse strain expressing the recombinase under control of a tissue-specific promoter (Fig. 5). In the offspring a Cre-mediated knockout is manifested in all cells that express or have expressed an active recombinase. The time-point

and cell type of Cre expression can be determined by the particular promoter selection. The conditional gene targeting strategy can overcome major limitations of a conventional knockout (Fig. 5). The permanent null-mutants with a gene knockout in all somatic cells often die during embryonic, or in case of the cGKI knockouts (Pfeifer et al., 1998), juvenile development, and have severe, complex phenotypes difficult to interpret. With the Cre-loxP system a mutant phenotype can be related to the specific cell type or tissue affected by the Cre-mediated recombination. The *floxed* cGKI mouse strain was generated recently (Wegener et al., 2002). These mice proofed to be an important tool to study the role of cGKI (Hofmann et al., 2006).

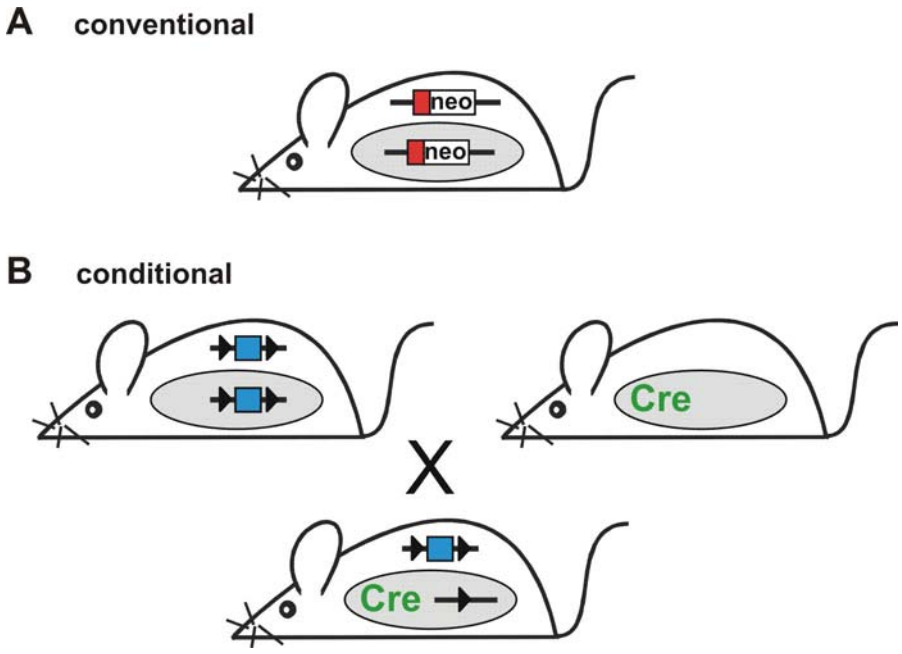

Fig. 5: Conventional and conditional deletion of mouse genes. (A) Permanent inactivation of genes by deletion of an essential exon (red rectangle) in the germ line using a neomycin (neo) resistance cassette. (B) Tissue-specific gene deletion. A target mouse with a floxed gene segment (essential exon, blue rectangle; loxP sites, black triangles) is crossed with a mouse expressing Cre recombinase under control of a tissue-specific promoter. Excision of the floxed exon is only manifested in cells with active promoter and Cre expression (gray ellipse) (modified from (Lukowski et al., 2005)).

1.4 Phenotypic modulation of smooth muscle cells

Vascular SMCs are among the most plastic cells of all mammalian cell types. The mature SMCs from the healthy vessel wall express a unique repertoire of contractile proteins (e.g. SM α-actin (α-SMA), SM22α, SM myosin heavy chain), cellular receptors, ion channels, and signaling molecules required for its contractile function. Under physiological conditions SMCs contribute to the regulation of vessel tone and blood pressure. However, in response to vascular injury or during *in vitro* culture SMCs switch from the differentiated contractile to an undifferentiated synthetic state (Berk, 2001; Owens et al., 2004). Being reversible, this process is characterized by a loss of contractile abilities and proteins, and an increase in proliferation rates, cell migration, and synthetic capacity of the cell. This phenotypic modulation, which is in general defined as a change in the normal structure and function of mature SMCs, plays an important role in the development and progression of vascular diseases, such as atherosclerosis, postangioplasty restenosis, vein graft disease, and transplant vasculopathy (Ferns and Avades, 2000).

1.4.1 Atherosclerosis versus restenosis

Atherosclerosis is a disease of large and medium-sized elastic and muscular arteries, including the aorta, the carotid and coronary arteries. Advanced atherosclerotic lesions or acute plaque rupture cause ischemia of the heart, brain, or extremities, resulting in infarction (Ross, 1999). Indeed, atherosclerosis is the principal cause of death in Western societies (Glass and Witztum, 2001; Lusis, 2000). It is characterized by an accumulation of lipids and fibrous elements in the vessel wall. Its progression involves many exogenous and endogenous factors, for example hypertension, elevated levels of lipoproteins, diabetes mellitus, gender (male), age, and smoking (Lusis, 2000). Proliferation of SMCs, endothelial dysfunction, circulating and tissue inflammatory cells, platelets, and matrix alterations contribute to plaque formation and remodeling of the vessel. The disease progresses by a series of characteristic changes in the vessel:

(1.) In the initial stage endothelial dysfunction and fatty-streak formation are observed. Typical changes are an increase in permeability of the endothelium for lipoproteins and other plasma components, such as prostacyclins, platelet-derived growth factor, accompanied by an up-regulation of vascular adhesion molecules. Initially, monocytes transmigrate across the

endothelial monolayer. The monocytes proliferate, differentiate into macrophages, and take up deposited lipoproteins, thereby, forming foam cells. (2.) Fatty streaks can progress to complicated and advanced lesions of artherosclerosis. The foam cells die and contribute to its necrotic core. SMCs are stimulated by secreted growth factors and cytokines to proliferate and migrate from the medial layer into the plaque. A fibrous cap develops, consisting of leukocytes, lipids, scattered SMCs and cell debris. While the lesion expands, inflammatory processes become apparent. (3.) In this stage vulnerable fibrous lesions are observed, which can result in plaque rupture. Inhibited matrix deposition, secretion of proteinases, and other proteolytic enzymes produced by plaque cells usually lead to thinning and finally rupture of the cap. The stability of the lesion might also be influenced by calcification. Rupture induces extensive thrombus formation (Dzau et al., 2002; Glass and Witztum, 2001; Lusis, 2000; Ross, 1999). Usually, mice are extremely resistant to the development of atherosclerosis. To overcome these limitations a murine model of apolipoprotein E (apoE) deficiency combined with a high-fat, high-cholesterol diet was generated. The combination of these genetic and nutritional manipulations results in greatly increased plasma cholesterol levels and severe atherosclerotic disease that has many features in common with plaque formation in humans (Zhang et al., 1992).

As mentioned above, occlusion of coronary arteries results from complex atherosclerotic lesions or plaque rupture (Ross, 1999). In the clinic, a common therapy to restore the blood flow in such narrowed arteries is angioplasty. However, every endovascular intervention may lead to a long-term risk of restenosis. Although, intra-vascular stents placed into coronary arteries significantly reduce the rate of restenosis, many patients still develop restenosis (Ferns and Avades, 2000). While atherosclerosis in humans develops slowly over many years, restenosis occurs within months after surgery. Additionally, vascular remodeling in restenosis usually does not involve the accumulation of lipids (Wang and Paigen, 2002). The exact pathophysiology of restenosis is unclear, although it is known that after the initial injury, SMCs contribute together with other vascular cell types to the remodeling and finally re-closure of a treated vessel. Restenosis of vessels has been studied in different experimental animal models, including rabbits, pigs, and rodents (Xu, 2004). Major differences in these models are the size of the artery injured, the susceptibility of the vessel to atherosclerosis induction before experimental injury, and the precise technique of injury-induction (Ferns and

Avades, 2000; Post et al., 1995). The commonly used model of restenosis in rats and rabbits is the balloon dilatation of the carotid arteries. However, this model is not practical in mice due to the extremely small diameter of the carotid artery. In mice several other vascular injury models have been established, such as the wire injury (Lindner et al., 1993), the carotid ligation (Kumar and Lindner, 1997), the perivascular electronic injury (Carmeliet et al., 1997), and the perivascular collar model (Moroi et al., 1998).

1.4.2 The NO-cGMP-cGKI pathway in vascular remodeling

In addition to the potent vasodilatory properties of NO, bioavailability and signaling of NO has also been related to vascular diseases (Barbato and Tzeng, 2004; Channon et al., 2000; Li and Forstermann, 2000), such as atherosclerosis (Lloyd-Jones and Bloch, 1996) and restenosis (Janssens et al., 1998; Varenne et al., 1998; von der Leyen et al., 1995; von der Thusen et al., 2004). Animal studies with transgenic mice that overexpress or lack the NO synthases indicated that NO can mediate beneficial effects on the vasculature under particular pathophysiological conditions (Kawashima et al., 2001; Knowles et al., 2000; Kuhlencordt et al., 2001b; Morishita et al., 2002; Moroi et al., 1998; Rudic et al., 1998). On the other hand, several studies reported that NO promoted the progression of vasculoproliferative processes, and, thus, that it was deleterious for the vasculature (Chyu et al., 1999; Detmers et al., 2000; Kuhlencordt et al., 2001a; Ozaki et al., 2002). This concept of bivalent functions of NO, even in the same biological setting, complicates the definition of its exact role in different pathophysiological situations (Wink et al., 2000).

cGKI was implicated as a main effector of the NO-cGMP pathway influencing the phenotypic modulation of SMCs (Brophy et al., 2002; Lincoln et al., 2001), which occurs in atherosclerosis and restenosis or during *in vitro* culture whilst SMCs switch from the contractile to a synthetic stage (Owens et al., 2004). Several studies (Boerth et al., 1997; Chiche et al., 1998; Garg and Hassid, 1989) suggested that cGKI has anti-mitogenic effects on SMCs *in vitro*, and, thus, might have a vasculo-protective potential *in vivo* (Anderson et al., 2000; Sinnaeve et al., 2002). Novel genetic evidence from the analysis of transgenic mice demonstrated that activation of SMC cGKI increases the growth of primary SMCs *in vitro* and promotes lesion formation in an apoE-deficient mouse model of hyperlipidemia-induced atherosclerosis (Wolfsgruber et al., 2003). These results oppose the common view

of a vasculo-protective role of cGKI and emphasize a proatherogenic potential of SMC cGKI (Feil et al., 2005a).

Recent data suggested that cGMP levels elevated by the PDE-5 inhibitor sildenafil were beneficial for the treatment of hypertrophic heart disease (Takimoto et al., 2005) and the vascular remodeling associated with pulmonary hypertension (Zhao et al., 2001). Activation of cGKI might mediate these inhibitory effects of sildenafil *in vivo* (Mendelsohn, 2005).

The role of the cGMP-cGKI signaling pathway in restenosis as well as the effect of cGMP-elevating drugs like sildenafil on its progression have not been clearly identified.

1.5 Aim of the work

In the present study, the functional role of SMC cGMP-cGKI signaling was examined in a mouse model of restenosis. It was hypothesized that the cGMP-cGKI pathway could mediate either the protective or deleterious effects that have been attributed to NO in restenosis. Since the reduced life expectancy of the conventional cGKI knockout mice made them inappropriate for long-term *in vivo* studies, the Cre-loxP system was used to generate a conditional deletion of cGKI in cardiomyocytes and SMCs. An established model of mechanical vascular injury resembling restenosis in humans (Kumar and Lindner, 1997) was used to study the remodeling in cGKI mutants and controls. Vascular remodeling was analyzed by morphometry and immunohistochemistry at different time points after injury induction in a normolipidemic situation as well as on an apoE-deficient background. In addition, a pharmacologic approach was used to chronically activate the cGMP-cGKI pathway in wild-type mice. To further characterize the NO-cGMP-cGKI and NP-cGMP-cGKI signaling in the vessel wall, additional *in vitro* studies were performed with primary wild-type and cGKI knockout SMCs.

2 MATERIAL AND METHODS

If not mentioned otherwise, all chemicals and drugs were purchased from Sigma Aldrich (München, Germany), Roth (Karlsruhe, Germany), Roche (Penzberg, Germany), Invitrogen (Karlsruhe, Germany), and Amersham (Freiburg, Germany). Sildenafil (Viagra®) was from Pfizer (Karlsruhe, Germany). Surgical instruments were purchased from Fine Science Tools (Heidelberg, Germany), suture devices were from Ethicon (Norderstedt, Germany).

2.1 Experimental animals

2.1.1 Animal welfare

All animals were maintained and bred in the animal facility of the Institut für Pharmakologie und Toxikologie, Technische Universität München. Experimental procedures were conducted according to the local government's committee on animal care and welfare in München. Mice were maintained at a 12-h light, 12-h dark cycle in type II (5 adult mice) or type III (12 adult mice) Makrolon cages. Environmental necessities of the laboratory animals were fulfilled by Nestlets as nesting material (Emsicon) and small shredded woodchip particles for bedding (Altromin). Drinking water was provided together with normal chow ad libidum. In general, adult females aged 6-20 weeks were used for breeding. Up to two sexually mature females were mated with one reproductive male (at least 9 weeks old). Tail biopsy DNA of 10- to 14-day-old offspring was used for genotyping by PCR (2.2.1). With 3-4 weeks male and female pubs were separated at weaning.

2.1.2 Transgenic mouse lines

For experiments, mice on a mixed 129Sv/C57BL6 genetic background were used. Genotyping of all animals was carried out as described (Holtwick et al., 2002; Soriano, 1999; Wegener et al., 2002). For genotyping of the apoE gene, protocols recommended by The Jackson Laboratory (Bar Harbor, ME) were used.

2.1.2.1 Floxed cGKI (cGKI$^{L2/L2}$) mice

Mice carrying the loxP-flanked essential exon 10 (L2) coding for the kinase activity of cGKI or the recombined, thus, knockout (L-) cGKI allele (Wegener et al., 2002) were described previously.

2.1.2.2 SM22α-Cre recombinase mice

The transgenic SM22α-Cre mice expressing Cre under control of the smooth muscle SM22α promoter fragment were described earlier (Holtwick et al., 2002).

2.1.2.3 ROSA26 Cre reporter mice

The ROSA26 Cre reporter (R26R) mouse strain (Soriano, 1999) was obtained from The Jackson Laboratory. LacZ expression in the R26R mouse strain is conditional. Only after Cre mediated excision of an intervening *floxed* DNA segment lacZ can be expressed. For recombination analysis, the transgenic SM22α-Cre mice (Holtwick et al., 2002) were crossed with heterozygous R26R mice. Tissue of adult offspring was stained with X-Gal for lacZ activity.

2.1.2.4 Apolipoprotein E-deficient (apoE$^{-/-}$) mice

The apolipoprotein E-deficient (apoE$^{-/-}$) mice (Piedrahita et al., 1992; Zhang et al., 1992) were obtained from The Jackson Laboratory. Mice lacking apoE have high plasma cholesterol levels and develop spontaneous artherosclerotic lesions.

2.1.2.5 Cardiac and smooth muscle cGKI knockout mice (cGKI^{csmko})

To generate offspring with a conditional knockout of cGKI in cardiac and smooth muscle cells (cGKI^{csmko}; genotype SM22α-Cre$^{tg/+}$, cGKI$^{L-/L2}$), and littermate controls (ctr; genotype SM22α-Cre$^{tg/+}$, cGKI$^{+/L2}$), the mice with modified cGKI alleles (cGKI$^{L2/L2}$) were crossed with SM22α-Cre mice heterozygous for cGKI (SM22α-Cre$^{tg/+}$, cGKI$^{L-/+}$). To generate cGKI^{csmko} and controls on an apoE-deficient genetic background (apoE$^{-/-}$), double transgenic (cGKI$^{L2/L2}$, apoE$^{-/-}$) animals were crossed with mice carrying SM22α-Cre$^{tg/+}$, cGKI$^{L-/+}$, and apoE$^{-/-}$.

2.1.3 Animal procedures

2.1.3.1 Carotid artery ligation

Reagents

8-0 nylon suture

1-2% Isoflurane (Forene) in oxygen

Anesthesia mixture

	[c]
Midazolamhydrochloride (Ratiopharm)	5 mg/ml
Medetomidin (Pfizer)	1 mg/ml
Fentanyldihydrogencitrate (Janssen-Cilag)	0.05 mg/ml

Anesthesia mixture (antagonists)

	[c]
Atipamezolhydrochloride (Pfizer)	5 mg/ml
Flumazenil (Roche)	0.1 mg/ml
Naloxonhydrochloride (Curamed Pharma)	0.4 mg/ml

Protocol

The experiments were performed with littermate male and female mice aged 6-18 weeks. Animals were deeply anesthetized with a mixture of Midazolam (Ratiopharm) (5 mg/kg), Medetomidin (Pfizer) (0.5 mg/kg), and Fentanyl (Janssen-Cilag) (0.05 mg/kg), which was injected intraperitoneally. The left common carotid artery was dissected by a midline incision in the neck and completely ligated proximal to its bifurcation with a 8-0 nylon suture. During the whole procedure, the animals received a continuous oxygen-isoflurane (1-2%) (Forene) inhalation. After surgery, the anesthesia was antagonized with Atipamezol (Pfizer) (2.5 mg/kg), Flumazenil (Roche) (0.5 mg/kg), and Naloxon (Curamed Pharma) (1.2 mg/kg). The animals were allowed to recover after surgery and showed no symptoms of a stroke. At 14 and 28 days (d) after the injury groups of animals were sacrificed and vascular remodeling was examined.

2.1.3.2 Chronic drug treatment

Reagents

Sildenafil citrate (Viagra®) 100 mg (Pfizer)

0.22 µm StericapPlus (Millipore)

0.2 µm Acrodisc Syringe (Pall)

Protocol

For PDE-5 inhibition, sildenafil citrate tablets (Pfizer) were used. Tablets were grounded into powder and dissolved in tap water at a final concentration of 0.2 mg/ml. The solution was filtered twice with a 0.22 µm StericapPlus (Millipore) and a 0.2 µm Acrodisc Syringe (Pall) filter, then stored at room temperature. This solution was administrated orally and substituted for the drinking water beginning from the day of surgery, whereas a control group received untreated water. The water intake was constantly monitored by weighing the bottle to assure a final drug dose of approximately 50 $mg \cdot kg^{-1} \cdot d^{-1}$. For cGMP measurements (2.2.3), mice were chronically treated for 14 d with sildenafil, whilst the morphometric analysis was done after 28 d (2.2.5).

2.2 Analysis of experimental animals

2.2.1 Genotyping

2.2.1.1 Tail tip biopsy

Reagents

1 M Tris-Cl pH 8.0

	MW [g/mol]	1 l	[c]
Tris-Cl	121.14	121.14 g	1 M
Adjust pH to 8.0 with HCl. Add ddH_2O to 1 l.			

0.5 M EDTA pH 8.0

	MW [g/mol]	1 l	[c]
$Na_2EDTA \bullet 2H_2O$	372.24	186.10 g	0.5 M
Adjust pH to 8.0 with NaOH. Add ddH_2O to 1 l.			

10x TE buffer

	0.5 l	[c]
1 M Tris-Cl pH 8.0	50 ml	0.1 M
0.5 M EDTA pH 8.0	10 ml	10 mM
Add ddH_2O to 500 ml.		

Proteinase K (PK) 50 mg/ml in 1x TE buffer

10x Taq DNA Polymerase buffer (Promega)

PK working solution

	50 µl	[c]
PK (50 mg/ml) in 1xTE buffer	1 µl	1 mg/ml
10x Taq DNA Polymerase buffer	5 µl	1x
ddH_2O	45 µl	-

Protocol

For genotyping 2 mm of mouse tail tip biopsy material from 10-14 d old animals was used. Tips were incubated over night at 55°C in 50 µl proteinase K (PK) buffer containing 1 mg/ml PK. Next, samples were centrifuged at 18000 xg for 1 min at room temperature (RT). The supernatant was transferred into a clean polymerase chain reaction (PCR) test tube. Remaining PK activity was inactivated by heating the samples to 95°C for 15 min. In general, the DNA solution was stored at –20°C until the genotyping PCR was performed on 1 µl of the samples (2.2.1.2).

2.2.1.2 Polymerase chain reaction (PCR)

Reagents

1 M KCl

	MW [g/mol]	1 l	[c]
KCl	74.56	74.56 g	1 M
Add ddH_2O to 1 l.			

1 M $MgCl_2$

	MW [g/mol]	0.1 l	[c]
$MgCl_2 \bullet 6H_2O$	203.30	20.3 g	1 M
Add ddH_2O to 100 ml.			

10x PCR buffer

	stock	10 ml	[c]
Tris-Cl pH 8.0	1 M	1 ml	100 mM
$MgCl_2 \bullet 6H_2O$	1 M	0.15 ml	15 mM
KCl	1 M	5 ml	500 mM
dNTPs	100 mM	0.2 ml each	2 mM (each)
Add ddH_2O to 10 ml.			

Taq DNA polymerase (Promega) (5 U/µl)

Protocol

The PCR is an enzymatically method to amplify defined DNA sequences *in vitro*. Components necessary for the DNA duplication are template DNA, large quantities of the four deoxynucleotide triphosphates (dNTPs), excess of primer, and a DNA polymerase. Here, the thermo stable Taq polymerase that was isolated from *Thermus aquaticus*

(Promega), was used. The PCR itself is a cyclic process and involves three steps carried out in the same test tube at different temperatures:

(1.) Denaturation - During this initial step the DNA chains of the double helix are separated at 94°C. (2.) Annealing - Sequence specific binding of the primers to the template DNA at 50°C-65°C. (3.) Elongation - Taq polymerase adds nucleotides to the primer and eventually makes a complementary copy of the template DNA at 72°C. Ideally, at the end of a cycle each template DNA strand in the tube has been duplicated once. Therefore, the DNA sequence flanked by the primer pair will accumulate selectively.

The PCR method was used on DNA isolated from tail biopsies for the genotyping of animals, and on DNA isolated from different organs for the analysis of SM22α-Cre mediated recombination of the *floxed* cGKI gene.

Standard PCR reaction mixture:

	stock	25 µl
Primer A	25 µM	0.25 µl
Primer B	25 µM	0.25 µl
Primer C	25 µM	0.25 µl
PCR buffer	10x	2.50 µl
Taq DNA polymerase	5 U/µl	0.25 µl
ddH_2O	-	20.5 µl
DNA (tissue or tail biopsy material)	100 ng/ml	1 µl

As template DNA for genotyping, genomic DNA (100 ng/ml) isolated from different tissues (2.2.2.1), and tail biopsy material were used (2.2.1.1). Primer (A, B, C), 10x PCR buffer, Taq DNA polymerase, and water were calculated for all samples of a reaction and combined to make a PCR master mix. 24 µl of the mixture were used together with 1 µl of DNA for the amplification. These standard quantities were varied slightly to improve the quality of the subsequent PCR.

Standard conditions for the amplification:

Initial denaturation	5 min, 94°C	
Denaturation	15 sec, 94°C	35x
Annealing	30 sec, 55°C	
Elongation	30 sec, 72°C	
Final elongation	5 min, 72°C	

These standard conditions were varied slightly depending on the size of the amplicon and the primer pairs used. Amplification was performed in a Biometra Thermocycler.

2.2.1.3 Agarose gel electrophoresis

Reagents

Ethidium bromide solution (10 mg/ml)

SeaKem LE Agarose (Biozym)

Bromphenol blue

	10 ml	[c]
Bromphenol blue	0.5 g	50 mg/ml
Add ddH_2O to 10 ml.		

Xylencyanol FF

	10 ml	[c]
Xylencyanol FF	0.5 g	50 mg/ml
Add ddH_2O to 10 ml.		

6x DNA loading dye

	stock	100 ml	[c]
Ficoll type 400	-	18 g	18%
EDTA, pH 8.0	0.5 M	24 ml	0.12 M
10x TBE	10x	60 ml	6x
Bromphenol blue	50 mg/ml	3 ml	0.15%
Xylencyanol FF	50 mg/ml	3 ml	0.15%
Add ddH_2O to 100 ml.			

10x TBE gel buffer

	MW [g/mol]	1 l	[c]
Tris-Cl	121.14	107.78 g	0.9 M
$Na_2EDTA \bullet 2H_2O$	372.24	7.44 g	20 mM
Boric acid	61.83	55.0 g	0.9 M
Add ddH_2O to 1 l.			

DNA electrophoresis standard

	6 ml
1 kb DNA ladder (1 µg/µl)	100 µl
6x DNA loading dye	1 ml
10x TE buffer	0.6 ml
Add ddH_2O to 6 ml.	

Protocol

DNA can be separated for analytic or preparative purposes by horizontal agarose gel electrophoresis. Negatively charged DNA will migrate in the electric field towards the positive electrode. Fragments of linear DNA migrate through agarose gels with a mobility that is inversely proportional to the $\log_{10}$ of their molecular weight. By using gels with different concentrations of agarose, one can separate DNA of different sizes. Higher agarose

concentrations facilitate the separation of small DNA fragments. For visualization of the fragments within the gel the fluorescent dye ethidium bromide can be incorporated into the gel, or added to the DNA samples before loading. Binding of the intercalating agent to DNA can be detected by UV light. A 1 kb DNA ladder of mixed DNA fragments of known size is used as a electrophoresis standard. The size of a DNA fragment that was separated is determined by its relative position in comparison to the ladder.

PCR fragments of tissues (2.2.2.1) and tail biopsy (2.2.1.1) DNA were diluted in 6x loading dye. In general, the agarose concentration in the gel was 1-2% (w/v) in 1x TBE gel buffer. Gel solutions were heated in a microwave oven before ethidium bromide was added (final concentration was 500 ng/ml). The electrophoresis was done in 1x TBE buffer at 150 V for 30 min depending on the size of the separated fragments.

2.2.2 Recombination analysis of the floxed cGKI gene

2.2.2.1 DNA isolation from mouse tissue

Reagents

DNA lysis buffer

	stock	50 ml	[c]
Tris-Cl, pH 7.4	1 M	2.5 ml	50 mM
EDTA, pH 8.0	0.5 M	0.5 ml	5 mM
SDS	10%	5.0 ml	1%
NaCl	5 M	2.0 ml	0.2 M
PK	50 mg/ml	0.5 ml	0.5 mg/ml
Add ddH_2O to 50 ml.			

1x PBS, pH 7.4

	MW [g/mol]	1 l	[c]
NaCl	58.44	8.00 g	135 mM
KCl	74.56	0.20 g	3 mM
$Na_2HPO_4 \bullet 2H_2O$	177.99	1.44 g	8 mM
KH_2PO_4	136.09	0.24 g	2 mM
Dissolve in 0.8 l ddH_2O and adjust pH to 7.4 with HCl. Add ddH_2O to 1 l.			

99% Trichloromethane p.a.

Roti-Phenol

100% Ethanol p.a.

Protocol

Tissue from adult experimental animals was collected, washed in ice cold 1x phosphate-buffered saline (PBS), frozen on liquid nitrogen, and stored at –80°C. For the DNA isolation, samples were incubated in 400 µl DNA lysis buffer at 55°C over night. After incubation, samples were centrifuged at 18000 xg for 1 min at RT. DNA was extracted by adding 1 volume of 400 µl phenol-chloroform (1:1) to the supernatant. Samples were vortexed and centrifuged at 18000 xg. DNA from the aqueous upper phase was precipitated at -20°C for 1 h with 2 volumes of 100% ethanol. Precipitated DNA was sedimented at 18000 xg for 10 min, then the pellet was washed carefully with 70% ethanol, and again centrifuged for 5 min at 18000 xg. DNA was dissolved in 50 µl ddH_2O after remaining traces of ethanol were allowed to evaporate at 37°C. The DNA solutions were stored at –20°C until further analysis. A 1:100 dilution of the concentrated samples in ddH_2O was used for the photometric DNA quantification (2.2.2.2). Eventually, the DNA was diluted to 100 ng/µl. PCRs were performed on 100 ng DNA with specific primer pairs to detect the L2, L- and wild-type allele of the cGKI gene locus.

2.2.2.2 Quantification of nucleic acids

Nucleic acids were quantified by standard UV photometry. The optical density (OD) measurements were performed at 260 nm (nucleic acids) and 280 nm (proteins). For the measurements a quartz cuvette of 1 cm thickness was used. Under these conditions a DNA solution containing 50 µg/ml corresponds to an OD of 1. The purity of a sample was determined by calculating the ratio of its absorbance at 260 nm versus 280 nm (OD_{260}/OD_{280}). For double stranded DNA this ratio should be >1.8.

The final concentration for a DNA sample was calculated as follows:

[DNA [µg/µl] = (50 µg/ml x OD_{260} x dilution factor)/1000]

2.2.2.3 Protein extraction from whole tissue

Reagents

1x PBS (2.2.2.1)

SDS lysis buffer

	stock	10 ml	[c]
Tris-Cl, pH 8.0	1 M	210 µl	21 mM
SDS	10%	670 µl	0.67%
2-mercaptoethanol	14.2 M	170 µl	238 mM
Phenylmethylsulphonylfluoride (PMSF)	100 mM	20 µl	0.2 mM
Add ddH_2O to 10 ml.			

Protocol

To analyze the cGKI expression in control animals and $cGKI^{csmko}$ mice whole protein was extracted from various mouse organs. Isolated organs were washed in ice cold 1x PBS and stored at –80°C until further usage. The frozen tissues were homogenized for 1 min in 1 ml SDS lysis buffer. To obtain the protein extracts, carotid arteries or aortas from six animals were pooled, whereas single hearts and cerebelli were used for the extraction. The homogenates were heated at 95°C for 10 min, then centrifuged for 5 min at 18000 xg and the supernatant was transferred to a clean test tube. After denaturation, proteins were stored at

–80°C until protein concentrations (2.2.2.4) were determined and Western blot (2.2.2.5) was performed.

2.2.2.4 Protein quantification assay after Lowry

Reagents

Micro Lowry Total protein kit (TP-0300):

Lowry reagent

0.15% (w/v) Deoxycholate solution

72% (w/v) Trichloroacetic acid solution

Folin-Ciocalteu's phenol reagent working solution

Bovine serum albumin (BSA) standard stock solutions (200 µg/ml, 100 µg/ml, 50 µg/ml, 25 µg/ml, 12.5 µg/ml)

Protocol

The Lowry method for determining protein concentrations is based on a biuret reaction that includes Folin-Ciocalteu's phenol reagent for an enhanced purple-color development. Proteins are treated with alkaline copper (Cu^{2+}) sulfate forming Cu^{2+}-protein complexes. These complexes reduce phospho-molybdic/phosphotungstic acid of the Folin–phenol reagent. The colorimetric protein determination is carried out at 750 nm. The protein concentration is determined from a BSA calibration curve.

BSA standard solutions were prepared from 200 µl BSA standard stock solutions (200 µg/ml, 100 µg/ml, 50 µg/ml, 25 µg/ml, 12.5 µg/ml), which were diluted with ddH_2O to a final volume of 1 ml. Protein samples were heated at 95°C for 5 min. For the quantification 2-30 µl denaturated extract were used and ddH_2O was added to a final volume of 1 ml. As a reference, an equal volume of lysis buffer was used in water. Blank samples (water only) were included in every assay. For precipitation, 100 µl deoxycholate (1.5 mg/ml) were added to each standard, blank, and sample. After mixing well, solutions were incubated for 10 min at RT. Next, 100 µl trichloroacetic acid solution (72%) were added and all tubes were mixed immediately. To precipitate the proteins a centrifugation step of 10 min at 18000 xg was carried out. The supernatant was discarded and the pellet dissolved in 200 µl Lowry reagent.

After adding 1 volume of ddH_2O, solutions were mixed well and incubated for 20 min at RT. Eventually, 100 µl Folin-Ciocalteu's phenol were added. Color developed within 30 min incubation at RT. Solutions were transferred to cuvettes and the absorbance was determined at a wavelength of 750 nm. Protein concentrations were calculated from the standard curve, which was plotted as absorbance values of the standards versus the corresponding concentration.

2.2.2.5 Western blot analysis

Reagents

4x Tris-Cl-SDS, pH 6.8

	MW [g/mol]	100 ml	[c]
Tris-Cl	121.14	6.05 g	0.5 M
SDS	288.38	0.4 g	0.4%
Add ddH_2O to 100 ml. Adjust pH with HCl.			

6x SDS sample buffer

	10 ml
4x Tris-Cl-SDS, pH 6.8	7 ml
Glycerol	3.6 g
SDS	1 g
1,4-Dithiothreit (DTT)	0.93 g
Bromphenol Blue	1.2 mg
Add ddH_2O to 10 ml.	

4x Tris-Cl-SDS, pH 8.8

	MW [g/mol]	100 ml	[c]
Tris-Cl	121.14	18.2 g	1.5 M
Sodium dodecyl sulfate (SDS)	288.38	0.4 g	0.4%
Add ddH_2O to 100 ml. Adjust pH with HCl.			

Separating gel

	8%	9%
30% acrylamide, 0.8% bisacrylamide solution	4 ml	4.5 ml
4x Tris-Cl-SDS, pH 8.8	3.75 ml	3.75 ml
ddH_2O	7.25 ml	6.75 ml
30% ammonium persulfate (APS)	50 µl	50 µl
N,N,N',N'-tetramethylethylenediamine (TEMED)	10 µl	10 µl

Stacking gel

30% acrylamide, 0.8% bisacrylamide solution	0.65 ml
4x Tris-Cl/SDS, pH 6.8	1.25 ml
ddH_2O	3.05 ml
30% APS	12.5 µl
TEMED	5 µl

10x SDS electrophoresis buffer

	MW [g/mol]	1 l	[c]
Tris-Cl	121.14	30.3 g	250 mM
Glycine	75.07	144.1 g	1.92 M
SDS	288.38	10.00 g	1%
Add ddH_2O to 1 l.			

Anode transfer buffer-I, pH 10.4

	MW [g/mol]	1 l	[c]
Tris-Cl	121.14	36.3 g	0.3 M
Methanol	100%	200 ml	20 %
Dissolve Tris-Cl in 800 ml ddH_2O and adjust pH to 10.4. Ad 200 ml methanol.			

Anode transfer buffer-II, pH 10.4

	MW [g/mol]	1 l	[c]
Tris-Cl	121.14	3.03 g	20 mM
Methanol	100%	200 ml	20 %
Dissolve Tris-Cl in 800 ml ddH_2O and adjust pH to 10.4. Ad 200 ml methanol.			

Cathode transfer buffer, pH 7.6

	MW [g/mol]	1 l	[c]
Tris-Cl	121.14	3.03 g	20 mM
6-Aminocaproic acid	131.18	5.2 g	40 mM
Methanol	100%	200 ml	20 %
Dissolve Tris-Cl in 800 ml ddH_2O and adjust pH to 7.6. Ad 200 ml methanol.			

10x TBS, pH 8.2

	MW [g/mol]	1 l	[c]
Tris-Cl	121.14	6.05 g	50 mM
NaCl	58.44	43.8 g	750 mM
Methanol	100%	200 ml	20 %
Dissolve Tris-Cl in 800 ml ddH_2O and adjust pH to 8.2. Ad 200 ml methanol.			

1x TBS-T (0.1% Tween)

10x TBS	50 ml
Tween20	0.5 ml
ddH_2O	add to 500 ml

1x TBS-T blocking solution (5% milk powder)

1x TBS-T	50 ml
Milk powder	2.5 g

1x TBS-T washing solution (1% milk powder)

1x TBS-T	50 ml
Milk powder	0.5 g

Molecular weight standards

See-Blue® (Invitrogen)

See-Blue Plus2® (Invitrogen)

Polyvinyliden difluoride (PVDF) membrane (Millipore)

ECL Western blotting analysis system (Amersham)

Detection reagent A

Detection reagent B

Protocol

By Western blot analysis a particular protein can be detected in a multi protein extract. Western blot technique was used to analyze the cGKI expression in different organs of experimental animals, and to investigate the cGMP-cGKI protein signaling machinery in extracts of primary vascular SMCs.

In general, samples of 10-30 µg protein were loaded on a gel. After quantification, the final concentration of the extracts was adjusted to 1-2 µg/µl protein in 2x SDS sample buffer. These solutions were made by diluting the extracts with 6x SDS sample buffer in ddH_2O. Alternatively, extracts of low protein content were concentrated using the Wessel-Flugge precipitation method (2.3.3) (Wessel and Flugge, 1984), then dissolved in 2x SDS sample buffer. In contrast, 1/15 (6-well plate) or 1/25 (10-cm culture dish) of the original protein extract isolated from primary SMCs culture was loaded on a gel after precipitation without prior protein quantification.

Before loading, the samples were heated at 95°C for 5 min. Proteins were separated by their molecular weight using denaturing SDS polyacrylamide gel (8-9%) electrophoresis. Next, the separated proteins were transferred (blotted) to a polyvinyliden difluoride (PVDF) membrane using a semi-dry transfer chamber. The transfer unit is composed of two closely spaced electrodes separated by filter papers, saturated with transfer buffer, including the gel and a PVDF membrane.

The setup of the blotting chamber was:

(1.) anode plate, (2.) 3x filter papers saturated with anode transfer buffer-I, (4.) 2x filter papers saturated with anode transfer buffer-II, (5.) PVDF membrane soaked in 100% methanol and saturated with anode transfer buffer-II, (6.) gel, (7.) 5x filter papers saturated with cathode transfer buffer, and (8.) cathode plate. The transfer was performed for 1 h at 50 mA for each gel.

Unspecific binding of the antibodies to the membrane was blocked with 5% milk powder in 1x TBS-T blocking solution for 1 h at RT. The membrane was then exposed sequentially to solutions containing the primary antibodies (over night at 4°C), followed by the horseradish peroxidase (HRP) conjugated secondary antibodies (RT for 45 min) diluted 1:2000 in 1.0% milk powder in 1x TBS-T. In between incubations with blocking-, primary-, and secondary-antibody solutions the membrane was regularly washed with three changes of 1.0% milk powder in 1x TBS-T. Before soaking of the membrane in the detection reagent to enable a color reaction, another washing was done with three changes of 1x TBS-T only. The enhanced chemiluminescent (ECL) method was used for detection of the antigen-antibody complexes. The detection is based on the peroxidase-catalyzed oxidation of the chemiluminescent substrate luminol. 1 ml of a 1:1 mixture of the detection solutions A and B was used for each membrane. Following exposure of the soaked membrane to a X-ray film the protein antigen was visualized as a band. A molecular weight standard containing proteins of known size provided information about the molecular weight of the protein.

2.2.3 Cyclic nucleotide measurements

Reagents

100% EtOH p.a.

EIA kit (Cayman Chemical)

Protocol

Cyclic nucleotides were extracted from homogenized hearts of control mice and mice treated with sildenafil (50 $mg \cdot kg^{-1} \cdot d^{-1}$) for 14 d (2.1.3.2). The hearts were homogenized in 1 ml ice-cold 100% EtOH for 1 min. Homogenates were centrifuged for 10 min at 18000 xg at RT, and then the supernatant containing the cyclic nucleotides was concentrated by evaporating the

alcohol in a speed vac for 3-4 h at RT. After evaporation, the final pellet was dissolved in 200 µl EIA-buffer provided in the EIA kit (Cayman Chemical). cGMP and cAMP concentrations were determined according to the manufactures recommendations using the standard protocol without acetylation.

Primary vascular SMCs were grown on a 10-cm culture dish to a confluency of 80-90% (2.3.1) then serum-starved for 48 h. The treatment with different drugs *in vitro* was carried out in Tyrode's solution (2.3.2) for 10 min. In general, serum-starved cells that were incubated in Tyrode's solution containing no drugs were included in every experiment as control. After stimulation, the cells were washed once in 1x PBS. For the extraction of cyclic nucleotides 1 ml ice-cold 100% EtOH was added per 10-cm SMCs culture dish. Using a cell scratcher, extracts were collected and transferred to test tubes. Samples were centrifuged for 10 min at 18000 xg. The supernatant was used for the cyclic nucleotides determination as described above, whereas the protein pellet was dissolved in 1.0 ml SDS lysis buffer and heated for 10 min at 95°C. The protein fraction was used for Western blot to investigate the cGMP-cGKI protein signaling machinery in SMCs after exposure to different drugs.

2.2.4 Histological methods

2.2.4.1 Paraffin sectioning of mouse tissue

Reagents

1x PBS, pH 7.4 (2.2.2.1)

Cellfix

	(w/v)	0.5 l	(v/v)
Formaldehyde solution	37%	27 ml	2%
Glutaraldehyde solution	25%	4 ml	0.2%
Add 1x PBS pH 7.4 to 0.5 l.			

Paraplast embedding medium

EtOH (50%, 60%, 70%, 80%, 90% 95% in ddH_2O, and 100%)

Toluol

Protocol

Experimental animals received a lethal dose of diethyl ether. The hearts were dissected by opening the chest with bone cutting scissors, which were passed through the sternum. To ensure the preservation of tissue architecture and cell morphology an in situ perfusion was performed using a 12-gauge needle inserted into the left ventricle. Perfusion fixation was carried out with cellfix for 10 min. The perfusate flow rate was adjusted to 1 ml/min by the use of a perfusion device. Tissue was isolated and rinsed in 1x PBS, then post-fixed in the same fixative for 1 h at RT. Next, the tissue was washed three times with 1x PBS for 1 h at RT each. The fixed and washed tissue was dehydrated successively in an alcohol series with increasing concentrations of EtOH. The incubation time was, if not otherwise mentioned 1 h: (1.) 50% EtOH, (2.) 60% EtOH, (3.) 70% EtOH, (4.) 80% EtOH, (5.) 90% EtOH, (6.) 95% EtOH, (7.) 3x 20 min 100% EtOH, (8.) 30 min EtOH (100%):Toluol 1:1, (9.) 3x 20 min Toluol. After dehydration, the tissue material was routinely passed trough 3 changes of liquid paraffin at 60°C in tissue processing cassettes for at least 1 h each. Finally, the material was embedded in freshly molten paraffin on an embedding system that combines cassettes and rings. The paraffin blocks were stored at RT until further processing. For histological analysis, serial sections of 6 μm thickness were cut, transferred to a clean water bath with distilled water, and mounted on poly-L-lysine coated slides. Before further applications the sections were allowed to dry at 37°C over night in an upright position in order to facilitate adhesion between sections and the charged glass surface. For immunohistochemistry (2.2.4.4) and hematoxylin and eosin (H&E) stainings (2.2.4.2) the slides were deparaffinized in toluol for 3x 10 min. Rehydration was carried out in an descending series of alcohol. (1.) 2x 5 min 100% EtOH, (2.) 5 min 95% EtOH, (3.) 5 min 90% EtOH, (4.) 5 min 70% EtOH, and (5.) 5 min 50% EtOH. Finally, sections were washed with tap water (2.2.4.2) or 1x PBS (2.2.4.4).

2.2.4.2 Hematoxylin and eosin (H&E) staining

Reagents

Hematoxylin after Harris (Roth)

Ammonia water

	stock	500 ml	[c]
Ammonia solution (NH_3)	32%	1.56 ml	0.1 %
Add ddH_2O to 0.5 l.			

100% acetic acid glacial p.a.

Acidic eosin Y (Sigma)

	stock	100 ml	[c]
Eosin Y aqueous solution	0.5%	20 ml	0.1 %
Add ddH_2O to 100 ml and acidify with 3 drops acetic acid.			

80% EtOH

DePex mounting medium (Serva)

Toluol

Protocol

For the hematoxylin and eosin (H&E) staining, fixed paraffin embedded 6 μm serial sections were rehydrated as described (2.2.4.1). Using this method the nuclei of cells were stained blue-black by the hematoxylin, whilst the cytoplasm was counterstained in red-pink by eosin. Slides washed in tap water were incubated for 10 s in hematoxylin after Harris, then washed again in two changes of tap water for 2 min each before the blue staining was developed by a short dip in ammonia water (0.1% ammonia hydroxide in ddH_2O). Next, sections were washed for 5 min in tap water and counterstained with acidic eosin (0.1% in ddH_2O) for 2-10 min followed by five rinses in tap water. The color was differentiated in 80% EtOH for a maximum of 1 min. Finally, the sections were dehydrated in 100% EtOH for 3 min and then passed through toluol for 5 min. Sections were mounted in DePex mounting medium.

2.2.4.3 5-Bromo-4-chloro-3-indolyl β–D-galactoside (X-Gal) staining

Reagents

1 µg/ml Hoechst No. 33258 (Sigma) in 80 % glycerol

X-Gal (5-Bromo-4-chloro-3-indolyl β–D-galactoside)

40 mg/ml in 100% dimethyl sulfoxide (DMSO)

X-Gal staining solution

	MW [g/mol]	500 ml	[c]
Potassium hexacyanoferrate (III)	329.26	0.83 g	2.5 mM
Potassium hexacyanoferrate (II) trihydrate	422.39	1.07 g	2.5 mM
$MgCl_2$ (1 M)	203.30	1.0 ml	2.0 mM
Ad X-Gal (1 mg/ml) to staining solution.			

Protocol

To examine the recombination pattern of the SM22α-Cre transgene, the SM22α-Cre mice were crossed with the R26R Cre reporter mouse strain. A β–galactosidase (β–gal) activity assay was used to visualize the Cre-mediated recombination events at the cellular level (Kuhbandner et al., 2000). Organs were isolated from perfusion fixed animals as described (2.2.4.1) including an additional staining step based on the β–gal activity. Precisely, the post-fixed material was incubated in a X-Gal (5-Bromo-4-chloro-3-indolyl β–D-galactoside) staining solution over night at RT followed by three changes of 1x PBS washing for 1 h each. Organs were dehydrated, paraffin embedded, and eventually cut in 6 µm sections. Whole-mount digital pictures were taken at the 70% EtOH dehydration step, whilst the rehydrated 6 µm sections were mounted in 80% glycerol containing 1 µg/ml Hoechst No. 33258, for the nuclei counterstain, and then photographed.

2.2.4.4 Immunohistochemistry

Reagents

1x PBS, pH 7.4 (2.2.2.1)

Permeabilization solution

	100 ml	[c]
Triton-X 100	0.3 ml	0.3%
Add 1x PBS pH 7.4 to 100 ml.		

Peroxidase blocking solution

	stock	10 ml	[c]
H_2O_2	30%	1 ml	3%
Methanol	100%	2 ml	20%
Add 1x PBS pH 7.4 to 10 ml.			

Antigen retrieval solution

	1 l	[c]
Tri-sodium citrate • $2H_2O$	2.94 g	10 mM
Adjust pH to 6.0 with HCl.		

Serum-PBS blocking solution

	50 ml	[c]
Normal goat serum (NGS)	750 µl	1.5%
Add 1x PBS pH 7.4 to 50 ml		

Biotinylated secondary antibody 1:200 in Serum-PBS blocking solution (6.3.2).

ABC-Solutions

Vectastain alkaline phosphatase (ABC-AP) standard kit (Vector Laboratories)

Vectastain peroxidase (ABC-Peroxidase) elite standard kit (Vector Laboratories)

	10 ml
Reagent A (Avidin DH)	100 µl
Reagent B (Biotinylated enzyme)	100 µl
Add 1x PBS pH 7.4 to 10 ml. Incubate 30 min before use in the dark.	

Reagent A and B are provided in the Vectastain alkaline phosphatase (ABC-AP) standard and Vectastain peroxidase (ABC-peroxidase) elite standard kit.

3,3´-diaminobenzidine tetrahydrochloride (DAB) stock solution

	50 ml	[c]
DAB	50 mg	0.1%
Add 1x PBS pH 7.4 to 50 ml.		

DAB staining solution

	stock	10 ml	[c]
DAB	0.1%	5 ml	0.05%
H_2O_2	30%	10 µl	0.03%
Add 1x PBS pH 7.4 to 10 ml.			

Alkaline phosphatase substrate III (Vector Laboratories)

	5 ml
Vector Blue substrate solution reagent 1	100 µl
Vector Blue substrate solution reagent 2	100 µl
Vector Blue substrate solution reagent 3	100 µl
1 M Tris-Cl pH 8.0	500 µl
Add ddH_2O to 5 ml.	

Aquatex mounting medium (VWR)

Protocol

Immunohistochemistry is the localization of protein antigens in tissue sections by the use of labeled antibodies. The antigen antibody complexes can be visualized by markers such as fluorescent dyes, enzymatic reporters, radioactive labeling, or colloidal gold attached to the antibodies used.

Here, using an indirect method, the localization of the primary antibody (6.3.1) antigen complexes was based on the successive application of (1.) biotinylated secondary antibodies (6.3.2), and (2.) avidin conjugated enzymes. (3.) For visualization, an enzyme-catalyzed chromogen reaction was carried out.

The sections were deparaffinized and rehydrated as described (2.2.4.1). To improve antibody penetration, a permeabilization step was included using 0.3% Triton-X in PBS for 30 min at RT followed by three washing steps in 1x PBS for 5 min each. For the detection based on the ABC-peroxidase reagent, a pretreatment of the slides was performed to inhibit endogenous tissue peroxidase activity. Therefore, sections were incubated in peroxidase blocking solution for 10 min. After the peroxidase block, the sections were washed with 1x PBS for 5 min, and, for some antibodies, an additional antigen retrieval based on sodium citrate was done. Next, all section were circled by a pap pen. To reduce unspecific binding of the antibodies, the sections were incubated for 1 h at RT in blocking solution containing 1.5% normal goat serum (NGS) in 1x PBS. The blocking solution was discarded and the primary

antibody was applied over night at 4°C in a humidified chamber (dilutions varied depending on the antibody (6.3.1)) followed by three washing steps in 1.5% NGS in 1x PBS for 5 min each. The appropriate biotinylated secondary antibodies (6.3.2) were diluted 1:200 in 1.5% NGS in PBS and applied for 45 min at RT. Unbound secondary antibodies were removed by three consecutive washes in 1x PBS 5 min each. The ABC-AP or ABC-peroxidase reagent was prepared by diluting reagent A and reagent B 1:100 in 1x PBS, respectively, and pre-incubated in the dark for 30 min before use. Sections were incubated in the dark with the ABC solutions for 30 min followed by 3 washing steps in 1x PBS 5 min each. Chromogens used to visualize the complexes were freshly prepared; 0.05% DAB in 1x PBS for the ABC-peroxidase and the Vector Blue substrate (Vector Laboratories) for the ABC-AP method. The ABC-AP substrate solution was prepared by diluting reagent 1, 2, and 3 provided with the alkaline phosphatase substrate kit 1:50 in 100 mM Tris-HCl (pH 8.0). Brown (DAB) or blue (Vector Blue substrate) staining was finished in 5 to 40 min depending on the antigen. Finally, sections were rinsed in ddH_2O and permanently covered in the Aquatex aqueous mounting medium (VWR) or in 1 µg/ml Hoechst 33258 (Sigma) in 80% Glycerol for the proliferating cell nuclear antigen (PCNA) stains.

2.2.5 Morphometric analysis

Evaluation of morphometric data was performed on the left carotid artery with the investigator being unaware of the genotype and/or drug treatment of the mice. Animals were perfused *in situ* via the left ventricle with formaldehyde (2%) and glutaraldehyde (0.2%) in 1x PBS. The arterial segment proximal to the bifurcation was excised, post-fixed for 1 hour, and embedded in paraffin as described (2.2.4.1). Starting from the ligation point used as reference, serial sections of 6 *µ*m thickness were obtained and H&E stained (2.2.4.2). In total, 30 H&E stained cross sections in 120 *µ*m intervals for each animal were included in the measurements. This procedure ensured the analysis of a representative vessel segment from the reference point at 0 mm to 3.6 mm of distance. Digital images of the H&E stained sections were analyzed by UTHSCSA ImageTool, version 3.0. The areas within the external elastic lamina (EEL), internal elastic lamina (IEL), and the lumen were determined by tracing their perimeter (Fig. 6). From these primary data all additional vessel parameters were calculated. In detail, the neointimal (NI) area was calculated by subtracting the luminal area

from the area defined by the IEL. By similar means the media was defined as the area between the IEL and the EEL. The degree of NI formation was expressed by the NI/media ratio. Taking all NI/media ratio measurements of the entire vessel into account, an individual mean value for each animal was calculated.

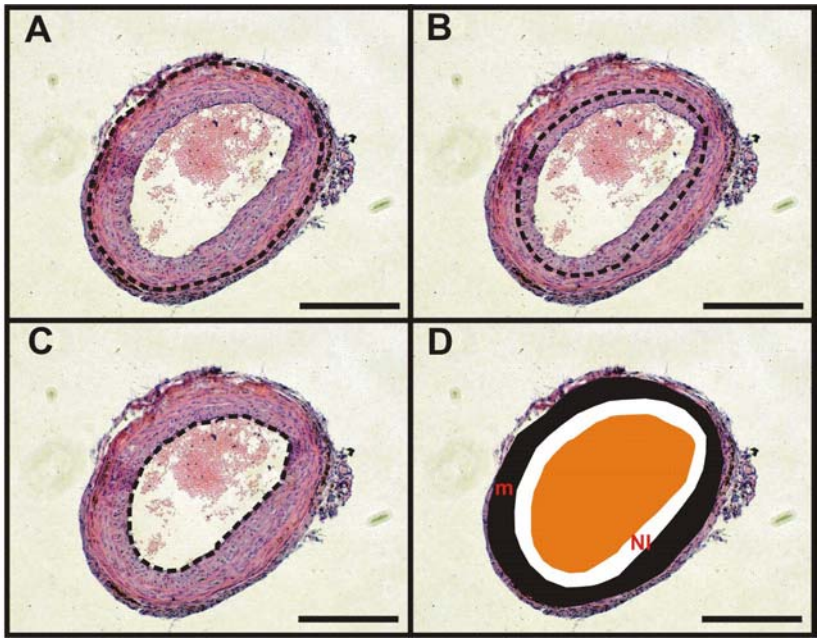

Fig. 6: Representative area measurements 28 d after ligation-induced injury of the CCA (A-D). The external elastic lamina (A), internal elastic lamina (B), and the lumen (C) were determined by tracing their perimeter (black broken lines). The UTHSCSA ImageTool program was used to estimate the corresponding areas inside the perimeters. From these primary data the media (m; black) and neointima (NI; white) were calculated (D). Further explanations in the text.

2.3 In vitro analysis of the cGMP-cGKI pathway in SMCs

2.3.1 Murine SMC culture

Reagents (SMC isolation)

0.2 µm Acrodisc Syringe filter (Pall)

Trypanblue solution 0.4%

Ca^{2+}-free medium

	MW [g/mol]	1 l	[c]
Na-glutamate	169.10	14.37 g	85.00 mM
NaCl	58.44	3.50 g	60.00 mM
HEPES	238.30	2.38 g	10.00 mM
KCl	74.56	0.42 g	5.60 mM
$MgCl_2 \bullet 6H_2O$	203.30	0.20 g	1.00 mM
Add ddH_2O to 1.0 l and adjust pH to 7.4 with 10 N NaOH.			

Enzyme stocks in Ca^{2+}-free medium

	[c]
Papain (Sigma)	7 mg/ml
Hyaluronidase type I-S (Sigma)	10 mg/ml
Collagenase type F (Sigma)	10 mg/ml

Bovine albumin fraction V (BSA) 100 mg/ml

1,4-Dithiothreit (DTT) 100 mg/ml

Enzyme working solutions

Solution A	[c]	Volume [µl]	Solution B	[c]	Volume [µl]
Papain	0.7 mg/ml	100	Hyaluronidase	1.0 mg/ml	100
BSA	1.0 mg/ml	10	Collagenase	1.0 mg/ml	100
DTT	1.0 mg/ml	10	BSA	1.0 mg/ml	10
Add Ca^{2+}-free medium to 1.0 ml.			Add Ca^{2+}-free medium to 1.0 ml.		

Reagents (SMC culture)

Dulbecco's modified Eagle's medium (DMEM) (Gibco)

4500 mg/l D-glucose

GlutaMAX-I

110 mg/l sodium pyruvate

Fetal calf serum (FCS) (Gibco)

Penicillin-streptomycin (Pen-strep) (Gibco)

10000 U/ml penicillin G

10000 µg/ml streptomycin

SMC complete medium

DMEM	500 ml
Pen-strep	5 ml
FCS	50 ml

SMC serum-free medium

DMEM	500 ml
Pen-strep	5 ml

Primary vascular SMCs were isolated from aortas of litter-matched wild-type (wt) and conventional cGKI-deficient ($cGKI^{L-/L-}$) mice aged approximately 3-5 weeks. The cells were cultured in SMC complete medium based on DMEM supplemented with 10% fetal calf serum (FCS), 100 U/ml penicillin, and 100 µg/ml streptomycin.

Protocol

Experimental animals received a lethal dose of diethyl ether. Aortas (aortic arch and descending aorta) were dissected and washed in 1x PBS. Using blunted forceps with atraumatic tips, the vessels were cleaned of adjacent fatty tissue and completely emptied of blood. Successive digestion of the aortas in solution A and B was performed at 37°C in a water bath. The amount of enzyme working solution needed for a maximum of eight aortas was 1 ml. Before digestion, the working solutions were filtered using a 0.2 µm Acrodisc

Syringe (Pall) filter and stored at 4°C. In general, pooled aortas were treated for 40-45 min in solution A by shaking them at regular intervals. After incubation, the aortas were centrifuged for 1 min at 300 xg. The supernatant was discarded and replaced by pre-warmed (37°C) solution B. The treatment of aortas in solution B did not exceed 10-20 min to prevent possible cell death induced by an enzymatic over digestion. Importantly, aortas were frequently mixed using a 1 ml pipette. In this manner the solution became turbid indicating a high quality and quantity of single SMCs. The enzymatic reaction was stopped by adding 10 ml of complete medium. Cells were then sedimented by centrifugation at 900 xrpm for 7 min and the resulting pellet was resuspended in an appropriate volume of freshly added complete medium (about 3 ml for 10 aortas yielding an approximate cell density of $1x10^6$ cells/ml). To determine the precise cell density counting was performed by the use of a haemocytometer. Using the trypanblue exclusion test, the proportion of viable cells was estimated. Therefore, an aliquot of the cell suspension was combined with trypanblue (final trypanblue dilution was 1:10). In general, $3x10^5$ cells were isolated from one particular aorta with an average viability of $>$95%.

The cells were grown in 6-well plates ($1x10^5$) or 10-cm culture dishes ($5x10^5$) in 3 ml or 10 ml complete medium, respectively, and maintained at 37°C and 6% CO_2 in humidified chambers. Regularly, the medium was aspirated on day three after the isolation procedure and exchanged by fresh SMC complete medium. Cells were grown to 80-90% confluence before serum withdrawal for the vasodilator-stimulated phosphoprotein (VASP) experiments (2.3.2) and cyclic nucleotide measurements (2.2.3).

2.3.2 VASP phosphorylation

Reagents

100% EtOH

Tyrode's solution

	MW [g/mol]	1 l	[c]
NaCl	58.44	8.18 g	140.00 mM
HEPES	238.30	1.19 g	5.00 mM
Glucose	180.2	1.80 g	10.00 mM
KCl (0.5 M)	74.56	10.00 ml	5.00 mM
$MgSO_4$ (0.12 M)	246.48	10.00 ml	1.20 mM
$CaCl_2$ (1 M)	147.02	2.00 ml	2.00 mM
Adjust pH to 7.4 with 6 N HCl. Add ddH_2O to 1.0 l.			

Drugs

	stock	dilution	[c]
8-Br-cGMP	100 mM in ddH_2O	1:100	1.0 mM
	10 mM in ddH_2O	1:100	0.1 mM
8-Br-cAMP	100 mM in ddH_2O	1:100	1.0 mM
	10 mM in ddH_2O	1:100	0.1 mM
ANP	100 µM in 1% AcOH	1:100	0.001 mM
CNP	100 µM in ddH_2O	1:100	0.001 mM
Sildenafil	1 mM in ddH_2O	1:10	0.1 mM
DEA-NO	100 mM in 10 mM NaOH	1:1000	0.1 mM
Drugs were diluted in an appropriate volume of Tyrode's solution or serum-free medium immediately before use.			

Protocol

To analyze VASP phosphorylation $1x10^5$ cells or $5x10^5$ cells were seeded in a 6-well chamber or 10-cm dish, respectively (2.3.1). The cells were grown to 80-90% confluence, then serum-starved for 48 h hours. Next, serum-free medium was removed and serum-starved-cells remained untreated in Tyrode's solution, as controls, or were stimulated in Tyrode's solution containing different drugs for 10 minutes at 37°C. Alternatively, serum-free medium instead of Tyrode's solution was used to dilute the drugs. In the latter case, stimulation with or without drugs (controls) was carried out for 30 min at 37°C. On 6-wells, 1.5 ml of the incubation solutions mentioned above were used for the treatment, whereas 5 ml were used on 10-cm dishes.

The stimulation was stopped by aspiration of the Tyrode's solution or serum-free medium after the time periods mentioned above. Aspiration was followed by one 1x PBS wash. After stimulation, 0.5 ml SDS-lysis buffer were added directly to the cells (6-well). The extracts were transferred to a clean 1.5 ml reaction tube and immediately heated to 95°C for 10 min. For extraction of cyclic nucleotides 1 ml ice-cold 100% EtOH was added per 10-cm SMCs culture dish as described (2.2.3). Finally, the protein fraction of 10-cm dishes was dissolved in 1.0 ml SDS-lysis buffer and heated to 95°C for 10 min as well.

Without prior quantification 150 µl of each protein extract was used for the Wessel-Flugge precipitation (Wessel and Flugge, 1984) (2.3.3) and further Western blot analysis (2.2.2.5). The NO-cGMP-cGKI and NP-cGMP-cGKI signaling machinery in SMCs after exposure to different drugs was analyzed by monitoring the phosphorylation of VASP, which has been described as a common target of cAK and cGKI (Eigenthaler et al., 1992).

2.3.3 Protein precipitation

Reagents

Methanol

99% Trichloromethane p.a.

6x SDS sample buffer (2.2.2.5)

Protocol

For concentration of protein extracts, a methanol- and chloroform-based precipitation method was used (Wessel and Flugge, 1984). The amount precipitated did not exceed 400 µg protein in a maximum volume of 150 µl. In general, 150 µl of the cell culture extracts were precipitated without prior quantification. In contrast, the precipitation of tissue lysates was only done after accurate quantification. Four volumes (600 µl) of methanol and 1 volume (150 µl) of chloroform were added to the sample and immediately vortexed. Next, three volumes of ddH_2O were added and the samples were vortexed again, then centrifuged at 18000 xg for 2 min. The upper phase was carefully removed without disturbing the proteins concentrated in the interphase. Again, three volumes (600 µl) of methanol were added. Finally, the samples were vortexed and centrifuged at 18000 xg for 2 min. After discarding the supernatant the pellet was air dried at RT for 5 min. The dried pellet was dissolved in an appropriate volume of 1x SDS sample buffer and heated at 95°C for 5 min.

2.4 Statistical analysis

The OriginPro-Software, version 6.1, was used for statistical analysis. Data are presented as mean±SEM. In order to compare groups an unpaired Student's *t*-test was used ($p<0.05$).

3 RESULTS

3.1 Recombination analysis of the SM22α-Cre mice

3.1.1 Analysis of recombination by X-gal staining of different tissues

To examine the recombination efficiency and pattern of the SM22α-Cre mouse line (Holtwick et al., 2002), this line was crossed to Cre reporter mice carrying the ROSA26 β-gal allele (Soriano, 1999). In the offspring, Cre mediates excision of an intervening *floxed* DNA segment at the ROSA26 β-gal allele, which removes a polyadenylation sequence and results in expression of lacZ in all cells that expressed the recombinase (2.1.2.3). The lacZ expression can be detected by X-gal staining of different organs for β-gal activity (Fig. 7). These stainings demonstrated recombination in the heart (Fig. 7A) and in vascular SMCs of the common carotid artery (CCA) (Fig. 7B). In comparison to vascular SMCs, recombination efficiency was reduced in visceral SMCs as shown by X-gal staining of the duodenum (Fig. 7C). In all control tissues analyzed, which lack SMCs, no recombination was detectable (data not shown).

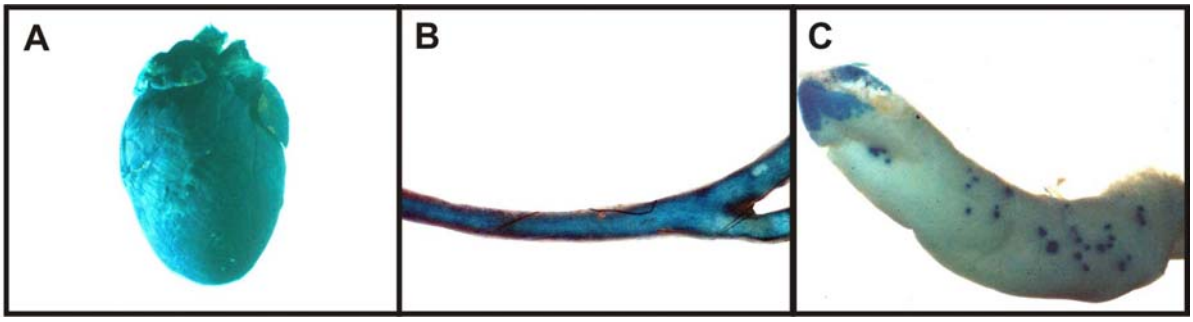

Fig. 7: X-gal staining for β-gal activity (blue) of whole mount organ preparations from the SM22α-Cre; ROSA26 β-gal reporter mouse. Recombination was detectable in cardiomyocytes and coronary arteries of the heart (A) and in vascular SMCs of the CCA (B), whereas the recombination efficiency in visceral SMCs of the duodenum was lower (C).

At the cellular level, blue staining was visible in the medial cell layer of the aorta (Fig. 8A) and CCA (Fig. 8B). In addition, recombination and vascular remodeling was analyzed 28 days after carotid ligation. At this time point severe morphological changes were apparent in the ligated vessel (Fig. 8C). A reproducible luminal obstruction was detectable proximal to the ligature. Inside the internal elastical lamina (IEL) a prominent neointima (NI) had formed. As shown by X-gal staining of ligated vessels, recombination occurred in the media, and importantly in cells of the NI as well (Fig. 8C). Cre recombinase was either directly active in a majority of these cells, or recombined progenitor cells in the media gave rise to blue progeny within the NI. It is very likely that these cells originated from the medial vessel layer and resemble a phenotypically modulated SMC type (Owens et al., 2004). However, it can not be excluded that bone marrow cells (Tanaka et al., 2003) or circulating progenitors (Margariti et al., 2006; Sata, 2006) contribute to the development of blue cells in the NI since they might give rise to a SMC-like phenotype (Saiura et al., 2001; Sata et al., 2002), and, thereby, express the SM22α-Cre transgene.

In conclusion, the X-gal stainings of the vessels showed that the recombination efficiency was very high in the common carotid artery before and after injury induction (Fig. 8B+C). Therefore, it was proposed that the SM22α-Cre mice would be a suitable tool to generate an effective knockout of cGKI in SMCs of the CCA under physiological conditions and after ligation-induced injury.

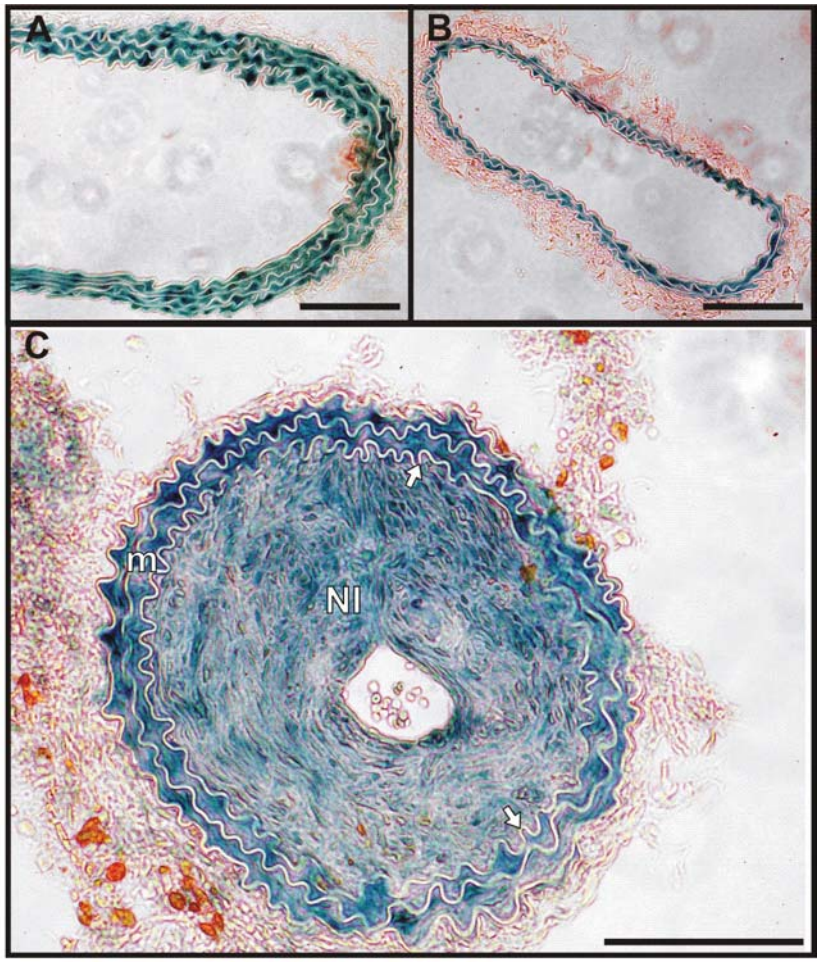

Fig. 8: Histological analysis of LacZ expression following SM22α-Cre mediated recombination in the ROSA26 β-gal reporter mouse. X-gal stainings of an uninjured aorta (A) and the CCA (B) are shown. 28 d after ligation of the CCA (C) blue cells were detectable in the media (m) and in the neointima (NI). Arrows indicate the internal elastic lamina (IEL). Scale bars, 100 µm.

3.1.2 Conditional deletion of cGKI in SMCs and the heart

A cGKI-null allele (L-) was generated by crossing the SM22α-Cre strain with mice carrying the conditional cGKI allele (L2) (Wegener et al., 2002), in which Cre mediated the excision of the loxP-flanked essential exon 10 of cGKI. The resulting L- allele was detectable by PCR analysis with specific primers in genomic DNA preparations of various SMC-containing tissues and in the heart (Fig. 9). Importantly, recombination of the L2 allele was detectable in the CCA and the aorta, whereas no conversion of the L2 allele was observed in non-smooth muscle control tissues, such as the cerebellum (Fig. 9).

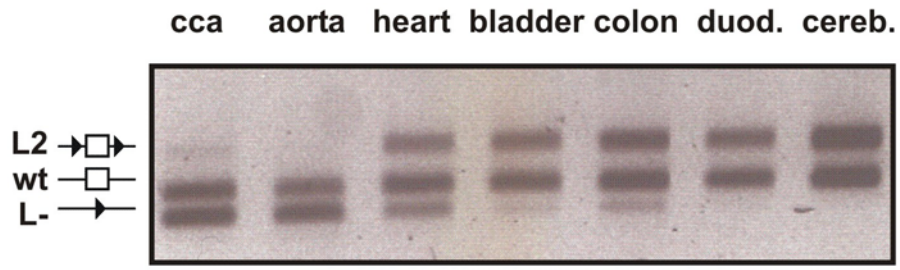

Fig. 9: PCR-analysis of the SM22α-Cre mediated deletion of cGKI in different tissues. PCR products amplified from the L2, wt, and L- alleles of SM22α-Cre$^{tg/+}$; cGKI$^{+/L2}$ mice are shown. The loxP sites (black triangles) and the exon 10 of cGKI (open box) are indicated (left). Abbreviations used are (duod) for duodenum and (cereb) for cerebellum.

Immunoblott analysis of control (ctr) mice in comparison to conditional cGKI knockouts (cGKI^{csmko}; csmko stands for "cardiac and smooth muscle knockout") demonstrated that cGKI protein expression was strongly reduced in the CCA and aorta, whilst a moderate reduction of cGKI protein was observed in the heart (Fig. 10). The decrease in cGKI protein levels in the hearts of the cGKI^{csmko} mutants might result from a transient SM22α gene promoter activity and subsequent Cre expression in embryonic cardiomyocytes (Li et al., 1996) as well as from a persistent expression of the Cre transgene in coronary SMCs of adult mice. In the cerebellum, which was used as negative control, cGKI protein levels were similar in control and cGKI^{csmko} mice (Fig. 10).

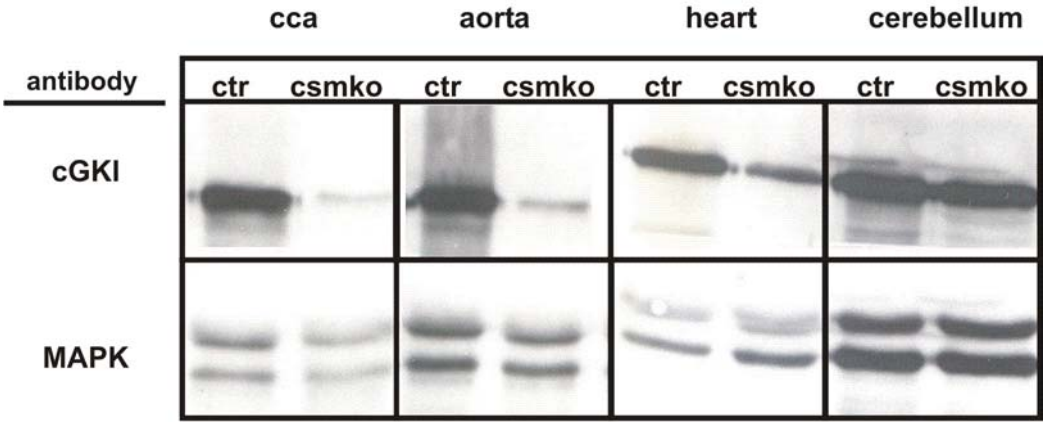

Fig. 10: Western blot analysis of cGKI protein expression in different organs of SM22α-Cre$^{tg/+}$; cGKI$^{+/L2}$ mice (ctr) and conditional SM22α-Cre$^{tg/+}$; cGKI$^{L-/L2}$ mice (csmko). By detecting the p42/p44 mitogen-activated protein kinase (MAPK) in the same protein homogenates equal loading of the gel was shown.

Immunohistochemical analysis of the CCA (Fig. 11A) and aorta (data not shown) from uninjured control animals using specific antibodies (Feil et al., 2005c) revealed a strong expression of the cGKI protein in the medial vessel layer. Remodeled vessels were obtained from mice at the age of 10-24 weeks 28 days after ligation of the common carotid artery (Kumar and Lindner, 1997). As a consequence of the complete cessation of blood flow, blood components were still present in the lumen after perfusion fixation (2.2.4.1). Ligation elicited an intensive remodeling of the injured vessels in both, control and cGKI^{csmko} mice. After injury, the cGKI protein was heterogeneously expressed in the media, and, in addition, it was clearly detectable in cells of the NI (Fig. 11B). In cGKI^{csmko} mice no cGKI staining could be identified in the uninjured CCA (Fig. 11C), at 14 d (data not shown), and at 28 d after ligation (Fig. 11D). It is important to note that under basal conditions, the cGKI^{csmko} mice showed no obvious phenotypic abnormalities including a normal blood pressure and heart rate (Dr. S. Feil, unpublished data 2006). Additionally, the arterial morphology and vessel structure in controls and cGKI^{csmko} was similar before the injury.

Taken together, it was shown that cGKI was expressed before and after injury in the CCA of control mice indicating that its expression might be of importance during the ligation-induced remodeling of vessels. On the other hand, the recombination analysis of the cGKI^{csmko} mice indicated that an efficient knockout of cGKI was generated in the vascular system, in particular in the CCA.

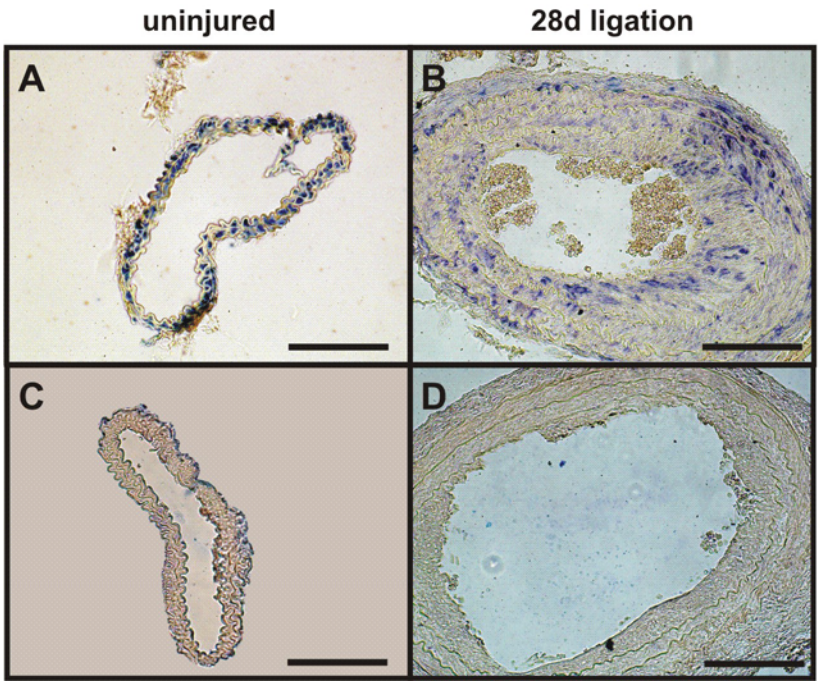

Fig. 11: Immunohistochemical analysis of cGKI expression in uninjured (A, C) and ligated carotid arteries (B, D) of control (upper) and cGKI^{csmko} (lower) mice. Scale bars, 100 µm.

3.2 Analysis of vascular changes induced by carotid ligation

3.2.1 Integrity of the vascular endothelium after injury

It is well accepted that the vascular endothelium plays an important role in regulating the vascular integrity. Under physiological conditions, endothelial cells secrete various vasoactive substances, including NO and prostacyclin, which are key molecules involved in vasoconstriction, inflammation, proliferative changes, and thrombus formation. In contrast to vascular injury models that are based on endothelial denudation, and, thus, lead to dysfunction of the endothelium, the carotid ligation model used here should preserve endothelial function including potential NO-cGMP signaling. The presence of an endothelial cell layer on the luminal surface of the vessels was verified by immunostaining for von Willebrand factor (vWF, factor VIII–related antigen). In a normal environment, aortas (Fig. 12A) and CCA (Fig. 12B) stained positive for the vWF. Importantly, 28 d after ligation-induced injury vWF was still detectable in a thin laminar cell layer, which marked the boundary of vessel lumen and NI in control (Fig. 12C) and cGKI^{csmko} mice (Fig. 12D). The vWF stain confirmed the existence of endothelial cells after injury, and, therefore, it was expected that the endothelial sources of NO were preserved during the entire injury period. eNOS derived NO is perhaps the most important activator of the cGMP-cGKI pathway in SMCs, and, thus, an essential stimulus.

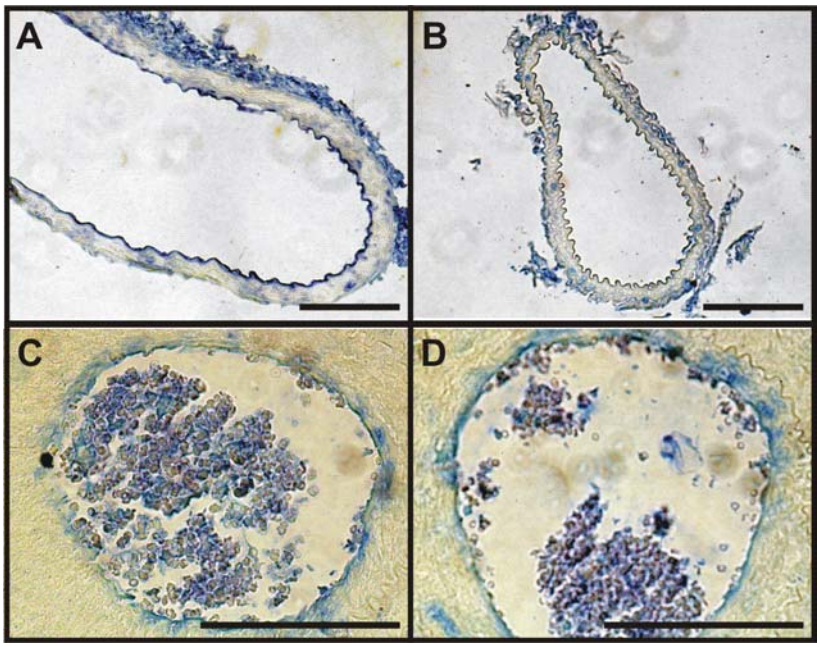

Fig. 12: Photomicrographs of 6 μm cross sections of uninjured aorta (A), carotid artery (B), and the CCA of control (C) and cGKI^{csmko} (D) mice 28 d after ligation demonstrating immunoreactivity for vWF on the luminal surface of the vessels. Scale bars, 100 μm.

3.2.2 Quantitative analysis of vascular lesions in ligated carotid arteries of normolipidemic mice

Quantitative assessment of the remodeling was performed by morphometric analysis of hematoxylin and eosin (H&E) stained sections. Based on the mean NI/media ratios, no differences could be detected between normolipidemic control mice (genotype, SM22α-Cre$^{tg/+}$; cGKI$^{+/L2}$) (NI/media ratio 0.38 $\pm$ 0.06; n=22) and littermate cGKI^{csmko} (genotype, SM22α-Cre$^{tg/+}$; cGKI$^{L-/L2}$) (NI/media ratio 0.45 $\pm$ 0.08; n=10) at 28 d after injury (Fig. 13). In an earlier period, after 14 d of injury, both genotypes showed significantly less intense remodeling of the vessels (ctr NI/media ratio 0.12 $\pm$ 0.03; n=18; cGKI^{csmko} NI/media ratio 0.14 $\pm$ 0.04; n=13) in comparison to the corresponding animals analyzed after 28 d of injury (Fig. 13). Based on the NI/media ratio, there was a significant time-dependent increase in the remodeling within both groups. Nevertheless, at all time-points evaluated, no differences could be detected between the genotypes.

In order to test whether an activation of the cGMP-cGKI pathway after injury had other functional consequences for the vascular response to ligation than the conditional deletion of

cGKI, a group of control animals (genotype, SM22α-Cre$^{tg/+}$; cGKI$^{+/L2}$) was continuously treated with the PDE-5 inhibitor sildenafil in their drinking water. As determined by the NI/media ratio 28 d after injury, no significant difference was detected between animals treated with sildenafil (NI/media ratio 0.29 $\pm$ 0.10; n=10) and the untreated control mice (Fig. 13).

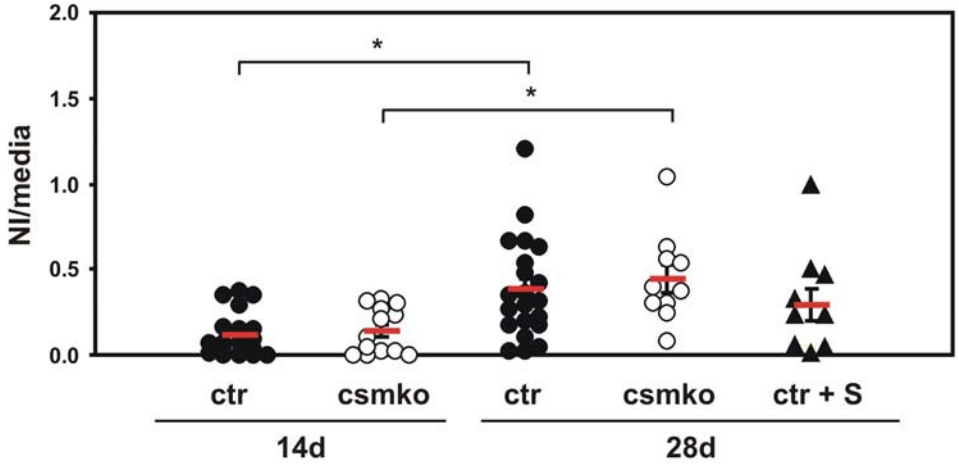

Fig. 13: Analysis of vascular remodeling after ligation-induced injury. The NI/media ratios shown were calculated from a representative vessel segment analyzed from the point of ligation at 0 mm to 3.6 mm distance. After 14 d of injury there were no differences between untreated controls (ratio 0.12 $\pm$ 0.03; n=18) and cGKI^{csmko} mutants (ratio 0.14 $\pm$ 0.04; n=13). Additionally, both groups showed a similar response to injury after 28 d (ctr, ratio 0.38 $\pm$ 0.06; n=22 and csmko, ratio 0.45 $\pm$ 0.08 n=10). Sildenafil treatment (50 mg·kg^{-1}·d^{-1}) did not change the remodeling as well (ctr+S, ratio 0.29 $\pm$ 0.10; n=10), whereas a significant time-dependent increase within the genotypes was clearly evident ($*$, $p<0.05$).

Effective administration of the drug was revealed by elevated cGMP levels (determined in the heart) (ctr 34.39 ± 9.71 fmol/mg protein; n=4 and ctr (+ sildenafil) 75.90 ± 3.81 fmol/mg protein; n=4) (Fig. 14). Apparently, this cGMP increase was without consequences for the remodeling as mentioned above.

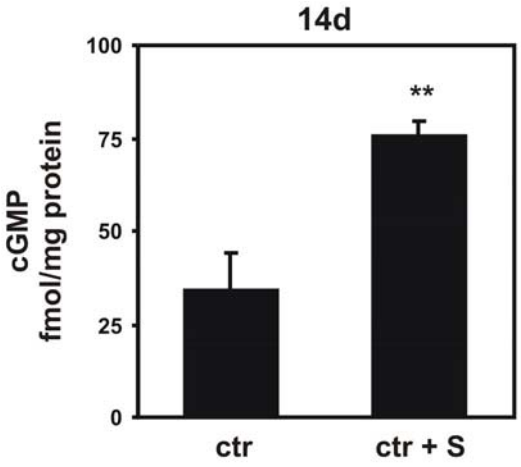

Fig. 14: cGMP measurements from untreated control mice (ctr 34.39 ± 9.71 fmol/mg protein; n=4) and mice (ctr+S 75.90 ± 3.81 fmol/mg protein; n=4) that continuously received sildenafil (50 $mg \cdot kg^{-1} \cdot d^{-1}$) for 14 d in their drinking water. Measurements were performed on extracts isolated from whole hearts (**, $p<0.01$).

A detailed NI/media profile was generated in order to focus on possible local consequences of the cGKI inactivation 28 d after injury. In ligated arteries a gradual decrease of the NI/media ratio with increasing distance to the ligation was observed in control mice and in the cGKI^{csmko} mutants (Fig. 15). Again, these continuous profiles confirmed a similar response to injury in both genotypes in a vessel segment analyzed from the point of ligation at 0 mm to 3.6 mm distance.

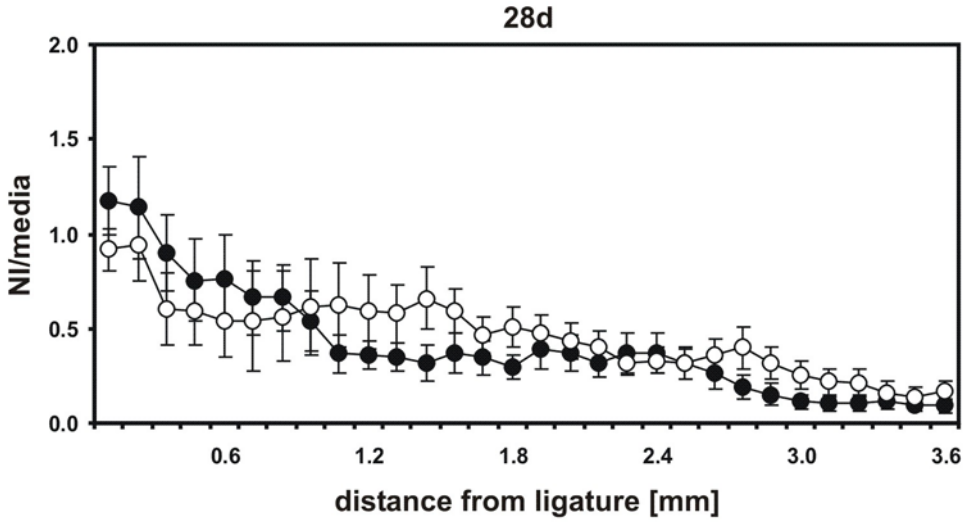

Fig. 15: Analysis of vascular remodeling after 28 d of injury. Based on the detailed NI/media profile of a representative vessel segment from 0-3.6 mm, no differences were found between controls (black circles; n=22) and conditional cGKI^{csmko} (open circles; n=10) mice.

Additional vessel parameters, such as the area inside the external elastic lamina (EEL) (ctr 58.1 ± 4.8 x10^3 µm^2; cGKI^{csmko} 72.8 ± 8.1 x10^3 µm^2), the medial area (ctr 25.8 ± 1.6 x10^3 µm^2; cGKI^{csmko} 31.3 ± 2.9 x10^3 µm^2), the NI (ctr 10.8 ± 1.8 x10^3 µm^2; cGKI^{csmko} 14.5 ± 2.7 x10^3 µm^2), and the vessel lumen (ctr 21.6 ± 2.3 x10^3 µm^2; cGKI^{csmko} 26.9 ± 3.9 x10^3 µm^2), again demonstrated that controls and cGKI^{csmko} responded equally to the injury (Fig. 16).

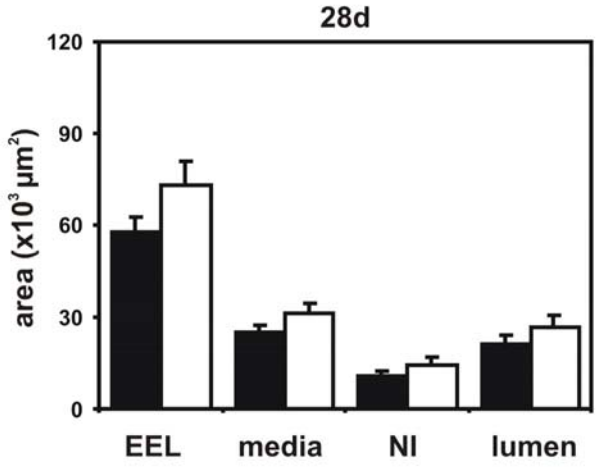

Fig. 16: Morphometric analysis of the left common carotid artery 28 d after injury. No differences were detectable between controls (black bars; n=22) and cGKI^{csmko} mice (open bars; n=10) in all areas analyzed 28 d after ligation-induced injury. Further explanations in the text.

In addition, all area parameters were determined after 14 d of injury as well. Corresponding with the data evaluated after 28 of injury, the EEL (ctr 61.9 ± 6.0 x10^3 µm^2; cGKI^{csmko} 59.7 ± 5.5 x10^3 µm^2), the media (ctr 25.3 ± 1.8 x10^3 µm^2; cGKI^{csmko} 24.8 ± 1.6 x10^3 µm^2), the NI (ctr 4.0 ± 1.0 x10^3 µm^2; cGKI^{csmko} 4.3 ± 1.1 x10^3 µm^2), the lumen (ctr 32.6 ± 3.6 x10^3 µm^2; cGKI^{csmko} 30.6 ± 3.4 x10^3 µm^2), and the NI/media profile were identical for both genotypes (Fig. 17A+B).

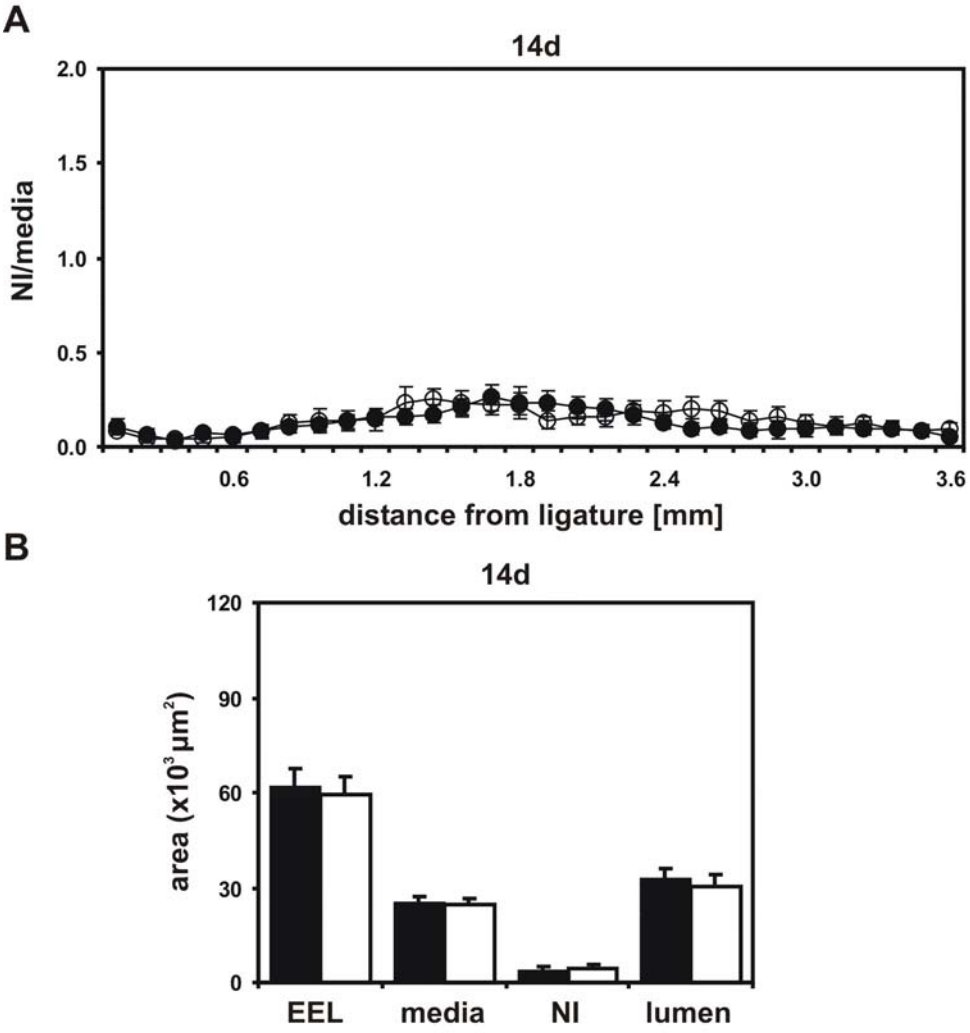

Fig. 17: Morphometric analysis of the left common carotid artery 14 d after injury. No differences were detectable between controls (black circles and bars; n=18) and cGKI^{csmko} mice (open circles and bars; n=13). Further explanations in the text.

Consistent with these morphometric results, the histological analysis of H&E stained sections showed the formation of an extensive NI within the IEL, but no differences were found between the genotypes 14 d (data not shown) and 28 d after injury (Fig. 18).

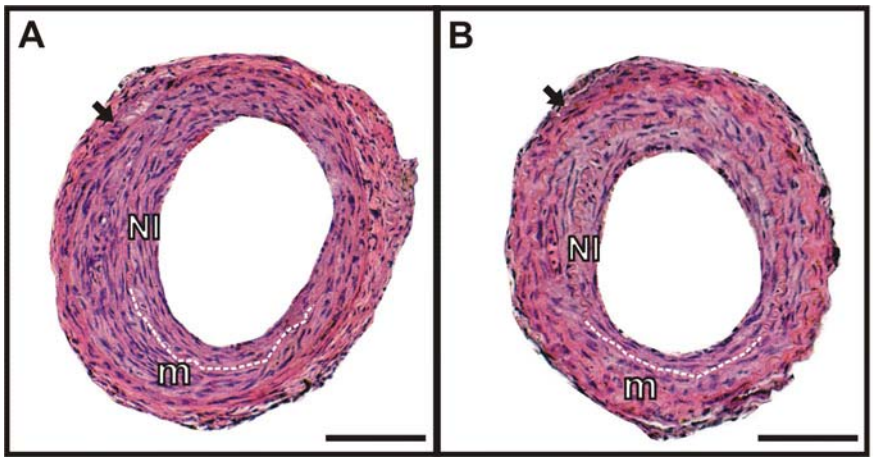

Fig. 18: Histological analysis of H&E stained 6 μm cross sections from control (A) and cGKI^{csmko} (B) mice 28 d after carotid ligation. Representative photomicrographs from the central region of the vessel segment studied are shown. Following the injury a prominent neointima (NI) inside the internal elastical lamina (white broken line) was detectable in both genotypes. Arrows indicate the external elastic lamina separating the tunica media (m) from the surrounding adventitial tissue. Scale bars, 100 μm.

3.2.3 Characterization of remodeled vessels by immunohistochemistry

3.2.3.1 Proliferating cell nuclear antigen (PCNA) staining

The experimental lesion formation in response to ligation-induced injury together with the data obtained from X-gal stainings of the Cre reporter vessels suggested that SMC proliferation was a prominent feature of this model. Indeed, it was shown previously that proliferation of cells from the vessel wall was involved in the remodeling after vascular injury (Kumar and Lindner, 1997). In order to assess this issue, a proliferation marker staining with an antibody against the proliferating cell nuclear antigen (PCNA) was performed on sections 28 d after injury and subsequently the proliferation index was determined. PCNA is a DNA polymerase δ associated co-factor and it is upregulated in the G_1 and S phases of the cell cycle. PCNA was detected in neointimal and underlying medial cells of controls and cGKI^{csmko} mice. The percentage of positively stained cells in the NI (ctr 3.13% $\pm$ 0.63%; n=12; cGKI^{csmko} 3.03% $\pm$ 0.92%; n=9) and the medial cell layer (ctr 3.06% $\pm$ 1.04%; n=12; cGKI^{csmko} 2.83% $\pm$ 0.80%; n=9) was not different between genotypes (Fig. 19). These results indicated that

proliferation of cells from the vessel wall contributed to the vascular remodeling after ligation, but the conditional deletion of cGKI in SMCs showed again no influence.

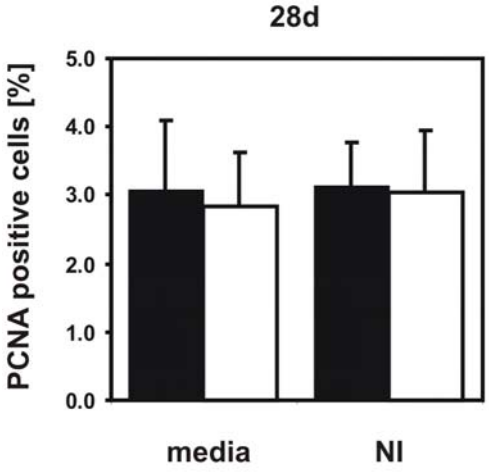

Fig. 19: Quantification of cellular proliferation in remodeled vessels from control (black bars) and cGKI^{csmko} (open bars) mice 28 d after injury. The statistics are based on the analysis of immunohistochemical staining for the proliferating cell nuclear antigen (PCNA). No differences were found between both genotypes in the media and NI (ctr n=12; cGKI^{csmko} n=9).

3.2.3.2 α-smooth muscle actin (α-SMA) immunohistochemistry

To further characterize the vascular changes after injury, immunostaining for α-smooth muscle actin (α-SMA) was performed on uninjured and ligated vessels. As expected, under physiological conditions the SM marker α-SMA was ubiquitously expressed in medial cells of the aorta (data not shown) and in carotid arteries of control (Fig. 20A) and cGKI^{csmko} (Fig. 20B) animals. After injury, remodeled vessels of both genotypes were positive for α-SMA. In the media, the α-SMA staining pattern was less homogeneous as compared to uninjured vessels. In addition, cells of the NI expressed the SM marker. The positive α-SMA staining indicated that many lesional cells still resembled the SMC-like phenotype. In correlation with the morphometric data again no differences were found between control and cGKI^{csmko} mice 14 d (data not shown) and 28 d after injury (Fig. 20).

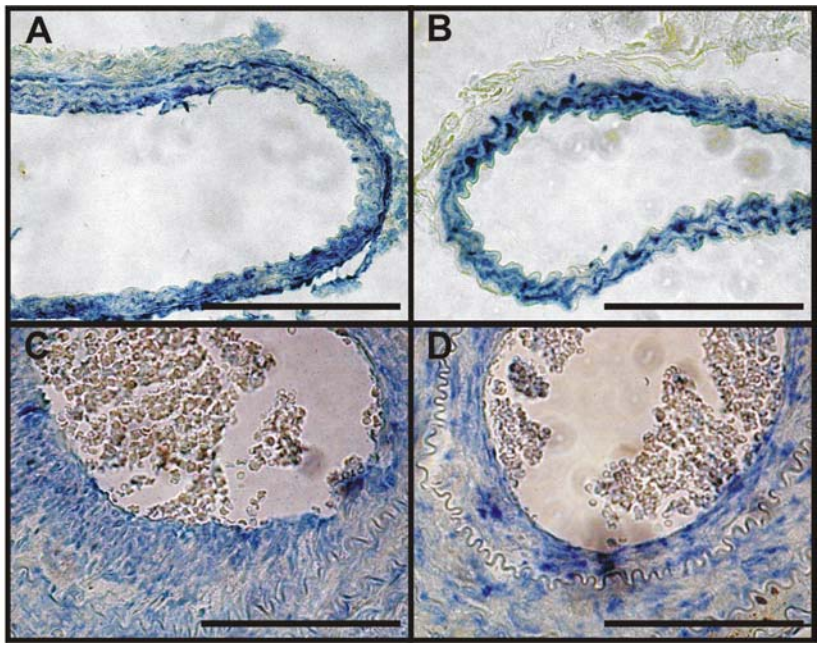

Fig. 20: Representative immunohistochemical staining for α-smooth muscle actin of unmanipulated (A and B) vessels and remodeled carotid arteries (C and D) 28 d after ligation. In carotid arteries α-SMA was expressed in medial cells of control (A) and cGKI^{csmko} (B) mice. After injury, positively stained cells were detectable in the media and neointima of control (C) and cGKI^{csmko} mice (D). Scale bars, 100 μm.

3.2.3.3 Immunostaining for inflammatory cells

Using a Mac-2 antibody detecting a carbohydrate-binding protein expressed on the surface of mature macrophages (Dong and Hughes, 1997), inflammatory events involved in the remodeling were analyzed. Immunohistochemistry showed clear up-regulation of Mac-2 after injury (Fig. 21B+C), whereas in sections of uninjured vessels Mac-2 staining was not detectable (Fig. 21A). Infiltration of the vascular wall after ligation by Mac-2 positive cells was found in controls (Fig. 21B) and cGKI^{csmko} mutants (Fig. 21C). In addition to macrophages, the Mac-2 positive cells might represent phenotypically modulated SMCs (Rong et al., 2003). In conclusion, the analysis of inflammation based on Mac-2 staining 28 d after injury revealed no differences between control and cGKI^{csmko} mice.

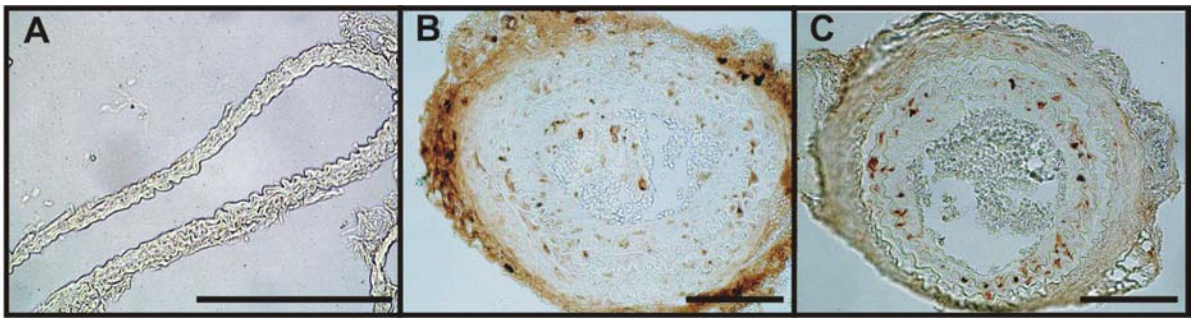

Fig. 21: Immunostaining for macrophages. To detect inflammatory cells the Mac-2 antibody was used on cross sections of unmanipulated vessels (A), or ligated controls (B) and cGKI^{csmko} mutants (B). 28 d after injury cells expressing Mac-2 were detectable in the media and NI of remodeled carotid arteries. Scale bars, 100 µm.

3.2.4 Quantitative analysis of vascular lesions in ligated carotid arteries of atherosclerosis-prone mice

Interestingly, in the apoE-deficient mouse model of atherosclerosis, the SMC-specific inactivation of cGKI reduced the formation of atherosclerotic plaques (Wolfsgruber et al., 2003). This study indicated that SMC cGKI modulates the progression of atherogenesis *in vivo* and promotes the growth of SMCs *in vitro*. Therefore, it was tested whether the genetic inactivation of cGKI in SMCs of apoE-deficient mice fed on normal chow influenced vascular remodeling after mechanical injury as well. However, the NI/media ratio (apoE-ko ctr NI/media ratio 0.59 ± 0.09; n=13 and littermate apoE-ko cGKI^{csmko} NI/media ratio 0.79 ± 0.15; n=12) 28 d after injury (Fig. 22) as well as the NI/media profile (Fig. 23A) in a representative vessel segment revealed no differences between apoE-ko controls and the apoE-deficient cGKI^{csmko} mutants.

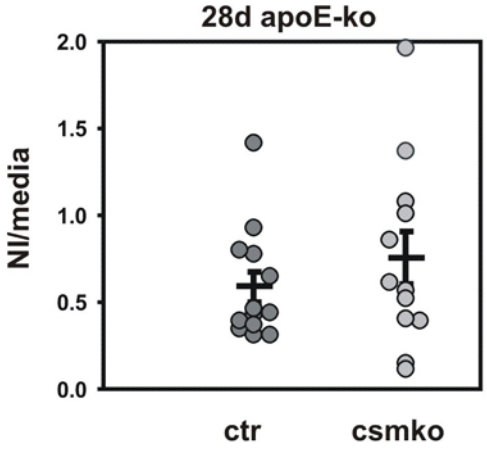

Fig. 22: Analysis of vascular remodeling 28 d after ligation-induced injury in apoE-deficient mice. The NI/media ratios were calculated from a representative vessel segment analyzed from 0-3.6 mm. Controls (ctr, n=13) and cGKI^{csmko} mice (csmko, n=12) on an apoE knockout background showed a similar response to the injury.

In line with these results, the morphometric data based on measurements of the EEL (apoE-ko ctr 86.8 ± 6.6 x10^3 µm^2; apoE-ko cGKI^{csmko} 94.1 ± 10.9 x10^3 µm^2), the medial area (apoE-ko ctr 36.7 ± 2.8 x10^3 µm^2; apoE-ko cGKI^{csmko} 37.5 ± 4.3 x10^3 µm^2), the NI (apoE-ko ctr 21.3 ± 3.2 x10^3 µm^2; apoE-ko cGKI^{csmko} 30.9 ± 7.4 x10^3 µm^2), and the vessel lumen (apoE-ko ctr 28.7 ± 2.6 x10^3 µm^2; apoE-ko cGKI^{csmko} 25.7 ± 3.7 x10^3 µm^2) showed that both genotypes responded equally to vascular injury on an apoE-deficient background (Fig. 23B).

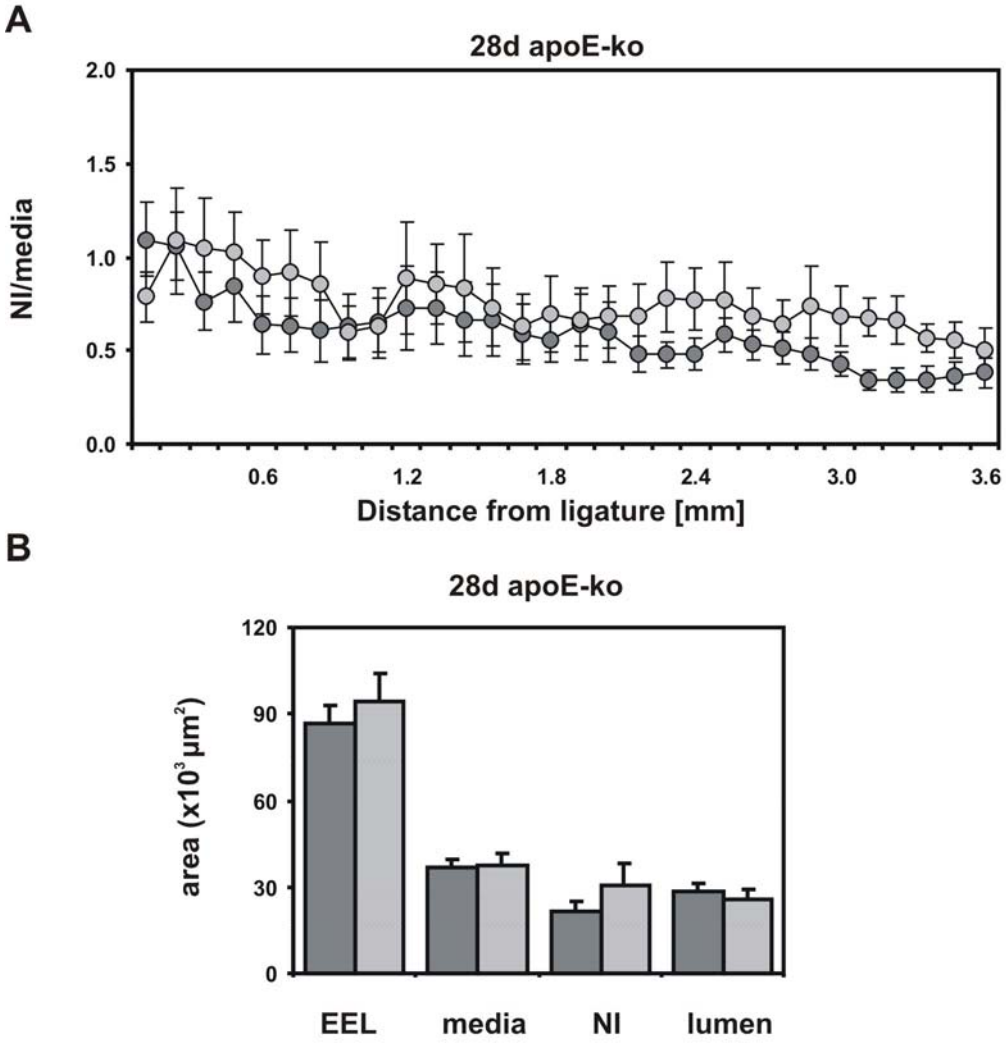

Fig. 23: Morphometric analysis of the left common carotid 28 d after injury in apoE knockout mice fed on a normal chow. No differences were detectable between control mice (dark gray circles and bars; n=13) and cGKI^{csmko} mutants (light gray circles and bars; n=12) on an apoE-deficient background. Further explanations in the text.

In addition, as shown before in normolipidemic mice (Fig. 11), the cGKI protein was expressed in the NI and media 28 d after injury in apoE-deficient controls (Fig. 24A). The cGKI expression in both the media and the NI was completely abolished in the apoE-deficient cGKI^{csmko} mutants (Fig. 24B). These observations from apoE-deficient controls and cGKI^{csmko} mice fed on a normal chow indicated that NI cells, which expressed cGKI, were indeed derived from medial SMCs.

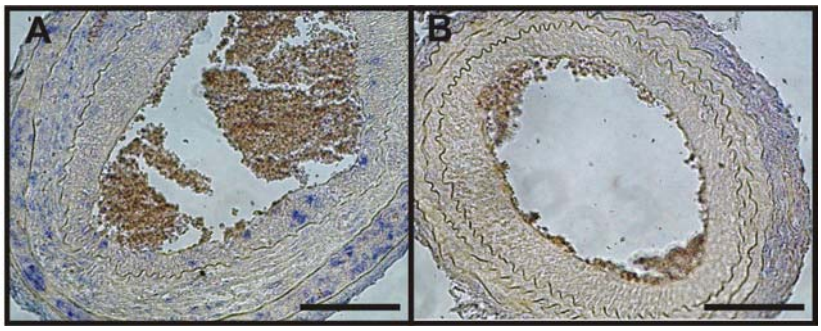

Fig. 24: Immunohistochemical detection of cGKI 28 d after carotid ligation in apoE-deficient control (A) and cGKI^{csmko} apoE knockout (B) mice. Scale bars, 100 µm.

3.3 Analysis of the cGMP-cGKI pathway in primary SMCs using the vasodilator-stimulated phosphoprotein (VASP) phosphorylation as a biomarker

3.3.1 Cyclic nucleotide- and sildenafil-induced phosphorylation of VASP in primary vascular SMCs

The VASP protein is known to be a common substrate for cGKI and cAK in several cell types, including SMCs (Krause et al., 2003). First, the effects of two membrane permeable cyclic nucleotide analogous on the phosphorylation of VASP were determined in primary vascular SMCs. For stimulation of primary SMCs, 8-bromoguanosine-3´,5´-cyclic monophosphate (8-Br-cGMP) and 8-bromoadenosine-3´,5´-cyclic monophosphate (8-Br-cAMP), which bind to and activate cGKI and cAK, respectively, were used.

Treatment of primary SMCs from wild-type (wt) (Fig. 25A) and conventional cGKI-deficient mice (cGKI$^{L-/L-}$) (Fig. 25B) with 8-Br-cAMP (1 mM) induced VASP phosphorylation on serine 157, which resulted in a characteristic shift in mobility of the protein on a denaturing SDS gel from 46 to 50 kDa (Halbrugge and Walter, 1989). A lower concentration of 100 µM 8-Br-

cAMP was less effective. Only a slight phosphorylation could be detected in both genotypes. Treatment of primary wild-type SMCs with a high (1 mM) or low (0.1 mM) concentration of 8-Br-cGMP induced a strong concentration-dependent phosphorylation of VASP (Fig. 25A). Interestingly, in cGKI knockout cells a relatively weak phosphorylation of VASP was induced by 1 mM 8-Br-cGMP, whereas no phosphorylation was detected in response to 0.1 mM 8-Br-cGMP (Fig. 25B). The VASP phosphorylation in SMCs from cGKI knockout mice was independent of cGKI activity since no protein was expressed. These data indicated a possible cross-activation of PKA by 1 mM 8-Br-cGMP. Therefore, it was hypothesized that SMC PKA might be cross-activated not only by the cyclic nucleotide analog 8-Br-cGMP but also directly by endogenous cGMP. To elucidate this in more detail, the effects of sildenafil on the phosphorylation of VASP were tested in primary SMCs of wild-type and cGKI-deficient mice. As shown before, the specific PDE-5 inhibitor sildenafil was effectively administrated *in vivo* in mice. The treatment successfully elevated cGMP levels in the heart (Fig. 14), but did not affect the vascular remodeling in control animals (Fig. 13). This indicated that the drug might be effective in raising cGMP levels of primary SMCs as well. Indeed, in primary SMCs a high concentration of sildenafil (0.1 mM) induced VASP phosphorylation in wild-type (Fig. 25A) and, interestingly, also in cGKI-deficient (Fig. 25B) cells.

The monitoring of VASP phosphorylation at serine 157 in wt and cGKI-deficient SMCs (Fig. 25) suggested that inhibition of PDE-5 might activate cAK either directly via binding of cGMP to the kinase or, alternatively, by a cross-talk of the two cyclic nucleotide pools.

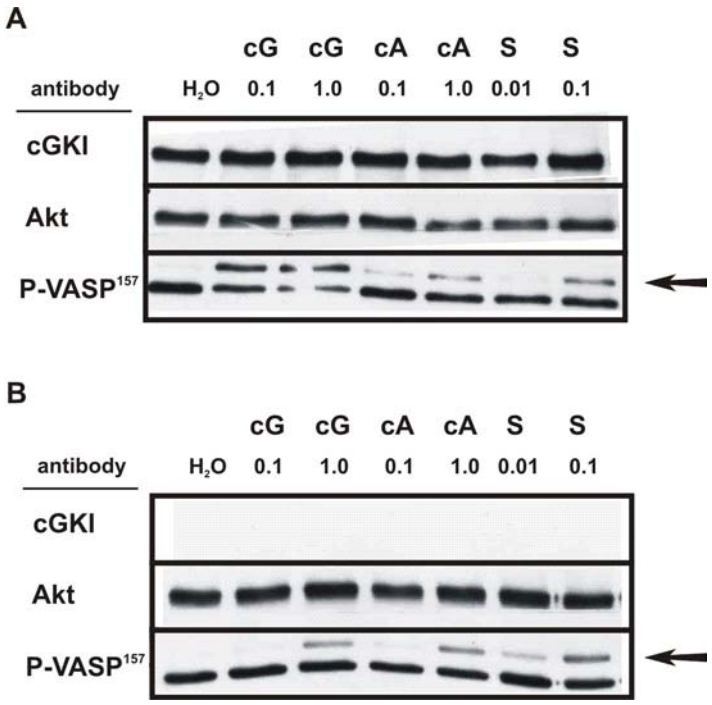

Fig. 25: Western blot analysis of protein extracts from wild-type (A) and cGKI-deficient (B) primary SMCs cultured in 6-well plates. Cells were serum-starved for 48 h before the treatment with serum-free medium (±drugs) for 30 min was performed. cGKI specific antibodies were used on loaded lysates from cells, which were stimulated with serum-free medium containing water as control (H_2O) or mM concentrations of the drugs as indicated. Stimulation was carried out with the membrane-permeable cyclic nucleotides 8-Br-cGMP (cG) or 8-Br-cAMP (cA), and the PDE-5 inhibitor sildenafil (S). A VASP antibody was used that detects both total VASP (lower band) and its phosphorylation at serine 157 ($P\text{-}VASP^{157}$) resulting in a mobility shift to 50 kDa (upper band, black arrow). Equal loading of the gels is demonstrated by detection of the protein kinase Akt. One of three representative experiments is shown.

3.3.2 Effect of natriuretic peptides on the phosphorylation of VASP in primary SMCs

The effects of cGMP-elevating peptides, which bind to and activate the pGCs, were tested in primary SMCs as well. In particular, VASP phosphorylation was analyzed upon treatment with the atrial (ANP), and C-type natriuretic (CNP) peptides. As shown before (Fig. 25) high concentrations of 8-Br-cGMP (1 mM), 8-Br-cAMP (1 mM), and sildenafil (0.1 mM) induced a phosphorylation-dependent shift of VASP in primary wild-type (Fig. 26A) and cGKI-deficient (Fig. 26B) cells. Interestingly, in response to ANP and CNP in all concentrations tested

(0.01 µM to 1 µM), phosphorylation of VASP was detectable in wild-type (Fig. 26A) and cGKI knockout (Fig. 26B) cells. Lower concentrations of ANP and CNP (0.01 nM to 1 nM; data not shown) were less effective than higher concentrations (0.01 µM to 1 µM; Fig. 26). Phosphorylation levels were comparable in both genotypes indicating that various cGMP-elevating agents induce phosphorylation of VASP, and, interestingly, in knockouts this phosphorylation is independent of cGKI and might therefore be mediated by cAK.

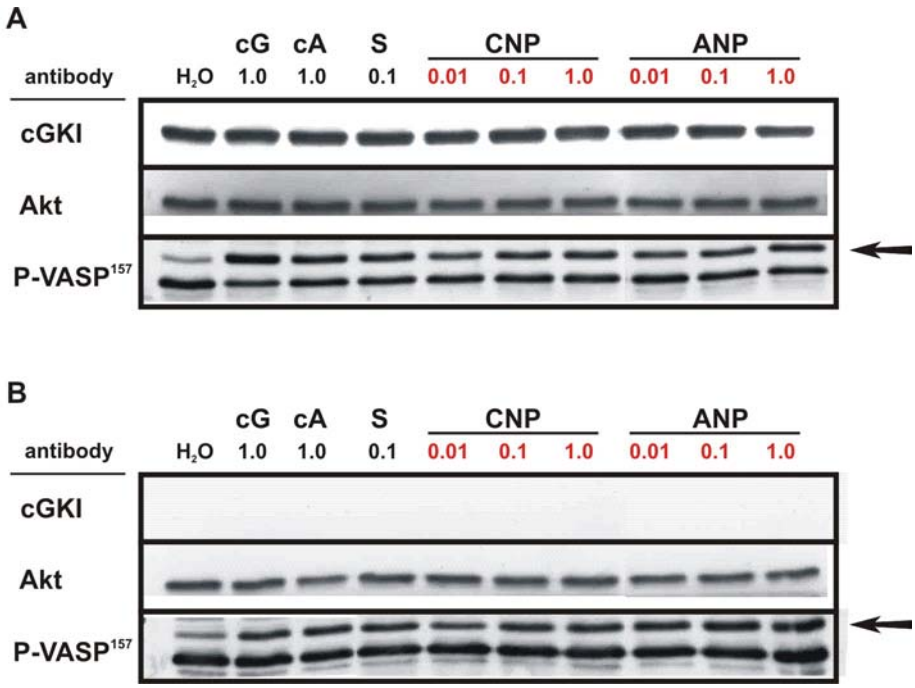

Fig. 26: Western blot analysis of lysates from serum-starved (48 h) wild-type (A) and cGKI-deficient (B) primary SMCs cultured in 6-well plates. Stimulation was carried out for 30 min with serum-free medium containing 8-Br-cGMP (cG), 8-Br-cAMP (cA), sildenafil (S) or the atrial (ANP) and C-type (CNP) natriuretic peptides. Concentrations of the agents used are indicated in black (mM) or red (µM). Extracts from cells treated with serum-free medium without agents but water (H_2O) were used as control. Antibodies used were the same as indicated in Fig. 25.

3.3.3 Phosphorylation of VASP and intracellular changes of cAMP and cGMP after treatment of primary SMCs with various cGMP-elevating agents

In order to analyze alterations of the two cyclic nucleotide pools in response to cGMP-elevating compounds, the VASP phosphorylation experiments were combined with cGMP

and cAMP measurements. Again, 8-Br-cGMP (1 mM), 8-Br-cAMP (1 mM), and sildenafil (0.1 mM), ANP (0.001 mM), and CNP (0.001 mM) induced VASP phosphorylation in primary wild-type (Fig. 27A) and cGKI-deficient (Fig. 27B) cells. Additionally, an alternative approach to stimulate the sGCs was performed using 0.1 mM of the NO-donor 2-(N,N-diethylamino)-diazenolate-2-oxide (DEA-NO). Stimulation with 0.1 mM DEA-NO resulted in a strong VASP phosphorylation in primary SMCs of wild-type (Fig. 27A) and cGKI knockout (Fig. 27B) cells. Using lower concentrations of DEA-NO (0.01 mM and 0.001 mM) the phosphorylation levels detectable in both genotypes were similar (data not shown).

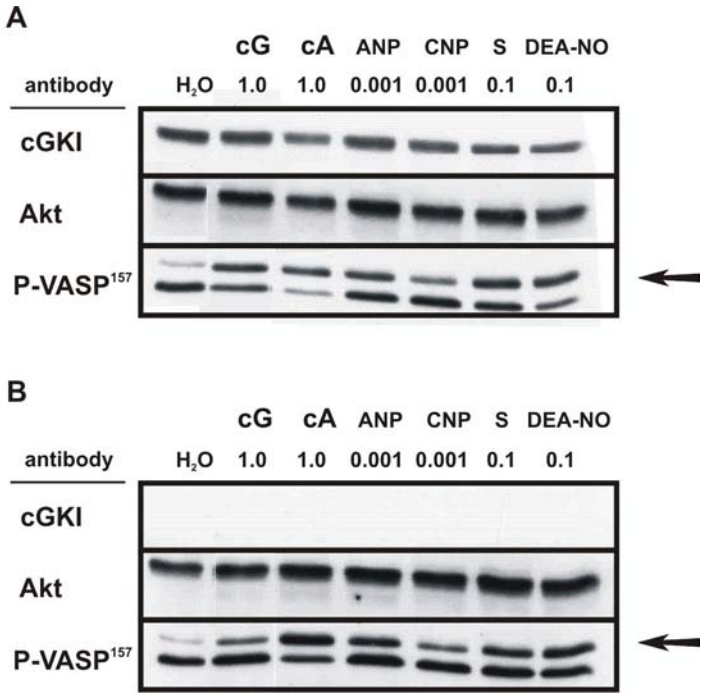

Fig. 27: Western blot analysis of lysates from serum-starved (48 h) wild-type (A) and cGKI-deficient (B) primary SMCs cultured on 10-cm dishes. Extracts loaded were isolated from cells treated for 10 min with Tyrode's solution containg water (H_2O) or mM concentrations of 8-Br-cGMP (cG), 8-Br-cAMP (cA), sildenafil (S), the atrial (ANP) or C-type (CNP) natriuretic peptides, and the NO-donor 2-(N,N-diethylamino)-diazenolate-2-oxide (DEA-NO). Antibodies used were the same as indicated in Fig. 25. One of three representative experiments is shown.

In parallel, cyclic nucleotide levels were determined in the same samples, which were used for the analysis of VASP phosphorylation shown in Fig. 27. Stimulation with 0.001 mM ANP (wt 6.44 ± 0.35 pmol/well; ko 7.64 ± 0.49 pmol/well), or CNP (wt 5.73 ± 1.41 pmol/well;

ko 6.62 ± 0.49 pmol/well), 0.1 mM sildenafil (wt 5.87 ± 0.11 pmol/well; ko 6.60 ± 0.66 pmol/well), and 0.1 mM DEA-NO (wt 6.53 ± 0.48 pmol/well; ko 7.19 ± 0.69 pmol/well) did not affect the global levels of cAMP of primary wild-type (wt) and cGKI knockout (ko) cells (Fig. 28A). In contrast, in response to these compounds, the low basal cGMP concentration (wt 0.34 ± 0.20 pmol/well; ko 0.31 ± 0.17 pmol/well) (Fig. 28B) was raised to levels comparable to those of baseline cAMP (wt 5.98 ± 0.69 pmol/well; ko 5.34 ± 0.50 pmol/well) (Fig. 28A). Both, the basal cAMP and cGMP pools were similar in wild-type as compared to cGKI knockout cells. Using the same drug concentrations for stimulation, the cGMP levels were highest after treatment with DEA-NO (wt 8.60 ± 3.73 pmol/well; ko 10.36 ± 2.85 pmol/well) and ANP (wt 7.91 ± 1.13 pmol/well; ko 8.91 ± 0.78 pmol/well), while CNP (wt 3.64 ± 0.62 pmol/well; ko 2.54 ± 0.92 pmol/well) and sildenafil (wt 2.93 ± 0.88 pmol/well; ko 2.83 ± 1.17 pmol/well) were less effective. No differences were detected between the two genotypes after stimulation with all agents tested.

Together, these results indicate that stimulation of primary wild-type and cGKI-deficient vascular SMCs with various cGMP-elevating agents leads to significant increases of cGMP levels, whereas cAMP levels are unaffected. Furthermore, the cGMP raises detected were similar in both genotypes and correlated with the phosphorylation of VASP at Ser 157 (Fig. 27).

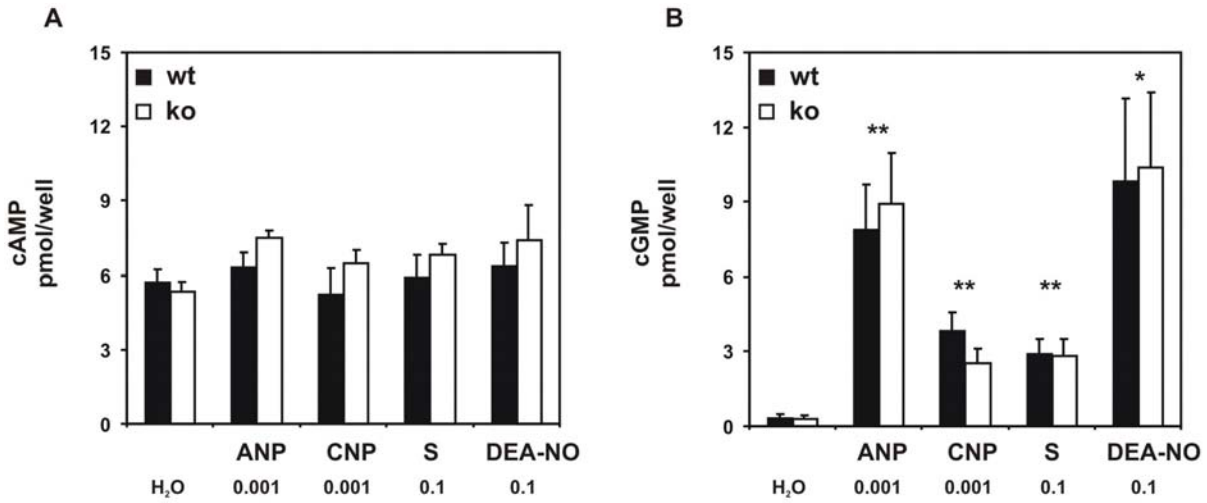

Fig. 28: Endogenous cAMP (A) and cGMP (B) levels of wild-type (black bars; n=4) and cGKI-deficient (open bars; n=4) primary SMCs in response to different cGMP-elevating compounds. Cells were maintained on 10-cm dishes in serum-free medium for 48 h and then stimulated for 10 min with

Tyrode's solution containing water (H_2O) or with Tyrode's solution containing mM concentrations of the agents as indicated. Abbreviations used are the same as in Fig. 27. Cyclic nucleotides were extracted using ice-cold 100% ethanol, concentrated by evaporating the alcohol, and resuspended in EIA buffer provided with the cAMP and cGMP EIA kit (Cayman chemical). cAMP and cGMP levels were determined successively from the same samples. All nucleotide measurements were carried out following the manufacture's recommendation without acetylation (*, $p<0.05$; **, $p<0.01$).

4 DISCUSSION

4.1 Functional analysis of the cGMP-cGKI pathway in ligation-induced restenosis of vessels

As shown by a recent work analyzing vascular proliferative disorders in transgenic mice, GKI in SMCs accelerated plaque formation in a hyperlipidemia-induced model of atherosclerosis in mice (Wolfsgruber et al., 2003). These results indicated that cGKI potentially mediated proatherogenic properties of the NO-cGMP pathway *in vivo*, being thus, in contrast to the common view that this pathway is vasculo-protective. In the present study, the role of cGKI in SMCs was investigated in a different model of vascular disease resembling restenosis. In order to solve the controversy about the role of the cGMP-cGKI pathway in vasculo-proliferative processes an effective conditional deletion of cGKI in SMCs was generated (Fig. 9-11) and a mouse model of restenosis (carotid ligation) was established. As compared to control mice, the deletion of cGKI in SMCs did not effect the NI/media ratio, cellular proliferation (Fig. 19), and various other vessel parameters that were determined by morphometry at different time-points after injury in normolipidemic (Fig. 13; 15-17) and in apoE-deficient mice (Fig. 22+23). Furthermore, the chronic activation of cGMP-cGKI signaling after injury by continuous administration of sildenafil had no effect on the remodeling response (Fig. 13). The efficiency of the sildenafil treatment was confirmed by the detection of increased cGMP levels in the heart (Fig. 14).

Previous analysis of NI formation after balloon injury of rat carotid arteries (Monks et al., 1998) showed that the media and the NI are positive for cGKI after injury. Similar data have been obtained in the ligation model used in the present study (Fig. 11+24). Further confirmation comes from the observation that cGKI was not detected in neointimal cells no matter whether normolipidemic (Fig. 11) or apoE-deficient cGKI^{csmko} (Fig. 24) mice have been used for the ligation. Thus, the NI cells, which expressed cGKI, were most likely derived from medial SMCs. However, the exact origin of the NI cells is not clear since it can not be excluded that alternative cell types, such as fibroblasts of the adventitia, circulating progenitor and/or bone marrow-derived cells (Margariti et al., 2006; Sata, 2006; Tanaka et al., 2003) contributed to the NI formation, and in course of the remodeling process acquired a

SMC-like phenotype expressing active Cre recombinase. Together, these immunohistochemical results from different models strongly implicate a potential relevance of the cGMP-cGKI pathway for injury-induced vascular remodeling.

Although, the increased cGMP levels in hearts of sildenafil-treated mice emphasized the effective administration of the drug (Fig. 14), the continuous treatment was without consequences for the remodeling response (Fig. 13). In this respect, it was assumed that the drug reached not only the heart but also the actual site of remodeling and, thus, was also effective in elevating the endogenous cGMP in the CCA. The finding that sildenafil increased basal cGMP levels in the heart is in contrast to a recent study that detected a sildenafil-induced rise of cardiac cGMP only after the injury procedure (aortic banding; (Takimoto et al., 2005)). Different dosage, application, and duration of the drug treatment might be reasons for these discrepancies.

Together, the results of the present work indicate that the effects of NO on ligation-induced restenosis of vessels (Sirsjo et al., 2003; Yogo et al., 2000) are apparently not mediated by the cGMP-cGKI pathway. Indeed, it has been suggested that many effects of NO are strongly concentration dependent and not always mediated by cGMP. Presumably, the spatio-temporal profile, the amount of NO synthesized, and the source of its production after ligation resulted in the activation of alternative mechanisms (e.g., S-nitrosylation, peroxynitrite formation, tyrosine nitration, regulation of hypoxia inducible factor 1) (Beckman and Koppenol, 1996; Foster et al., 2003; Hanafy et al., 2001).

It is well accepted that SMCs from the vessel wall show a variety of phenotypes (Hao et al., 2003). Additionally, within the developing embryo SMCs of coronary arteries, the aortic arch, and the descending aorta originate from different sources (Margariti et al., 2006). This biological heterogeneity of SMCs possibly may result in a functional divergence of the cGMP-cGKI pathway depending on the cell´s phenotypic state. Specifically, as shown in this study, during restenosis of individual vessels the lack of SMC cGKI or, conversely, the chronic stimulation of the cGMP pathway with sildenafil did not change the remodeling process (Fig. 13). In contrast, cGKI signaling was central to the phenotypic modulation of SMCs in response to systemic atherosclerosis in apoE-deficient mice. The combined results of the atherosclerosis study and the present restenosis study provide evidence that the role of the smooth muscle cGMP-cGKI signaling pathway in vascular disorders might be context-

specific, being more important in systemic atherosclerosis than in ligation-induced restenosis of particular vessels. Furthermore, the lack of cGKI during ontogenesis in the present injury model might lead to a functional compensation of the pathway, whereas in the atherosclerosis model a tamoxifen-inducible Cre recombinase was used to delete cGKI selectively in SMCs of adult mice (Kuhbandner et al., 2000; Wolfsgruber et al., 2003). The different susceptibility of selected mouse strains to atherosclerosis and injury-induced lesion formation was anticipated because the main cause of lesion development following ligation is a drastic reduction of shear stress and turbulence of blood flow in the injured vessel (Kumar and Lindner, 1997). In addition to these changes in flow, plaque formation in systemic atheroslerosis of apoE-deficient mice involves other cell types, such as monocyte-derived macrophages, lymphocytes, chondrocytes, and platelets, other molecular signaling pathways (e.g. inflammatory response), and other effectors (e.g. lipid accumulation) (Wang and Paigen, 2002). This comparison indicates that vascular lesion formation in different models is perhaps mediated by a different set of proteins (Harmon et al., 2000; Kuhel et al., 2002). Indeed, as discussed above, the relevance of cGMP-cGKI signaling for vascular proliferative disorders appears to be context-specific.

The cGMP-cGKI signaling cascade has also been analyzed in models of vascular injury that differ from the ligation model. The balloon injury model in rats has been used to evaluate the contribution of cGMP and cGKI to the restenosis process (Sinnaeve et al., 2002; Sinnaeve et al., 2001; Tulis et al., 2002). Adenoviral transfer of a constitutively active cGKI (Sinnaeve et al., 2002) or sGC in conjunction with the exogenous application of the NO-donor molsidomine (Sinnaeve et al., 2001) significantly reduced NI formation. Importantly, transfer of the cGKIβ isoform (Sinnaeve et al., 2002) or solely sGC (Sinnaeve et al., 2001) had no effect on vascular remodeling. In the same model, YC-1, reported to be a NO-independent activator of the sGC (Mulsch et al., 1997), prevented NI formation (Tulis et al., 2002). In these studies, endogenous cGMP levels after drug treatment were not determined. Furthermore, the authors did not differentiate strictly between effects carried by cGMP and SMC cGKI and those mediated by NO and other endothelial factors. Indeed, it was shown recently that YC-1 not only failed to elevate cGMP, but instead modified the activity of matrix metalloproteinases, a family of zinc-endopeptidases that degrade components of the extracellular matrix (Kuzuya and Iguchi, 2003), in a cGMP-independent manner (Liu et al.,

2006). The rat model differs significantly from the one used in the present study. Balloon injury damages the endothelium and completely changes the local transmitter environment. In contrast, as shown in this study, after ligation the endothelial cell layer is preserved (Fig. 12), and, therefore vasoactive substances should still be generated. Nevertheless, endothelial dysfunction might also occur in response to ligation. The injury exposes endothelial cells to a disturbed blood flow, and altered shear stress, which might result in an abnormal or disordered release of endothelium-derived factors, such as NO, due to e.g. a hypoxic environment (Cooke, 2003). Furthermore, after ligation-induced injury it remained unclear whether substrate proteins targeted by the cGMP-cGKI pathway are still functional or are even expressed. It is therefore likely that the relevant signaling pathway in the carotid ligation model differ significantly from those important in the balloon injury model. In the latter model, as already mentioned, cGKI expression was shown, and, remarkably, the cGKI substrate VASP was found as well (Monks et al., 1998).

As it is the case for many animal models, the carotid ligation injury has several limitations as a proper model for restenosis in human arteries. First, the injury is conducted in healthy vessels, whereas human restenosis progresses after the surgical intervention in atherosclerotic coronary arteries. Second, species-specific differences of cGMP-cGKI signaling during restenosis might lead to an underestimation of this pathway as a therapeutic target in human patients. Taken together, this study clearly demonstrates the presence of cGKI signaling after injury, however, the results shown here in conjunction with the data from other cGKI-deficient mouse models do not support a protective role of the smooth muscle cGMP-cGKI signaling cascade in vascular remodeling.

4.2 Cyclic nucleotide signaling in primary SMCs

The VASP protein is a common substrate for cGKI and cAK that was identified in various cell types including SMCs (Haffner et al., 1995). VASP is involved in the regulation of cytoskeletal dynamics, migration, and growth of SMCs (Krause et al., 2003). Additionally, VASP was proposed to be a valuable marker for the intracellular activity of cGKI and cAK (Feil et al., 2005a; Oelze et al., 2000).

In this study, phosphorylation of VASP was used as a biochemical marker to analyze the activity of both kinases after stimulation of primary SMCs with cyclic nucleotide analogs and

various cGMP-elevating agents. Platelets isolated from wild-type mice showed phosphorylation of VASP at Ser 157 upon treatment with 8-Br-cAMP and 8-Br-cGMP (Butt et al., 1994). Using antibodies that recognize total VASP, the analogs induced a dosage-dependent mobility shift of VASP from an apparent molecular weight of 46 kDa to 50 kDa indicating Ser 157 phosphorylation (Halbrugge and Walter, 1989). Interestingly, both 8-Br-cAMP and 8-Br-cGMP were effective in cGKI-deficient cells as well (Fig. 25). Recently, it was demonstrated in permeabilized aortas of wild-type and cGKI-deficient mice that the cGMP-dependent relaxation via Ca^{2+}-desensitization at high cGMP concentrations was mostly mediated by cAK (Worner et al., 2006). Together, these results suggest that, at least high concentrations of 8-Br-cGMP have the potential to either cross-activate cAK directly or to inhibit the SMC cAMP-hydrolyzing PDE-3 (Rybalkin et al., 2003). Both cGMP and cAMP levels depend on the rates of their synthesis by cyclases and degradation by PDEs. The cGMP-mediated inhibition of PDE-3 (Rybalkin et al., 2003) results in an increase of the intracellular cAMP level. Indeed, it was shown before that the NO-induced inhibition of platelet aggregation was caused partially by an accumulation of cAMP, resulting from a cGMP-induced PDE-3 inhibition (Maurice and Haslam, 1990). Stimulatory effects of NO-donors on cardiac calcium currents were explained by a similar mechanism (Kirstein et al., 1995). Novel findings obtained by using cGMP analogs and NO donors in human platelets depict that phosphorylation of VASP was independent of cGKI (Li et al., 2003a). In this study only cAK inhibitors efficiently diminished the phosphorylation, whereas cyclic nucleotide analogs that should inhibit cGKI were ineffective. In this context, it is important to note that the properties of several cGKI inhibitors used in the study mentioned above were questioned recently (P. Weinmeister and Prof. Dr. R. Feil, unpublished data 2006). In contrast to the analysis of VASP phophorylation in primary SMCs from wild-type and cGKI knockout mice, the phosphorylation in human platelets was accomplished by a cGMP-induced accumulation of cAMP. Opposing this view it was demonstrated in aortic rings of cGKI knockout mice that high concentrations of NO donors produced enough cGMP to directly activate the cAK (Sausbier et al., 2000). Direct activation of cAK by cGMP was also observed after downregulation of cGKI in SMCs (Soff et al., 1997). To determine in more detail whether a cross-talk of the two cyclic nucleotide pools via PDE-3 or a direct cross-activation of cAK by

cGMP accounted for the VASP phosphorylation in primary SMCs, several cGMP-elevating compounds were tested.

Sildenafil caused VASP phosphorylation at Ser 157 independently of cGKI (Fig. 25), and stimulated endogenous cGMP accumulation about 10-fold in wild-type and knockout cells, whereas no changes in the cAMP levels were detectable (Fig. 28). Consistent with these findings, it has been reported before that the specific PDE-5 inhibitor caused VASP phosphorylation in SMCs (Osinski et al., 2001). This phosphorylation event was at least in part abolished by the highly selective cAK inhibitor peptide PKI. Nevertheless, it remained unclear whether the accumulation of cGMP resulted in PDE-3 inhibition and/or in the direct stimulation of cAK. The current data suggest that cAK was rather activated directly by an increase in cGMP than by changes in cAMP following cGMP-mediated inhibition of PDE-3 since the cAMP level was unchanged after stimulation of primary SMCs with several cGMP-elevating agents (Fig. 28). Assuming the possibility that compartmentalization, i.e. the localization of the cGMP signal to different cellular regions, might lead to spatial cGMP peaks exceeding the global measurements performed in the present study, it is even more likely that cAK was activated directly (Piggott et al., 2006). Indeed, it is unclear whether cGMP-mediated events are dependent on the absolute level of a cGMP signal, or whether the relative increase is more important. Using natriuretic peptides, which elevate cGMP via the pGCs, and the NO-donor DEA-NO, which stimulates the sGC, endogenous cGMP levels were raised about 10-fold (CNP) to 30-fold (ANP and DEA-NO) as compared to basal levels (Fig. 28). The lower fold stimulation of cGMP accumulation elicited by CNP as compared to ANP and DEA-NO was in line with relatively weak phosphorylation of VASP at Ser 157 in cells stimulated with CNP (Fig. 27). Notably, previous findings using NO-donors (Sausbier et al., 2000) are in agreement with the cGMP measurements performed in this study (Fig. 28). Using different approaches, there is clear evidence that cGMP increases in wild-type and cGKI knockouts are similar after stimulation with DEA-NO, sildenafil, ANP and CNP. By a feedback regulation the PDE-5 is known to be phosphorylated by cGKI. This phosphorylation increases the enzyme activity to hydrolyze cGMP (Mullershausen et al., 2003). It is therefore likely that the major PDE regulating cGMP levels in SMCs is not the PDE-5 isoform (Hofmann et al., 2004). In particular, in primary SMCs lacking cGKI this feedback mechanism that regulates the activity of PDE-5 is assumed to be inactive, and, thus, cGMP should be

increased. However, the cGMP levels in wild-type and knockout cells were similar after stimulation with various cGMP-elevating agents (Fig. 28). Additionally, the phosphorylation might be carried solely by cAK in cGKI-deficient cells (Murthy, 2001). Again, the cGMP-elevating compounds confirmed the concept of a direct cross-activation of cAK in primary SMCs since there was no raise or fall in cAMP levels detectable.

Apart from 8-Br-cGMP (Fig. 25), the VASP phosphorylation kinetics and levels detected in primary SMCs isolated from wild-type cells were comparable to those from cGKI knockouts (Fig. 26+27). These findings indicate once more that the cellular changes in cGMP, induced by various elevating drugs, directly stimulated the SMC cAK of cGKI-deficient cells. It might be possible that in knockout cells a functional compensation of cGKI in the cGMP-cGKI-VASP[157] pathway by cAK accounts for these phosphorylation events. This hypothesis could be tested by using a variety of genetic tools. A small interfering RNA (siRNA) based knockdown strategy could be applied to deplete cGKI in SMCs of wild-type animals (Tuschl and Borkhardt, 2002). This reversible short-term suppression of the cGKI protein by targeting its transcipt should prevent a functional compensation of the pathway. Furthermore, to bypass possible compensation, the floxed cGKI mouse line (Wegener et al., 2002) in combination with an inducible SMC-specific Cre-loxP recombination approach based on e.g. tamoxifen (Kuhbandner et al., 2000), or alternatively a cell-permeable Cre (Lin et al., 2004) would also be helpful. In these experimental systems the importance of cAK for the cGMP-induced VASP phosphorylation could be tested by a pharmacological approach using the highly selective cAK inhibitor peptide PKI (Worner et al., 2006). Furthermore, green fluorescent protein mutants fused to the cAK subunits might provide further insights into a direct activation of the cAK tetramer. By the use of this technique the dissociation of the catalytic cAK subunits from the regulatory subunits upon cyclic nucleotide binding could be measured (Zaccolo et al., 2000).

In contrast to endogenously generated cGMP, low and high amounts of 8-Br-cGMP were less efficient in cGKI-deficient cells as compared to the wild-type (Fig. 25). This might arise from minor intracellular concentration or unfavorable localization of the analog as compared to endogenous cGMP accumulation following the stimulation of sGC, pGC, or the inhibition of PDE-5. Additionally, the bromo substitution of the analog might hinder an optimal activation of cAK. Indeed, it was shown that the C-8 modification of cGMP caused a significant

decrease in affinity to a noncatalytic binding site of the PDE-6 expressed in rod cells (Hebert et al., 1998). This implicates that the binding of cGMP to cAK might as well involve multiple sites of interaction. Thus, in contrast to the binding affinity of 8-Br-cGMP to cGKI (Francis et al., 1988; Pohler et al., 1995; Sekhar et al., 1992), binding and activation of the derivate to cAK might be reduced by the 8-bromo substituent.

Although the functional relevance of the Ser 157 phosphorylation of VASP is still under investigation, it was implicated in VASP-mediated modulation of the cytoskeleton (Laurent et al., 1999). In addition, it was shown that the growth effects of VASP in SMCs were dependent on the Ser 157 phosphorylation site (Chen et al., 2004). Recently, VASP was identified as a substrate for protein kinase C (PKC) (Chitaley et al., 2004). PKC phosphorylation of VASP is also carried out at Ser 157. Thus, it is tempting to speculate that after stimulation of SMCs with cGMP-elevating drugs, such as sildenafil, NPs, and DEA-NO, the PKC was activated. So far, a potential mechanism underlying this postulated activation of PKC in SMCs is not known.

In conclusion, as monitored by the phosphorylation of VASP, the *in vitro* data presented here indicate that cAK plays an important role in the cGMP-induced VASP phosphorylation. This suggests that cAK might be an effector protein of many compounds that elevate endogenous cGMP levels, and, in addition, cAK might compensate for many mechanisms carried by cGKI under normal conditions. Certainly, this hypothesis needs further confirmation by future experiments. The current data supports the concept of a possible NO-cGMP signaling pathway via cAK (Feil et al., 2005a; Hofmann et al., 2006; Osinski et al., 2001; Worner et al., 2006). This pathway might under certain conditions, in particular cells, and/or once cGKI is lacking or inactive, be as important as the NO-cGMP-cGKI pathway. Due to the fact that cAK and cGKI are expressed together in many cells an analysis of their individual functions might be complicated since they perhaps carry out the same, different, or opposing functions. In the present study, the *in vitro* findings implicate for the *in vivo* situation that, at least in ligation-induced restenosis of vessels, the downstream target of NO signals might rather be cAK than cGKI. Indeed, the *in vivo* analysis of restenosis showed that cGKI is not important for the vascular remodeling.

5 SUMMARY

Nitric oxide (NO) is of crucial importance for smooth muscle cell (SMC) function and exerts numerous, sometimes opposing, effects on vascular proliferative diseases. Among these disorders is restenosis, the narrowing of an artery after intra-arterial intervention, such as balloon angioplasty or stent placement. The molecular downstream effectors of NO in restenosis are not clear. In SMCs, NO exerts many of its effects via the second messenger cyclic guanosine-3´,5´-monophosphate (cGMP). The cGMP-dependent protein kinase type I (cGKI) is presumably the major mediator of NO-cGMP signaling in SMCs. The purpose of this study was to examine the functional role of the SMC NO-cGMP-cGKI pathway in restenosis. By using the Cre-loxP site-specific recombination system, tissue-specific mouse mutants were generated in which the cGKI protein was efficiently ablated in SMCs and, to a lesser extent, also in cardiomyocytes. It was tested whether this conditional inactivation of cGKI would effect vascular remodeling after carotid ligation. Remodeling was analyzed by morphometry and immunohistochemistry. Based on the neointima/media ratio and other vessel parameters as well as on various immunostainings, no significant differences were detected between the conditional cGKI mutants and controls at different time points after injury, in normolipidemic as well as in apolipoprotein E-deficient mice. Moreover, continuous treatment of injured wild-type mice with the phosphodiesterase 5 inhibitor sildenafil (Viagra®) indicated that elevated cGMP levels had no influence on ligation-induced remodeling. Thus, vascular remodeling after mechanical injury was altered neither by the deletion of smooth muscle cGKI nor by sildenafil treatment. Finally, this work addressed the effects of different cGMP-elevating agents, such as sildenafil, 2-(N,N-diethylamino)-diazenolate-2-oxide (DEA-NO), and natriuretic peptides, on cyclic nucleotide signaling in primary vascular SMCs. These experiments indicated that endogenously generated cGMP might cross-activate cAMP-dependent protein kinase (cAK), at least in the absence of cGKI. Together, the results of the present study indicate that NO signaling in restenosis is independent of the cGMP-cGKI pathway and perhaps mediated via an unconventional NO-cGMP-cAK pathway.

6 APPENDIX

6.1 Abbreviations

α-SMA	α-smooth muscle actin
$[Ca^{2+}]_i$	intracellular calcium concentration
µM	micromoles per liter
8-Br-cAMP	8-bromoadenosine-3´,5´-cyclic monophosphate
8-Br-cGMP	8-bromoguanosine-3´,5´-cyclic monophosphate
AMP	adenosine-5´-monophosphate
ANP	atrial natriuretic peptide
apoE	apolipoprotein E
APS	ammonium persulfate
ATP	adenosine-5´-triphosphate
bp	base pairs
$BK_{Ca}{}^{2+}$-channel	calcium-sensitive potassium channel
BNP	brain natriuretic peptide
BSA	bovine serum albumin
cAK	cAMP-dependent protein kinase
Ca^{2+}-CaM	Ca^{2+}-calmodulin
cAMP	cyclic adenosine-3´,5´-monophosphate
CCA	common carotid artery
cereb	cerebellum
CFTR channel	cystic fibrosis trans-membrane conductance regulator ion channel
cGK	cGMP-dependent protein kinase
cGKI	cGMP-dependent protein kinase type I
cGKIα	cGK type Iα
cGKIβ	cGK type Iβ
$cGKI^{csmko}$	conditional knockout of cGKI in cardiac and smooth muscle cells
cGKII	cGK type II
cGMP	cyclic guanosine-3´,5´-monophosphate
CNG channel	cyclic nucleotide-gated cation channel
CNP	C-type natriuretic peptide
COS-7	african green monkey kidney cell line
Cre	cyclization recombination
ctr	control
Cu^{2+}	copper-ion
d	days
DAB	3,3´-diaminobenzidine tetrahydrochloride
ddH_2O	double distilled water
DEA-NO	2-(N,N-diethylamino)-diazenolate-2-oxide
DMEM	Dulbecco's modified Eagle's medium
DMSO	dimethyl sulfoxide
DNA	deoxyribonucleic acid
dNTP	deoxynucleotide tri-phosphate
DTT	1,4-Dithiothreitol
duod	duodenum
ECL	enhanced chemiluminescent
EDTA	ethylenediaminetetraacetic acid tetrasodium salt
EEL	external elastic lamina
eNOS	endothelial NOS
ER	endoplasmic reticulum
EtOH	ethanol
f	forward primer
FCS	fetal calfserum
Fig.	figure
floxed	loxP-flanked
g	grams or relative centrifugal force
GMP	guanosine-5´-monophosphate
GPCR	G-protein-coupled receptor
GTP	guanosine-5´-triphosphate
h	hour
H&E	hematoxilin and eosin

HEPES	4-(2-hydroxyethyl)-1-piperazineethanesulfonic acid
HRP	horseradish peroxidase
IEL	internal elastic lamina
iNOS	inducible NOS
IP_3	inositol 1,4,5-triphosphate
IP_3RI	IP_3-receptor-I
IRAG	IP_3-receptor associated cGMP-kinase substrate
kb	kilo-base
KCl	potassium chloride
kDa	kilo dalton
ko	knockout
L-	cGKI knockout allele
L2	loxP-flanked exon 10 of cGKI
LacZ	β-galactosidase
loxP	locus of X-over of P1
LPS	lipopolysaccharide
m	media
M	moles per liter
mM	millimoles per liter
MW	molecular weight
MAPK	p42/p44 mitogen-activated protein kinase
$MgCl_2$	magnesium chloride
MLCK	myosin light chain kinase
MLCP	myosin light chain phosphatase
mol	mole
nM	nanomoles per liter
MYPT1	myosin phosphatase regulatory targeting subunit-1
NaOH	sodium hydroxide
neo	neomycine-resistance gene
NGS	normal goat serum
NI	neointima
nNOS	neuronal NOS
NO	nitric oxide
NOS	NO synthase
NP	natriuretic peptide
OD	optical density
p.a.	pro analysi
PBS	phosphate buffered saline
PCNA	proliferating cell nuclear antigen
PCR	polymerase chain reaction
PDE	phosphodiesterase
Pen/strep	Penicillin-streptomycin
pGC	particulate guanylyl cyclase
PK	proteinase K
PKC	protein kinase C
PLC-β	phospholipase C-β
PMSF	phenylmethylsulphonyl-fluoride
P-VASP^{157}	phospho-Ser^{157}-VASP
PVDF	polyvinyliden difluoride
prkg	gene locus for cGK
r	reverse primer
R26R	ROSA26 Cre reporter
RGS-2	regulator of G-protein signaling-2
RLC	myosin regulatory light chain
RT	room temperature
S	sildenafil
SDS	sodium dodecyl sulfate
Ser	serine
siRNA	small interfering RNA
sGC	soluble guanylyl cyclase
SM	smooth muscle
SM22α	smooth muscle specific protein with 22 kDa
SMCs	smooth muscle cells
TBE	Tris-borate-EDTA buffer
TBS	Tris-buffered saline
TBS-T	Tris-Tween-buffered saline
TE	Tris-EDTA buffer
TEMED	N,N,N',N'-tetramethylethylenediamine
tg	transgene
Tris	2-amino-2-hydroxymethyl-1,3-propanediol
U	units
UV	ultraviolett
v	volume
VASP	vasodilator-stimulated phosphoprotein
vWF	von Willebrand factor
w	weight
wt	wild-type
X-Gal	5-Bromo-4-chloro-3-indolyl β–D-galactoside
YC-1	3-(5'-hydroxymethyl-2'furyl)-1-benzyl indazole

6.2 Primer

6.2.1 Oligonucleotides

primer	sequence	gene
RF53	5´-cct ggc tgt gat ttc act cca-3´	cGKI_f
RF118	5´-aaa tta taa ctt gtc aaa ttc ttg-3´	cGKI_r
RF125	5´-gtc aag tga cca cta tg-3´	cGKI_r
RF115 (oIMR180)	5´-gcc tag ccg agg gag agc cg-3´	apoE_f
RF116 (oIMR181)	5´-tgt gac ttg gga gct ctg cag c-3´	apoE_r
RF117 (oIMR182)	5´-gcc gcc ccg act gca tct-3´	apoE_r
MG-Cre800	5´-gct gcc acg acc aag tga cag caa tg-3´	Cre_f
MG-Cre1200	5´-gta gtt att cgg atc atc agc tac ac-3´	Cre_r
RF126 (oIMR0883)	5´-aaa gtc gct ctg agt tgt tat-3´	R26R_f
RF127 (oIMR0315)	5´-gcg aag agt ttg tcc tca acc-3´	R26R_r
RF128 (oIMR0316)	5´-gga gcg gga gaa atg gat atg-3´	R26R_r

6.2.2 Mouse genotyping PCRs

mouse line	primer pair(s)	detectable allele	amplicon
floxed cGKI	RF53+ RF118	L-	250 bp
	RF53+ RF125	L2	338 bp
	RF53+ RF125	wt	284 bp
apoE	RF115+RF116	wt	155 bp
	RF115+RF117	ko	245 bp
SM22α-Cre	MG-Cre800+ MG-Cre1200	tg	402 bp
R26R Cre reporter	RF126+RF127	tg	250 bp
	RF126+ RF128	wt	550 bp

6.3 Antibodies

6.3.1 Primary antibodies

antibody	origin	application (dilution)	references
cGKI	polyclonal rabbit	Immunohistochemistry (1:50)	Prof. Dr. F. Hofmann (München)
cGKI	polyclonal rabbit	Western blot (1:200)	Prof. Dr. F. Hofmann (München)
MAPK	polyclonal rabbit	Western blot (1:1000)	Cell signaling (9102)
vWF	polyclonal rabbit	Immunohistochemistry (1:400)	DAKO (A0082)
Mac-2	monoclonal rat	Immunohistochemistry (1:100)	Cedarlane (CL8942AP)
PCNA	polyclonal rabbit	Immunohistochemistry (1:100)	Santa Cruz (sc-7907)
αSMA	monoclonal mouse	Immunohistochemistry (1:5000)	Sigma (A-2547)
VASP	polyclonal rabbit	Western blot (1:4000)	Alexis (ALX-210-880)
Akt	polyclonal rabbit	Western blot (1:1000)	Cell signaling (9272)

6.3.2 Secondary antibodies

antibody	origin	application (dilution)	references
biotinylated-anti-rabbit	goat	Immunohistochemistry (1:200)	Vector (BA-1000)
biotinylated-anti-rat	rabbit	Immunohistochemistry (1:200)	Vector (BA-4001)
biotinylated-anti-mouse	horse	Immunohistochemistry (1:200)	Vector (BA-2000)
anti-rabbit-HRP	goat	Western blot (1:2000)	Cell signaling (7074)

7 REFERENCES

Alioua, A., Tanaka, Y., Wallner, M., Hofmann, F., Ruth, P., Meera, P. and Toro, L. (1998) The large conductance, voltage-dependent, and calcium-sensitive K+ channel, Hslo, is a target of cGMP-dependent protein kinase phosphorylation in vivo. *J Biol Chem*, **273**, 32950-32956.

Anderson, P.G., Boerth, N.J., Liu, M., McNamara, D.B., Cornwell, T.L. and Lincoln, T.M. (2000) Cyclic GMP-dependent protein kinase expression in coronary arterial smooth muscle in response to balloon catheter injury. *Arterioscler Thromb Vasc Biol*, **20**, 2192-2197.

Barbato, J.E. and Tzeng, E. (2004) Nitric oxide and arterial disease. *J Vasc Surg*, **40**, 187-193.

Beckman, J.S. and Koppenol, W.H. (1996) Nitric oxide, superoxide, and peroxynitrite: the good, the bad, and ugly. *Am J Physiol*, **271**, C1424-1437.

Berk, B.C. (2001) Vascular smooth muscle growth: autocrine growth mechanisms. *Physiol Rev*, **81**, 999-1030.

Boerth, N.J., Dey, N.B., Cornwell, T.L. and Lincoln, T.M. (1997) Cyclic GMP-dependent protein kinase regulates vascular smooth muscle cell phenotype. *J Vasc Res*, **34**, 245-259.

Brophy, C.M., Woodrum, D.A., Pollock, J., Dickinson, M., Komalavilas, P., Cornwell, T.L. and Lincoln, T.M. (2002) cGMP-dependent protein kinase expression restores contractile function in cultured vascular smooth muscle cells. *J Vasc Res*, **39**, 95-103.

Butt, E., Abel, K., Krieger, M., Palm, D., Hoppe, V., Hoppe, J. and Walter, U. (1994) cAMP- and cGMP-dependent protein kinase phosphorylation sites of the focal adhesion vasodilator-stimulated phosphoprotein (VASP) in vitro and in intact human platelets. *J Biol Chem*, **269**, 14509-14517.

Carmeliet, P., Moons, L., Stassen, J.M., De Mol, M., Bouche, A., van den Oord, J.J., Kockx, M. and Collen, D. (1997) Vascular wound healing and neointima formation induced by perivascular electric injury in mice. *Am J Pathol*, **150**, 761-776.

Channon, K.M., Qian, H. and George, S.E. (2000) Nitric oxide synthase in atherosclerosis and vascular injury: insights from experimental gene therapy. *Arterioscler Thromb Vasc Biol*, **20**, 1873-1881.

Chao, D.S., Silvagno, F., Xia, H., Cornwell, T.L., Lincoln, T.M. and Bredt, D.S. (1997) Nitric oxide synthase and cyclic GMP-dependent protein kinase concentrated at the neuromuscular endplate. *Neuroscience*, **76**, 665-672.

Chen, L., Daum, G., Chitaley, K., Coats, S.A., Bowen-Pope, D.F., Eigenthaler, M., Thumati, N.R., Walter, U. and Clowes, A.W. (2004) Vasodilator-stimulated phosphoprotein regulates proliferation and growth inhibition by nitric oxide in vascular smooth muscle cells. *Arterioscler Thromb Vasc Biol*, **24**, 1403-1408.

Chiche, J.D., Schlutsmeyer, S.M., Bloch, D.B., de la Monte, S.M., Roberts, J.D., Jr., Filippov, G., Janssens, S.P., Rosenzweig, A. and Bloch, K.D. (1998) Adenovirus-mediated gene transfer of cGMP-dependent protein kinase increases the sensitivity of cultured vascular smooth muscle cells to the antiproliferative and pro-apoptotic effects of nitric oxide/cGMP. *J Biol Chem*, **273**, 34263-34271.

Chitaley, K., Chen, L., Galler, A., Walter, U., Daum, G. and Clowes, A.W. (2004) Vasodilator-stimulated phosphoprotein is a substrate for protein kinase C. *FEBS Lett*, **556**, 211-215.

Chyu, K.Y., Dimayuga, P., Zhu, J., Nilsson, J., Kaul, S., Shah, P.K. and Cercek, B. (1999) Decreased neointimal thickening after arterial wall injury in inducible nitric oxide synthase knockout mice. *Circ Res*, **85**, 1192-1198.

Cooke, J.P. (2003) Flow, NO, and atherogenesis. *Proc Natl Acad Sci U S A*, **100**, 768-770.

Corbin, J.D., Ogreid, D., Miller, J.P., Suva, R.H., Jastorff, B. and Doskeland, S.O. (1986) Studies of cGMP analog specificity and function of the two intrasubunit binding sites of cGMP-dependent protein kinase. *J Biol Chem*, **261**, 1208-1214.

Demoliou-Mason, C.D. (1998) G-protein-coupled receptors in vascular smooth muscle cells. *Biol Signals Recept*, **7**, 90-97.

Detmers, P.A., Hernandez, M., Mudgett, J., Hassing, H., Burton, C., Mundt, S., Chun, S., Fletcher, D., Card, D.J., Lisnock, J., Weikel, R., Bergstrom, J.D., Shevell, D.E., Hermanowski-Vosatka, A., Sparrow, C.P., Chao, Y.S., Rader, D.J., Wright, S.D. and Pure, E. (2000) Deficiency in inducible nitric oxide synthase results in reduced atherosclerosis in apolipoprotein E-deficient mice. *J Immunol*, **165**, 3430-3435.

Dong, S. and Hughes, R.C. (1997) Macrophage surface glycoproteins binding to galectin-3 (Mac-2-antigen). *Glycoconj J*, **14**, 267-274.

Draijer, R., Vaandrager, A.B., Nolte, C., de Jonge, H.R., Walter, U. and van Hinsbergh, V.W. (1995) Expression of cGMP-dependent protein kinase I and phosphorylation of its substrate, vasodilator-stimulated phosphoprotein, in human endothelial cells of different origin. *Circ Res*, **77**, 897-905.

Dzau, V.J., Braun-Dullaeus, R.C. and Sedding, D.G. (2002) Vascular proliferation and atherosclerosis: new perspectives and therapeutic strategies. *Nat Med*, **8**, 1249-1256.

Eigenthaler, M., Nolte, C., Halbrugge, M. and Walter, U. (1992) Concentration and regulation of cyclic nucleotides, cyclic-nucleotide-dependent protein kinases and one of their major substrates in human platelets. Estimating the rate of cAMP-regulated and cGMP-regulated protein phosphorylation in intact cells. *Eur J Biochem*, **205**, 471-481.

El-Husseini, A.E., Williams, J., Reiner, P.B., Pelech, S. and Vincent, S.R. (1999) Localization of the cGMP-dependent protein kinases in relation to nitric oxide synthase in the brain. *J Chem Neuroanat*, **17**, 45-55.

Feil, R., Feil, S. and Hofmann, F. (2005a) A heretical view on the role of NO and cGMP in vascular proliferative diseases. *Trends Mol Med*, **11**, 71-75.

Feil, R., Hartmann, J., Luo, C., Wolfsgruber, W., Schilling, K., Feil, S., Barski, J.J., Meyer, M., Konnerth, A., De Zeeuw, C.I. and Hofmann, F. (2003a) Impairment of LTD and cerebellar learning by Purkinje cell-specific ablation of cGMP-dependent protein kinase I. *J Cell Biol*, **163**, 295-302.

Feil, R., Hofmann, F. and Kleppisch, T. (2005b) Function of cGMP-dependent protein kinases in the nervous system. *Rev Neurosci*, **16**, 23-41.

Feil, R., Lohmann, S.M., de Jonge, H., Walter, U. and Hofmann, F. (2003b) Cyclic GMP-dependent protein kinases and the cardiovascular system: insights from genetically modified mice. *Circ Res*, **93**, 907-916.

Feil, S., Zimmermann, P., Knorn, A., Brummer, S., Schlossmann, J., Hofmann, F. and Feil, R. (2005c) Distribution of cGMP-dependent protein kinase type I and its isoforms in the mouse brain and retina. *Neuroscience*, **135**, 863-868.

Ferns, G.A. and Avades, T.Y. (2000) The mechanisms of coronary restenosis: insights from experimental models. *Int J Exp Pathol*, **81**, 63-88.

Foster, M.W., McMahon, T.J. and Stamler, J.S. (2003) S-nitrosylation in health and disease. *Trends Mol Med*, **9**, 160-168.

Francis, S.H., Noblett, B.D., Todd, B.W., Wells, J.N. and Corbin, J.D. (1988) Relaxation of vascular and tracheal smooth muscle by cyclic nucleotide analogs that preferentially activate purified cGMP-dependent protein kinase. *Mol Pharmacol*, **34**, 506-517.

Fukao, M., Mason, H.S., Britton, F.C., Kenyon, J.L., Horowitz, B. and Keef, K.D. (1999) Cyclic GMP-dependent protein kinase activates cloned BKCa channels expressed in mammalian cells by direct phosphorylation at serine 1072. *J Biol Chem*, **274**, 10927-10935.

Furchgott, R.F. and Zawadzki, J.V. (1980) The obligatory role of endothelial cells in the relaxation of arterial smooth muscle by acetylcholine. *Nature*, **288**, 373-376.

Gambaryan, S., Hausler, C., Markert, T., Pohler, D., Jarchau, T., Walter, U., Haase, W., Kurtz, A. and Lohmann, S.M. (1996) Expression of type II cGMP-dependent protein

kinase in rat kidney is regulated by dehydration and correlated with renin gene expression. *J Clin Invest*, **98**, 662-670.
Garbers, D.L. and Lowe, D.G. (1994) Guanylyl cyclase receptors. *J Biol Chem*, **269**, 30741-30744.
Garg, U.C. and Hassid, A. (1989) Nitric oxide-generating vasodilators and 8-bromo-cyclic guanosine monophosphate inhibit mitogenesis and proliferation of cultured rat vascular smooth muscle cells. *J Clin Invest*, **83**, 1774-1777.
Geiselhoringer, A., Gaisa, M., Hofmann, F. and Schlossmann, J. (2004) Distribution of IRAG and cGKI-isoforms in murine tissues. *FEBS Lett*, **575**, 19-22.
Glass, C.K. and Witztum, J.L. (2001) Atherosclerosis. the road ahead. *Cell*, **104**, 503-516.
Gross, S.S. and Wolin, M.S. (1995) Nitric oxide: pathophysiological mechanisms. *Annu Rev Physiol*, **57**, 737-769.
Haffner, C., Jarchau, T., Reinhard, M., Hoppe, J., Lohmann, S.M. and Walter, U. (1995) Molecular cloning, structural analysis and functional expression of the proline-rich focal adhesion and microfilament-associated protein VASP. *Embo J*, **14**, 19-27.
Halbrugge, M. and Walter, U. (1989) Purification of a vasodilator-regulated phosphoprotein from human platelets. *Eur J Biochem*, **185**, 41-50.
Hanafy, K.A., Krumenacker, J.S. and Murad, F. (2001) NO, nitrotyrosine, and cyclic GMP in signal transduction. *Med Sci Monit*, **7**, 801-819.
Hao, H., Gabbiani, G. and Bochaton-Piallat, M.L. (2003) Arterial smooth muscle cell heterogeneity: implications for atherosclerosis and restenosis development. *Arterioscler Thromb Vasc Biol*, **23**, 1510-1520.
Harmon, K.J., Couper, L.L. and Lindner, V. (2000) Strain-dependent vascular remodeling phenotypes in inbred mice. *Am J Pathol*, **156**, 1741-1748.
Hebert, M.C., Schwede, F., Jastorff, B. and Cote, R.H. (1998) Structural features of the noncatalytic cGMP binding sites of frog photoreceptor phosphodiesterase using cGMP analogs. *J Biol Chem*, **273**, 5557-5565.
Hepler, J.R. (1999) Emerging roles for RGS proteins in cell signalling. *Trends Pharmacol Sci*, **20**, 376-382.
Hofmann, F. (2005) The biology of cyclic GMP-dependent protein kinases. *J Biol Chem*, **280**, 1-4.
Hofmann, F., Ammendola, A. and Schlossmann, J. (2000) Rising behind NO: cGMP-dependent protein kinases. *J Cell Sci*, **113 (Pt 10)**, 1671-1676.
Hofmann, F., Biel, M., Feil, R. and Kleppisch, T. (2004) Mouse models of NO/Natriuretic Peptide/cGMP Kinase Signaling. In Offermanns, S. (ed.), *Handbook of Experimental Pharmacology (Vol. 159)*. Springer-Verlag, Berlin Heidelberg, Vol. 159, pp. 95-130.
Hofmann, F., Feil, R., Kleppisch, T. and Schlossmann, J. (2006) Function of cGMP-dependent protein kinases as revealed by gene deletion. *Physiol Rev*, **86**, 1-23.
Hofmann, F. and Sold, G. (1972) A protein kinase activity from rat cerebellum stimulated by guanosine-3':5'-monophosphate. *Biochem Biophys Res Commun*, **49**, 1100-1107.
Holtwick, R., Gotthardt, M., Skryabin, B., Steinmetz, M., Potthast, R., Zetsche, B., Hammer, R.E., Herz, J. and Kuhn, M. (2002) Smooth muscle-selective deletion of guanylyl cyclase-A prevents the acute but not chronic effects of ANP on blood pressure. *Proc Natl Acad Sci U S A*, **99**, 7142-7147.
Ignarro, L.J., Buga, G.M., Wood, K.S., Byrns, R.E. and Chaudhuri, G. (1987) Endothelium-derived relaxing factor produced and released from artery and vein is nitric oxide. *Proc Natl Acad Sci U S A*, **84**, 9265-9269.
Janssens, S., Flaherty, D., Nong, Z., Varenne, O., van Pelt, N., Haustermans, C., Zoldhelyi, P., Gerard, R. and Collen, D. (1998) Human endothelial nitric oxide synthase gene transfer inhibits vascular smooth muscle cell proliferation and neointima formation after balloon injury in rats. *Circulation*, **97**, 1274-1281.
Joyce, N.C., DeCamilli, P., Lohmann, S.M. and Walter, U. (1986) cGMP-dependent protein kinase is present in high concentrations in contractile cells of the kidney vasculature. *J Cyclic Nucleotide Protein Phosphor Res*, **11**, 191-198.

Karaki, H., Ozaki, H., Hori, M., Mitsui-Saito, M., Amano, K., Harada, K., Miyamoto, S., Nakazawa, H., Won, K.J. and Sato, K. (1997) Calcium movements, distribution, and functions in smooth muscle. *Pharmacol Rev*, **49**, 157-230.

Kaupp, U.B. and Seifert, R. (2002) Cyclic nucleotide-gated ion channels. *Physiol Rev*, **82**, 769-824.

Kawashima, S., Yamashita, T., Ozaki, M., Ohashi, Y., Azumi, H., Inoue, N., Hirata, K., Hayashi, Y., Itoh, H. and Yokoyama, M. (2001) Endothelial NO synthase overexpression inhibits lesion formation in mouse model of vascular remodeling. *Arterioscler Thromb Vasc Biol*, **21**, 201-207.

Keilbach, A., Ruth, P. and Hofmann, F. (1992) Detection of cGMP dependent protein kinase isozymes by specific antibodies. *Eur J Biochem*, **208**, 467-473.

Kirstein, M., Rivet-Bastide, M., Hatem, S., Benardeau, A., Mercadier, J.J. and Fischmeister, R. (1995) Nitric oxide regulates the calcium current in isolated human atrial myocytes. *J Clin Invest*, **95**, 794-802.

Kleppisch, T. (1999) Langzeitpotenzierung im Hippocampus: Die funktionelle Rolle von zyklischem Guanosinmonophosphat und der Zyklo-Guanosinmonophosphat-abhängigen Proteinkinase. *Habilitationsschrift*.

Kleppisch, T., Pfeifer, A., Klatt, P., Ruth, P., Montkowski, A., Fassler, R. and Hofmann, F. (1999) Long-term potentiation in the hippocampal CA1 region of mice lacking cGMP-dependent kinases is normal and susceptible to inhibition of nitric oxide synthase. *J Neurosci*, **19**, 48-55.

Kleppisch, T., Wolfsgruber, W., Feil, S., Allmann, R., Wotjak, C.T., Goebbels, S., Nave, K.A., Hofmann, F. and Feil, R. (2003) Hippocampal cGMP-dependent protein kinase I supports an age- and protein synthesis-dependent component of long-term potentiation but is not essential for spatial reference and contextual memory. *J Neurosci*, **23**, 6005-6012.

Knowles, J.W., Reddick, R.L., Jennette, J.C., Shesely, E.G., Smithies, O. and Maeda, N. (2000) Enhanced atherosclerosis and kidney dysfunction in eNOS(-/-)Apoe(-/-) mice are ameliorated by enalapril treatment. *J Clin Invest*, **105**, 451-458.

Koeppen, M., Feil, R., Siegl, D., Feil, S., Hofmann, F., Pohl, U. and de Wit, C. (2004) cGMP-dependent protein kinase mediates NO- but not acetylcholine-induced dilations in resistance vessels in vivo. *Hypertension*, **44**, 952-955.

Komalavilas, P. and Lincoln, T.M. (1996) Phosphorylation of the inositol 1,4,5-trisphosphate receptor. Cyclic GMP-dependent protein kinase mediates cAMP and cGMP dependent phosphorylation in the intact rat aorta. *J Biol Chem*, **271**, 21933-21938.

Krause, M., Dent, E.W., Bear, J.E., Loureiro, J.J. and Gertler, F.B. (2003) Ena/VASP proteins: regulators of the actin cytoskeleton and cell migration. *Annu Rev Cell Dev Biol*, **19**, 541-564.

Kuhbandner, S., Brummer, S., Metzger, D., Chambon, P., Hofmann, F. and Feil, R. (2000) Temporally controlled somatic mutagenesis in smooth muscle. *Genesis*, **28**, 15-22.

Kuhel, D.G., Zhu, B., Witte, D.P. and Hui, D.Y. (2002) Distinction in genetic determinants for injury-induced neointimal hyperplasia and diet-induced atherosclerosis in inbred mice. *Arterioscler Thromb Vasc Biol*, **22**, 955-960.

Kuhlencordt, P.J., Chen, J., Han, F., Astern, J. and Huang, P.L. (2001a) Genetic deficiency of inducible nitric oxide synthase reduces atherosclerosis and lowers plasma lipid peroxides in apolipoprotein E-knockout mice. *Circulation*, **103**, 3099-3104.

Kuhlencordt, P.J., Gyurko, R., Han, F., Scherrer-Crosbie, M., Aretz, T.H., Hajjar, R., Picard, M.H. and Huang, P.L. (2001b) Accelerated atherosclerosis, aortic aneurysm formation, and ischemic heart disease in apolipoprotein E/endothelial nitric oxide synthase double-knockout mice. *Circulation*, **104**, 448-454.

Kumar, A. and Lindner, V. (1997) Remodeling with neointima formation in the mouse carotid artery after cessation of blood flow. *Arterioscler Thromb Vasc Biol*, **17**, 2238-2244.

Kumar, R., Joyner, R.W., Komalavilas, P. and Lincoln, T.M. (1999) Analysis of expression of cGMP-dependent protein kinase in rabbit heart cells. *J Pharmacol Exp Ther*, **291**, 967-975.

Kuzuya, M. and Iguchi, A. (2003) Role of matrix metalloproteinases in vascular remodeling. *J Atheroscler Thromb*, **10**, 275-282.

Lakso, M., Sauer, B., Mosinger, B., Jr., Lee, E.J., Manning, R.W., Yu, S.H., Mulder, K.L. and Westphal, H. (1992) Targeted oncogene activation by site-specific recombination in transgenic mice. *Proc Natl Acad Sci U S A*, **89**, 6232-6236.

Laurent, V., Loisel, T.P., Harbeck, B., Wehman, A., Grobe, L., Jockusch, B.M., Wehland, J., Gertler, F.B. and Carlier, M.F. (1999) Role of proteins of the Ena/VASP family in actin-based motility of Listeria monocytogenes. *J Cell Biol*, **144**, 1245-1258.

Li, H. and Forstermann, U. (2000) Nitric oxide in the pathogenesis of vascular disease. *J Pathol*, **190**, 244-254.

Li, L., Miano, J.M., Cserjesi, P. and Olson, E.N. (1996) SM22 alpha, a marker of adult smooth muscle, is expressed in multiple myogenic lineages during embryogenesis. *Circ Res*, **78**, 188-195.

Li, Z., Ajdic, J., Eigenthaler, M. and Du, X. (2003a) A predominant role for cAMP-dependent protein kinase in the cGMP-induced phosphorylation of vasodilator-stimulated phosphoprotein and platelet inhibition in humans. *Blood*, **101**, 4423-4429.

Li, Z., Xi, X., Gu, M., Feil, R., Ye, R.D., Eigenthaler, M., Hofmann, F. and Du, X. (2003b) A stimulatory role for cGMP-dependent protein kinase in platelet activation. *Cell*, **112**, 77-86.

Lin, Q., Jo, D., Gebre-Amlak, K.D. and Ruley, H.E. (2004) Enhanced cell-permeant Cre protein for site-specific recombination in cultured cells. *BMC Biotechnol*, **4**, 25.

Lincoln, T.M., Dey, N. and Sellak, H. (2001) Invited review: cGMP-dependent protein kinase signaling mechanisms in smooth muscle: from the regulation of tone to gene expression. *J Appl Physiol*, **91**, 1421-1430.

Lindner, V., Fingerle, J. and Reidy, M.A. (1993) Mouse model of arterial injury. *Circ Res*, **73**, 792-796.

Liu, Y.N., Pan, S.L., Peng, C.Y., Guh, J.H., Huang, D.M., Chang, Y.L., Lin, C.H., Pai, H.C., Kuo, S.C., Lee, F.Y. and Teng, C.M. (2006) YC-1 [3-(5'-hydroxymethyl-2'-furyl)-1-benzyl indazole] inhibits neointima formation in balloon-injured rat carotid through suppression of expressions and activities of matrix metalloproteinases 2 and 9. *J Pharmacol Exp Ther*, **316**, 35-41.

Lloyd-Jones, D.M. and Bloch, K.D. (1996) The vascular biology of nitric oxide and its role in atherogenesis. *Annu Rev Med*, **47**, 365-375.

Lohmann, S.M., Walter, U., Miller, P.E., Greengard, P. and De Camilli, P. (1981) Immunohistochemical localization of cyclic GMP-dependent protein kinase in mammalian brain. *Proc Natl Acad Sci U S A*, **78**, 653-657.

Lukowski, R., Weber, S., Weinmeister, P., Feil, S. and Feil, R. (2005) Cre/loxP-vermittelte konditionale Mutagenese des cGMP-Signalwegs in der Maus. *Biospektrum*, Vol. 3, pp. 287-290.

Lusis, A.J. (2000) Atherosclerosis. *Nature*, **407**, 233-241.

Margariti, A., Zeng, L. and Xu, Q. (2006) Stem cells, vascular smooth muscle cells and atherosclerosis. *Histol Histopathol*, **21**, 979-985.

Markert, T., Vaandrager, A.B., Gambaryan, S., Pohler, D., Hausler, C., Walter, U., De Jonge, H.R., Jarchau, T. and Lohmann, S.M. (1995) Endogenous expression of type II cGMP-dependent protein kinase mRNA and protein in rat intestine. Implications for cystic fibrosis transmembrane conductance regulator. *J Clin Invest*, **96**, 822-830.

Massberg, S., Sausbier, M., Klatt, P., Bauer, M., Pfeifer, A., Siess, W., Fassler, R., Ruth, P., Krombach, F. and Hofmann, F. (1999) Increased adhesion and aggregation of platelets lacking cyclic guanosine 3',5'-monophosphate kinase I. *J Exp Med*, **189**, 1255-1264.

Maurice, D.H. and Haslam, R.J. (1990) Molecular basis of the synergistic inhibition of platelet function by nitrovasodilators and activators of adenylate cyclase: inhibition of cyclic AMP breakdown by cyclic GMP. *Mol Pharmacol*, **37**, 671-681.

Mendelsohn, M.E. (2005) Viagra: now mending hearts. *Nat Med*, **11**, 115-116.

Metzger, D. and Feil, R. (1999) Engineering the mouse genome by site-specific recombination. *Curr Opin Biotechnol*, **10**, 470-476.

Monks, D., Lange, V., Silber, R.E., Markert, T., Walter, U. and Nehls, V. (1998) Expression of cGMP-dependent protein kinase I and its substrate VASP in neointimal cells of the injured rat carotid artery. *Eur J Clin Invest*, **28**, 416-423.

Morishita, T., Tsutsui, M., Shimokawa, H., Horiuchi, M., Tanimoto, A., Suda, O., Tasaki, H., Huang, P.L., Sasaguri, Y., Yanagihara, N. and Nakashima, Y. (2002) Vasculoprotective roles of neuronal nitric oxide synthase. *Faseb J*, **16**, 1994-1996.

Moroi, M., Zhang, L., Yasuda, T., Virmani, R., Gold, H.K., Fishman, M.C. and Huang, P.L. (1998) Interaction of genetic deficiency of endothelial nitric oxide, gender, and pregnancy in vascular response to injury in mice. *J Clin Invest*, **101**, 1225-1232.

Mullershausen, F., Friebe, A., Feil, R., Thompson, W.J., Hofmann, F. and Koesling, D. (2003) Direct activation of PDE5 by cGMP: long-term effects within NO/cGMP signaling. *J Cell Biol*, **160**, 719-727.

Mulsch, A., Bauersachs, J., Schafer, A., Stasch, J.P., Kast, R. and Busse, R. (1997) Effect of YC-1, an NO-independent, superoxide-sensitive stimulator of soluble guanylyl cyclase, on smooth muscle responsiveness to nitrovasodilators. *Br J Pharmacol*, **120**, 681-689.

Munzel, T., Feil, R., Mulsch, A., Lohmann, S.M., Hofmann, F. and Walter, U. (2003) Physiology and pathophysiology of vascular signaling controlled by guanosine 3',5'-cyclic monophosphate-dependent protein kinase [corrected]. *Circulation*, **108**, 2172-2183.

Murthy, K.S. (2001) Activation of phosphodiesterase 5 and inhibition of guanylate cyclase by cGMP-dependent protein kinase in smooth muscle. *Biochem J*, **360**, 199-208.

Murthy, K.S., Zhou, H., Grider, J.R. and Makhlouf, G.M. (2003) Inhibition of sustained smooth muscle contraction by PKA and PKG preferentially mediated by phosphorylation of RhoA. *Am J Physiol Gastrointest Liver Physiol*, **284**, G1006-1016.

Nagy, A. (2000) Cre recombinase: the universal reagent for genome tailoring. *Genesis*, **26**, 99-109.

Ny, L., Pfeifer, A., Aszodi, A., Ahmad, M., Alm, P., Hedlund, P., Fassler, R. and Andersson, K.E. (2000) Impaired relaxation of stomach smooth muscle in mice lacking cyclic GMP-dependent protein kinase I. *Br J Pharmacol*, **129**, 395-401.

Oelze, M., Mollnau, H., Hoffmann, N., Warnholtz, A., Bodenschatz, M., Smolenski, A., Walter, U., Skatchkov, M., Meinertz, T. and Munzel, T. (2000) Vasodilator-stimulated phosphoprotein serine 239 phosphorylation as a sensitive monitor of defective nitric oxide/cGMP signaling and endothelial dysfunction. *Circ Res*, **87**, 999-1005.

Orban, P.C., Chui, D. and Marth, J.D. (1992) Tissue- and site-specific DNA recombination in transgenic mice. *Proc Natl Acad Sci U S A*, **89**, 6861-6865.

Osinski, M.T., Rauch, B.H. and Schror, K. (2001) Antimitogenic actions of organic nitrates are potentiated by sildenafil and mediated via activation of protein kinase A. *Mol Pharmacol*, **59**, 1044-1050.

Owens, G.K., Kumar, M.S. and Wamhoff, B.R. (2004) Molecular regulation of vascular smooth muscle cell differentiation in development and disease. *Physiol Rev*, **84**, 767-801.

Ozaki, M., Kawashima, S., Yamashita, T., Hirase, T., Namiki, M., Inoue, N., Hirata, K., Yasui, H., Sakurai, H., Yoshida, Y., Masada, M. and Yokoyama, M. (2002) Overexpression of endothelial nitric oxide synthase accelerates atherosclerotic lesion formation in apoE-deficient mice. *J Clin Invest*, **110**, 331-340.

Palmer, R.M., Ferrige, A.G. and Moncada, S. (1987) Nitric oxide release accounts for the biological activity of endothelium-derived relaxing factor. *Nature*, **327**, 524-526.

Persson, K., Pandita, R.K., Aszodi, A., Ahmad, M., Pfeifer, A., Fassler, R. and Andersson, K.E. (2000) Functional characteristics of urinary tract smooth muscles in mice lacking cGMP protein kinase type I. *Am J Physiol Regul Integr Comp Physiol*, **279**, R1112-1120.

Pfeifer, A., Aszodi, A., Seidler, U., Ruth, P., Hofmann, F. and Fassler, R. (1996) Intestinal secretory defects and dwarfism in mice lacking cGMP-dependent protein kinase II. *Science*, **274**, 2082-2086.

Pfeifer, A., Klatt, P., Massberg, S., Ny, L., Sausbier, M., Hirneiss, C., Wang, G.X., Korth, M., Aszodi, A., Andersson, K.E., Krombach, F., Mayerhofer, A., Ruth, P., Fassler, R. and Hofmann, F. (1998) Defective smooth muscle regulation in cGMP kinase I-deficient mice. *Embo J*, **17**, 3045-3051.

Piedrahita, J.A., Zhang, S.H., Hagaman, J.R., Oliver, P.M. and Maeda, N. (1992) Generation of mice carrying a mutant apolipoprotein E gene inactivated by gene targeting in embryonic stem cells. *Proc Natl Acad Sci U S A*, **89**, 4471-4475.

Piggott, L.A., Hassell, K.A., Berkova, Z., Morris, A.P., Silberbach, M. and Rich, T.C. (2006) Natriuretic Peptides and Nitric Oxide Stimulate cGMP Synthesis in Different Cellular Compartments. *J Gen Physiol*, **128**, 3-14.

Pohler, D., Butt, E., Meissner, J., Muller, S., Lohse, M., Walter, U., Lohmann, S.M. and Jarchau, T. (1995) Expression, purification, and characterization of the cGMP-dependent protein kinases I beta and II using the baculovirus system. *FEBS Lett*, **374**, 419-425.

Post, M.J., Borst, C., Pasterkamp, G. and Haudenschild, C.C. (1995) Arterial remodeling in atherosclerosis and restenosis: a vague concept of a distinct phenomenon. *Atherosclerosis*, **118 Suppl**, S115-123.

Pryzwansky, K.B., Kidao, S., Wyatt, T.A., Reed, W. and Lincoln, T.M. (1995) Localization of cyclic GMP-dependent protein kinase in human mononuclear phagocytes. *J Leukoc Biol*, **57**, 670-678.

Qian, Y., Chao, D.S., Santillano, D.R., Cornwell, T.L., Nairn, A.C., Greengard, P., Lincoln, T.M. and Bredt, D.S. (1996) cGMP-dependent protein kinase in dorsal root ganglion: relationship with nitric oxide synthase and nociceptive neurons. *J Neurosci*, **16**, 3130-3138.

Rong, J.X., Shapiro, M., Trogan, E. and Fisher, E.A. (2003) Transdifferentiation of mouse aortic smooth muscle cells to a macrophage-like state after cholesterol loading. *Proc Natl Acad Sci U S A*, **100**, 13531-13536.

Ross, R. (1999) Atherosclerosis--an inflammatory disease. *N Engl J Med*, **340**, 115-126.

Rudic, R.D., Shesely, E.G., Maeda, N., Smithies, O., Segal, S.S. and Sessa, W.C. (1998) Direct evidence for the importance of endothelium-derived nitric oxide in vascular remodeling. *J Clin Invest*, **101**, 731-736.

Rybalkin, S.D., Yan, C., Bornfeldt, K.E. and Beavo, J.A. (2003) Cyclic GMP phosphodiesterases and regulation of smooth muscle function. *Circ Res*, **93**, 280-291.

Saiura, A., Sata, M., Hirata, Y., Nagai, R. and Makuuchi, M. (2001) Circulating smooth muscle progenitor cells contribute to atherosclerosis. *Nat Med*, **7**, 382-383.

Sata, M. (2006) Role of circulating vascular progenitors in angiogenesis, vascular healing, and pulmonary hypertension: lessons from animal models. *Arterioscler Thromb Vasc Biol*, **26**, 1008-1014.

Sata, M., Saiura, A., Kunisato, A., Tojo, A., Okada, S., Tokuhisa, T., Hirai, H., Makuuchi, M., Hirata, Y. and Nagai, R. (2002) Hematopoietic stem cells differentiate into vascular cells that participate in the pathogenesis of atherosclerosis. *Nat Med*, **8**, 403-409.

Sauer, B. and Henderson, N. (1988) Site-specific DNA recombination in mammalian cells by the Cre recombinase of bacteriophage P1. *Proc Natl Acad Sci U S A*, **85**, 5166-5170.

Sausbier, M., Schubert, R., Voigt, V., Hirneiss, C., Pfeifer, A., Korth, M., Kleppisch, T., Ruth, P. and Hofmann, F. (2000) Mechanisms of NO/cGMP-dependent vasorelaxation. *Circ Res*, **87**, 825-830.

Schlossmann, J., Ammendola, A., Ashman, K., Zong, X., Huber, A., Neubauer, G., Wang, G.X., Allescher, H.D., Korth, M., Wilm, M., Hofmann, F. and Ruth, P. (2000) Regulation of intracellular calcium by a signalling complex of IRAG, IP3 receptor and cGMP kinase Ibeta. *Nature*, **404**, 197-201.

Sekhar, K.R., Hatchett, R.J., Shabb, J.B., Wolfe, L., Francis, S.H., Wells, J.N., Jastorff, B., Butt, E., Chakinala, M.M. and Corbin, J.D. (1992) Relaxation of pig coronary arteries by new and potent cGMP analogs that selectively activate type I alpha, compared with type I beta, cGMP-dependent protein kinase. *Mol Pharmacol*, **42**, 103-108.

Sinnaeve, P., Chiche, J.D., Gillijns, H., Van Pelt, N., Wirthlin, D., Van De Werf, F., Collen, D., Bloch, K.D. and Janssens, S. (2002) Overexpression of a constitutively active protein kinase G mutant reduces neointima formation and in-stent restenosis. *Circulation*, **105**, 2911-2916.

Sinnaeve, P., Chiche, J.D., Nong, Z., Varenne, O., Van Pelt, N., Gillijns, H., Collen, D., Bloch, K.D. and Janssens, S. (2001) Soluble guanylate cyclase alpha(1) and beta(1) gene transfer increases NO responsiveness and reduces neointima formation after balloon injury in rats via antiproliferative and antimigratory effects. *Circ Res*, **88**, 103-109.

Sirsjo, A., Lofving, A., Hansson, G.K., Wagsater, D., Tokuno, S. and Valen, G. (2003) Deficiency of nitric oxide synthase 2 results in increased neointima formation in a mouse model of vascular injury. *J Cardiovasc Pharmacol*, **41**, 897-902.

Soff, G.A., Cornwell, T.L., Cundiff, D.L., Gately, S. and Lincoln, T.M. (1997) Smooth muscle cell expression of type I cyclic GMP-dependent protein kinase is suppressed by continuous exposure to nitrovasodilators, theophylline, cyclic GMP, and cyclic AMP. *J Clin Invest*, **100**, 2580-2587.

Somlyo, A.P. and Somlyo, A.V. (2003) Ca2+ sensitivity of smooth muscle and nonmuscle myosin II: modulated by G proteins, kinases, and myosin phosphatase. *Physiol Rev*, **83**, 1325-1358.

Sonnenburg, W.K. and Beavo, J.A. (1994) Cyclic GMP and regulation of cyclic nucleotide hydrolysis. *Adv Pharmacol*, **26**, 87-114.

Soriano, P. (1999) Generalized lacZ expression with the ROSA26 Cre reporter strain. *Nat Genet*, **21**, 70-71.

Surks, H.K., Mochizuki, N., Kasai, Y., Georgescu, S.P., Tang, K.M., Ito, M., Lincoln, T.M. and Mendelsohn, M.E. (1999) Regulation of myosin phosphatase by a specific interaction with cGMP- dependent protein kinase Ialpha. *Science*, **286**, 1583-1587.

Takimoto, E., Champion, H.C., Li, M., Belardi, D., Ren, S., Rodriguez, E.R., Bedja, D., Gabrielson, K.L., Wang, Y. and Kass, D.A. (2005) Chronic inhibition of cyclic GMP phosphodiesterase 5A prevents and reverses cardiac hypertrophy. *Nat Med*, **11**, 214-222.

Tanaka, K., Sata, M., Hirata, Y. and Nagai, R. (2003) Diverse contribution of bone marrow cells to neointimal hyperplasia after mechanical vascular injuries. *Circ Res*, **93**, 783-790.

Tang, K.M., Wang, G.R., Lu, P., Karas, R.H., Aronovitz, M., Heximer, S.P., Kaltenbronn, K.M., Blumer, K.J., Siderovski, D.P., Zhu, Y. and Mendelsohn, M.E. (2003) Regulator of G-protein signaling-2 mediates vascular smooth muscle relaxation and blood pressure. *Nat Med*, **9**, 1506-1512.

Tulis, D.A., Bohl Masters, K.S., Lipke, E.A., Schiesser, R.L., Evans, A.J., Peyton, K.J., Durante, W., West, J.L. and Schafer, A.I. (2002) YC-1-mediated vascular protection through inhibition of smooth muscle cell proliferation and platelet function. *Biochem Biophys Res Commun*, **291**, 1014-1021.

Tuschl, T. and Borkhardt, A. (2002) Small interfering RNAs: a revolutionary tool for the analysis of gene function and gene therapy. *Mol Interv*, **2**, 158-167.

Vaandrager, A.B., Smolenski, A., Tilly, B.C., Houtsmuller, A.B., Ehlert, E.M., Bot, A.G., Edixhoven, M., Boomaars, W.E., Lohmann, S.M. and de Jonge, H.R. (1998) Membrane targeting of cGMP-dependent protein kinase is required for cystic fibrosis

transmembrane conductance regulator Cl- channel activation. *Proc Natl Acad Sci U S A*, **95**, 1466-1471.

Varenne, O., Pislaru, S., Gillijns, H., Van Pelt, N., Gerard, R.D., Zoldhelyi, P., Van de Werf, F., Collen, D. and Janssens, S.P. (1998) Local adenovirus-mediated transfer of human endothelial nitric oxide synthase reduces luminal narrowing after coronary angioplasty in pigs. *Circulation*, **98**, 919-926.

von der Leyen, H.E., Gibbons, G.H., Morishita, R., Lewis, N.P., Zhang, L., Nakajima, M., Kaneda, Y., Cooke, J.P. and Dzau, V.J. (1995) Gene therapy inhibiting neointimal vascular lesion: in vivo transfer of endothelial cell nitric oxide synthase gene. *Proc Natl Acad Sci U S A*, **92**, 1137-1141.

von der Thusen, J.H., Fekkes, M.L., Passier, R., van Zonneveld, A.J., Mainfroid, V., van Berkel, T.J. and Biessen, E.A. (2004) Adenoviral transfer of endothelial nitric oxide synthase attenuates lesion formation in a novel murine model of postangioplasty restenosis. *Arterioscler Thromb Vasc Biol*, **24**, 357-362.

Wagner, C., Pfeifer, A., Ruth, P., Hofmann, F. and Kurtz, A. (1998) Role of cGMP-kinase II in the control of renin secretion and renin expression. *J Clin Invest*, **102**, 1576-1582.

Waldmann, R., Bauer, S., Gobel, C., Hofmann, F., Jakobs, K.H. and Walter, U. (1986) Demonstration of cGMP-dependent protein kinase and cGMP-dependent phosphorylation in cell-free extracts of platelets. *Eur J Biochem*, **158**, 203-210.

Wang, X. and Paigen, B. (2002) Comparative genetics of atherosclerosis and restenosis: exploration with mouse models. *Arterioscler Thromb Vasc Biol*, **22**, 884-886.

Wegener, J.W., Nawrath, H., Wolfsgruber, W., Kuhbandner, S., Werner, C., Hofmann, F. and Feil, R. (2002) cGMP-dependent protein kinase I mediates the negative inotropic effect of cGMP in the murine myocardium. *Circ Res*, **90**, 18-20.

Werner, C.G., Godfrey, V., Arnold, R.R., Featherstone, G.L., Bender, D., Schlossmann, J., Schiemann, M., Hofmann, F. and Pryzwansky, K.B. (2005) Neutrophil dysfunction in guanosine 3',5'-cyclic monophosphate-dependent protein kinase I-deficient mice. *J Immunol*, **175**, 1919-1929.

Wessel, D. and Flugge, U.I. (1984) A method for the quantitative recovery of protein in dilute solution in the presence of detergents and lipids. *Anal Biochem*, **138**, 141-143.

Wink, D.A., Miranda, K.M., Espey, M.G., Mitchell, J.B., Grisham, M.B., Fukuto, J. and Feelisch, M. (2000) The chemical biology of nitric oxide. Balancing nitric oxide with oxidative and nitrosative stress. In *Handbook of Experimental Pharmacology*, Vol. 143.

Wolfsgruber, W., Feil, S., Brummer, S., Kuppinger, O., Hofmann, F. and Feil, R. (2003) A proatherogenic role for cGMP-dependent protein kinase in vascular smooth muscle cells. *Proc Natl Acad Sci U S A*, **100**, 13519-13524.

Wooldridge, A.A., MacDonald, J.A., Erdodi, F., Ma, C., Borman, M.A., Hartshorne, D.J. and Haystead, T.A. (2004) Smooth muscle phosphatase is regulated in vivo by exclusion of phosphorylation of threonine 696 of MYPT1 by phosphorylation of Serine 695 in response to cyclic nucleotides. *J Biol Chem*, **279**, 34496-34504.

Worner, R., Lukowski, R., Hofmann, F. and Wegener, J.W. (2006) cGMP signals mainly through cAMP kinase in permeabilized murine aorta. *Am J Physiol Heart Circ Physiol*.

Xia, C., Bao, Z., Yue, C., Sanborn, B.M. and Liu, M. (2001) Phosphorylation and regulation of G-protein-activated phospholipase C-beta 3 by cGMP-dependent protein kinases. *J Biol Chem*, **276**, 19770-19777.

Xu, Q. (2004) Mouse models of arteriosclerosis: from arterial injuries to vascular grafts. *Am J Pathol*, **165**, 1-10.

Yogo, K., Shimokawa, H., Funakoshi, H., Kandabashi, T., Miyata, K., Okamoto, S., Egashira, K., Huang, P., Akaike, T. and Takeshita, A. (2000) Different vasculoprotective roles of NO synthase isoforms in vascular lesion formation in mice. *Arterioscler Thromb Vasc Biol*, **20**, E96-E100.

Zaccolo, M., De Giorgi, F., Cho, C.Y., Feng, L., Knapp, T., Negulescu, P.A., Taylor, S.S., Tsien, R.Y. and Pozzan, T. (2000) A genetically encoded, fluorescent indicator for cyclic AMP in living cells. *Nat Cell Biol*, **2**, 25-29.

Zhang, S.H., Reddick, R.L., Piedrahita, J.A. and Maeda, N. (1992) Spontaneous hypercholesterolemia and arterial lesions in mice lacking apolipoprotein E. *Science*, **258**, 468-471.

Zhao, L., Mason, N.A., Morrell, N.W., Kojonazarov, B., Sadykov, A., Maripov, A., Mirrakhimov, M.M., Aldashev, A. and Wilkins, M.R. (2001) Sildenafil inhibits hypoxia-induced pulmonary hypertension. *Circulation*, **104**, 424-428.

8 PUBLICATIONS

Reviews:

Lukowski R., Weber S., Weinmeister P., Feil S., Feil R. (2005). Cre/loxP-vermittelte konditionale Mutagenese des cGMP-Signalwegs in der Maus. *Biospektrum,* 3/05

Journal articles:

Worner R., **Lukowski R.**, Hofmann F., Wegener J.W. (2006). cGMP signals mainly through cAMP kinase in permeabilized murine aorta. Am J Physiol Heart Circ Physiol. (*published online*).

Lukowski R., Weinmeister P., Feil S., Gotthardt M., Herz J., Massberg S., Hofmann F., Feil R. (2006). Role of smooth muscle cGMP/cGKI signaling in a mouse model of restenosis. (*in preparation*).

Abstracts:

Weinmeister P., **Lukowski R.**, Linder S., Feil S., Hofmann F., Feil R. (2006). Die Wachstumsregulation durch zyklische Nukleotide unterscheidet sich in primären und subkultivierten glatten Gefäßmuskelzellen. *47. Frühjahrstagung der DGPT.* (Mainz, Germany)

Lukowski R., Weinmeister P., Feil S., Gotthardt M., Herz J., Massberg S., Hofmann F., Feil R. (2006). Bedeutung des cGMP/cGMP-abhängigen Proteinkinase Typ I Signalweges für die Restenose im Mausmodell. *47. Frühjahrstagung der DGPT.* (Mainz, Germany)

Worner R., **Lukowski R.**, Hofmann F., Wegener J. W. (2006). cGMP signals through cGMP- and cAMP-kinase in murine aorta. *Joint meeting of the German Society of Physiology and the Federation of European Physiological Societies*. (München, Germany)

Lukowski R., Weinmeister P., Vogl A., Feil S., Gotthardt M., Herz J., Massberg S., Hofmann F., Feil R. (2005). Function of smooth muscle cGMP-dependent protein kinase type I in a

mouse model of restenosis. *2nd International Conference on cGMP Generators, Effectors and Therapeutic Implications.* (Potsdam, Germany)

Weinmeister P., **Lukowski R.**, Linder S., Erl W., Brandl R., Feil S., Hofmann F., Feil R. (2005). Regulation of vascular smooth muscle growth by cyclic nucleotides and cGMP-dependent protein kinase. *2nd International Conference on cGMP Generators, Effectors and Therapeutic Implications.* (Potsdam, Germany)

Feil R., Weinmeister P., **Lukowski R.**, Weber S., Brummer S., Feil S., Hofmann F. (2005). Genetic dissection of signaling via cGMP-dependent protein kinases. *2nd International Conference on cGMP Generators, Effectors and Therapeutic Implications.* (Potsdam, Germany)

Lukowski R., Weinmeister P., Feil S., Gotthardt M., Herz J., Massberg S., Hofmann F., Feil R. (2005). Vascular remodeling in response to carotid ligation in mice with a smooth muscle-specific deletion of cGMP-dependent protein kinase type I. *46. Frühjahrstagung der DGPT.* (Mainz, Germany)

Feil R., Weinmeister P., **Lukowski R.**, Weber S., Brummer S., Feil S., Hofmann F. (2005). Role of cGMP/cGKI signaling in vascular smooth muscle growth. *46. Frühjahrstagung der DGPT.* (Mainz, Germany)

Feil R., Weinmeister P., **Lukowski R.**, Weber S., Feil S., Hofmann F. (2005). NO/cGMP signaling in smooth muscle cells and atherosclerosis. *Gordon Research Conference „Vascular Cell Biology".* (Ventura Beach, USA)

Lukowski R., Weinmeister P., Feil S., Gotthardt M., Herz J., Massberg S., Hofmann F., Feil R. (2005). Role of smooth muscle cGMP/cGKI signaling in restenosis. *Gordon Research Conference „Vascular Cell Biology".* (Ventura Beach, USA)

9 ACKNOWLEDGMENTS

I am very grateful to Prof. Dr. F. Hofmann (*Institut für Pharmakologie und Toxikologie, TU München, Germany*) for giving me the opportunity to perform this thesis in his laboratory. Thank you for helpful discussions, advice, and support. *Danke Chef!*

Many thanks to Prof. Dr. R. Feil (*Interfakultäres Institut für Biochemie, Universität Tübingen, Germany*) for supervising this work. His intensive support had major influence on the success of this thesis. Thanks for your interest in my research, many fruitful discussions that stimulated my mind, and being patient with my ideas. *Danke Robert!*

I am grateful to Prof. Dr. M. Schemann (*Department of Human Biology, TU München, Germany*) who represented this work to the faculty committee.

Thanks to Prof. Dr. J. Herz (*Department of Molecular Genetics, UT Southwestern, Dallas, USA)* and Dr. M. Gotthardt (*Max-Delbrück-Centrum für Molekulare Medizin, Berlin-Buch, Germany*) for making the SM22α-Cre mice available.

I thank Dr. S. Massberg (*Deutsches Herzzentrum, TU München, Germany*) for teaching the carotid ligation model of vascular injury to me.

I thank Prof. Dr. M. Gratzl and Dr. K. Schmidt-Bäse (*Anatomisches Institut, LMU München, Germany*) for accepting me as a graduate student in the “Biology of Human Diseases” training program and for the financial support.

For an interesting collaboration I thank Prof. M.E. Rosenfeld (MD., PhD.) and Prof. S.M. Schwartz (MD., PhD.) at the University of Washington (*Department of Pathology, UW Seattle, USA*). Thanks for giving me the opportunity to experience your laboratories.

Thanks to Dr. S. Feil (*Interfakultäres Institut für Biochemie, Universität Tübingen, Germany*) for familiarizing me with all important secrets of mouse breeding and handling.

I like to thank all colleagues at the *Institut für Pharmakologie und Toxikologie* contributing to the institute´s stimulating scientific atmosphere. In this respect, even more thanks to everyone for teamwork and friendship. Special thanks to Pascal who was the best company and co-worker, and, importantly, also a friend always as a friend was needed. I appreciated to work with you! Many thanks to Sabine and Doris for their technical support.

I dedicate many thanks to my friends from Munich for accepting me the way I am, being authentic, and above all making life more interesting and enjoyable. Thanks for the countless amusing discussions, marvelous activities, and many beers to Thombastisch, Pilts, Sascha, Olli, RalpHammer, and Andy. In addition, I thank my friends who came the long way to visit me: Joghurt, Alexito, Flo, Maddin, Guliani, Edi, Eduardo, Tobsche, Le Jens, Nik, and Daniel.

I apologize to all mice that participated in this study.

My greatest thanks are dedicated to my parents because they were, are, and will be the most important persons in my life. *Danke liebe Eltern!*